

Buckling Analysis of Nano-Composite Laminate Using Finite Element Analysis

Submitted in fulfilment of the requirements for the degree of

Master of Science (MSc)

In

Engineering

By

Siphelele Mthokoziseni Mziwandile Mhlongo

Student No.: 213540877

Under the Guidance of

Dr Georgios A. Drosopoulos



Date of submission:DECEMBER 2019.....

EXAMINER'S COPY

DECLARATION OF AUTHENTICITY

I, Siphelele Mthokoziseni Mziwandile Mhlongo declare that:

1. The research reported in this Dissertation, except where otherwise indicated, is my original research.
2. This Dissertation has not been submitted for any degree or examination at any other university.
3. This Dissertation does not contain other persons' data, pictures, graphs or other information, unless specifically acknowledged as being sourced from other persons.
4. This Dissertation does not contain other persons' writing, unless specifically acknowledged as being sourced from other researchers. Where other written sources have been quoted, then:
 - Their words have been re-written but the general information attributed to them has been referenced
 - Where their exact words have been used, then their writing has been placed in italics and inside quotation marks, and referenced.
5. This Dissertation does not contain text, graphics or tables copied and pasted from the Internet, unless specifically acknowledged, and the source being detailed in the Dissertation and in the References sections.

I Dr. Georgios A. Drosopoulos, as the candidate's Supervisor, agree to the submission of this dissertation.

.....

Student's Signature

.....

Date

.....

Supervisor's Signature

.....

Date

ABSTRACT

In this dissertation, the buckling problem of a nanocomposite laminate is investigated. The laminate consists of uni-directional nanocomposite plies fabricated with a graphene filled polymer matrix reinforced with carbon or glass fibres. The nanocomposite laminate is subjected to uniaxial and biaxial loading. The effective mechanical properties of the nanocomposite plies are determined using micromechanical equations. The structural analysis of the nanocomposite laminate is completed using a commercial finite element analysis software (ANSYS). Due to the geometry of the nanocomposite laminate, the classical laminate plate theory applies. Thus, it is assumed that there are no flaws between the plies and there is no shear deformation experienced by the nanocomposite laminate. The results show that the increase in the number of layers, weight fraction of graphene nanoplatelets (W_{GPL}) and aspect ratio results in the increase of critical buckling stress. The critical stress of a laminate can be increased or reduced when the fibre volume content (V_F) is increased, depending on the W_{GPL} of the laminate. For a uniaxially loaded laminate with all layers having an equal fibre orientation, the critical stress is maximum when the fibre orientation of the layers are parallel to the load applied and becomes minimum when the fibre orientation of layers is perpendicular to the applied load. When the boundary conditions are CFFF the buckling stress is minimum and when the boundary conditions are CCCC the buckling stress of is maximum.

ACKNOWLEDGEMENT

This dissertation became a reality because of the input and assistance of the following individuals and organizations. I would like to express my deepest appreciation to them.

Firstly, I would like to thank the almighty God for the wisdom and strength he gave me to complete this research.

My supervisor, Dr Georgios Drosopoulos, for his invaluable encouragement, suggestions and support throughout the process of writing this Dissertation.

Mrs Ntombenhle Nombuso Dlamini, for her assistance in registering for MSc, and her support whenever I needed help or clarity on anything related to MSc.

My fellow MSc students, namely: Senzo Nhlabasti, Shaverndarm Moonsamy and Thando Nqasha, for assisting me connect remotely to my computer on campus every time I needed to use ANSYS and for their advice and suggestions.

The school of Engineering in the University of KwaZulu-Natal for providing me with all the resources and support I needed to complete this dissertation.

Lastly, I would like to thank my employer Ithala Development Finance Corporation for allowing me to use office resources in order to complete this dissertation.

Siphelele M. Mhlongo

TABLE OF CONTENTS

DECLARATION OF AUTHENTICITY.....	i
ABSTRACT.....	ii
ACKNOWLEDGEMENT	iii
LIST OF ABBREVIATIONS	vi
LIST OF SYMBOLS	vii
LIST OF FIGURES	1
LIST OF TABLES.....	4
CHAPTER 1 INTRODUCTION	6
1.1 Introduction to study	6
1.2 Research goals and objectives.....	6
CHAPTER 2 LITERATURE REVIEW	7
2.1 Introduction.....	7
2.2 Literature review	7
2.2.1 Composites, nanocomposite and laminated composites	7
2.2.2 Reinforcement and nanofiller material.....	9
2.2.3 Fibre volume content	12
2.2.4 Boundary conditions	13
2.2.5 Layer fibre orientation	16
2.2.6 Aspect ratio	18
2.2.7 Composite laminate material stacking sequence.....	18
2.2.8 Nanocomposite studies and other findings	20
2.3 Literature review summary	21
CHAPTER 3 MODELS.....	22
3.1 Problem formulation	22
3.2 Micromechanical modelling	23
3.2.1 Graphene reinforced polymer matrix	24
3.2.2 Graphene and Fibre Reinforced Nanocomposite laminate	26
3.3 ANSYS modelling.....	27
3.3.1 Engineering data	28
3.3.2 ACP (pre)	29
3.3.3 Static structural and eigenvalue buckling	33

CHAPTER 4 RESULTS AND DISCUSSIONS	35
4.1. Effect of Boundary conditions on buckling stress	35
4.1.1 Results.....	35
4.1.2 Discussion of Results	38
4.2. Effect of Fibre Orientation on Buckling Stress.....	39
4.2.1 Results.....	39
4.2.2 Discussion of results	43
4.3. Effect of Number of Layers and Stacking Sequence on Buckling Stress.....	44
4.3.1 Results.....	44
4.3.2 Discussion of results	49
4.4. Effect of Thickness Ratio on Buckling Stress.....	50
4.4.1 Results.....	50
4.4.2 Discussion of results	52
4.5. Effect of Aspect Ratio on Buckling Stress.....	53
4.5.1 Results.....	53
4.5.2 Discussion of results	55
4.6. Effect of Weight Fraction (W_{GPL}) on Buckling Stress	56
4.6.1 Results.....	56
4.6.2 Discussion of results	61
4.7. Effect of Fibre Volume Content on Buckling Stress	62
4.7.1 Results.....	62
4.7.2 Discussion of results	66
4.8. Discussion on the practicality of results	67
CHAPTER 5 CONCLUSION AND RECOMMENDATIONS	68
REFERENCES	70
APPENDIX A.....	75
A.1 Glass fibre reinforcement properties.....	75
A.1.1 Material properties where V_F is kept constant while varying W_{GPL}	75
A.1.2 Material properties where W_{GPL} is kept constant while varying V_F	80
A.2. Carbon fibre reinforcement	83
A.2.1 Material properties where V_F is kept constant while varying W_{GPL}	83
A.2.2 Material properties where W_{GPL} is kept constant while varying V_F	88

LIST OF ABBREVIATIONS

2D	– Two dimensional
3D	– Three Dimensional
CFRL	– Carbon Fibre Reinforced Laminate
CMC	– Ceramic Matrix Composite
CMNC	– Ceramic Matrix NanoComposite
CNTs	– Carbon NanoTubes
DoF	– Degrees of Freedom
DWCNTs	– Double Walled Carbon Nanotubes
GFRL	– Glass Fibre Reinforced Laminate
GFRNL	– Graphene and Fibre Reinforced Nanocomposite Laminate
MMC	– Metal Matric Composite
MMNC	– Metal Matrix NanoComposite
MSc	– Master of Science
PMC	– Polymer Matric Composite
PMNC	– Polymer Matrix NanoComposite
SWCNTs	– Single Walled Carbon NanoTubes
UDL	– Uniformly Distributed load

LIST OF SYMBOLS

E	- Young's modulus
E_{11}	- Young's modulus X direction
E_{22}	- Young's modulus Y direction
E_{GM}	- Young's modulus of graphene reinforced polymer matrix
E_{GPL}	- Young's modulus of graphene nanoplatelets
E_M	- Young's modulus of polymer matrix
ρ	- Density
ρ_c	- Density of composite
ρ_f	- Density of fibre
ρ_m	- Density of matrix
ρ_{GPL}	- Mass density of graphene nanoplatelets
ρ_M	- Mass density of polymer matrix
ν	- Poisons ratio
ν_{12}	- poisons ratio in the XY direction
ν_{GPL}	- Poisson's ratio of graphene nanoplatelet
ν_M	- Poisson's ratio of polymer matrix
ν_f	- Volume content of fibre
G	- Shear Modulus
G_{12}	- Shear modulus in the XY direction
θ_x	- Rotation about the x-axis
θ_y	- Rotation about the y-axis
θ_z	- Rotation about the z-axis
P_{cr}	- Critical buckling
I	- Moment of inertia
L	- Effective length factor

σ^c	- Compressive stress
σ^T	- Tensile stress
M	- Moment
H	- Full thickness of laminate
h_s	- Full thickness of surface layers
$h_s/2$	- Thickness of single surface layer
h_m	- Thickness of middle layer
θ_s	- Fibre orientation of surface layer
θ_m	- Fibre orientation of middle layer
α	- Thickness ratio
a	- Width
b	- height
l_{GPL}	- Length of graphene nanoplatelets
h_{GPL}	- Thickness of graphene nanoplatelets
w_{GPL}	- width of graphene nanoplatelets
V_{GPL}	- Volume content of graphene nanoplatelets
V_F	- fibre volume content
W_{GPL}	- Weight fraction of graphene nanoplatelets
N_X	- Dimensional buckling stress
N_0	- Non-dimensional stress
D1	- Dimension one
D2	- Dimension two
D3	- Dimension three

LIST OF FIGURES

Figure 2-1 Composite material classifications based on matrix material with further sub-categories (Idowu, et al., 2015).	8
Figure 2-2 Composite material classifications based on reinforcement material, including further sub-categories (Idowu, et al., 2015).....	8
Figure 2-3 The three classifications of nanofillers; (a) one dimensional nanofiller,(b) two dimensional nanofiller and (c) three dimensional nanofiller (Akpan, et al., 2019).	10
Figure 2-4 Volume fraction vs critical load by Battawi (2008) for different slenderness ratios of beam length.	13
Figure 2-5 Degrees of freedom experienced by a point in 3D (Carleton, 2016).....	14
Figure 2-6 Theoretical and recommended effect length factors (Halkyard, 2005).	15
Figure 2-7 Results obtained by Hamani (2013) on fibre angle vs buckling load.....	16
Figure 2-8 Results obtained by Dhuban (2017) on fibre angle vs buckling load.....	17
Figure 2-9 Stresses acting on a plate under bending (Mao, et al., 2008).	18
Figure 2-10 Different types of stacking sequences. (a) Symmetric ply laminate, (b) Anti-symmetric laminate, (c) Cross ply laminate and (d) Angle ply laminate.	19
Figure 3-1 A 3 layer composite laminate, used in multiples analysis in this paper.	22
Figure 3-2 Schematic diagram of how composite micromechanical equations get the different results. The diagram shows the inputs and outputs of the micromechanical equations (Chamis, 1983).....	23
Figure 3-3 Project schematic in ANSYS used to analyse a laminate nanocomposite material and an enlarged image of the different analysis systems, (b) engineering data, (c)ACP (Pre), (d) Static structural and (e) Eigenvalue buckling.	27
Figure 3-4 New materials created on ANSYS and the data entered for a surface layer with $W_{GPL} = 0.05$ and $V_F = 0.5$	28
Figure 3-5 A 2d diagram of the plate created using design modeller. The dimensions of the plate is 1m x 1m.	29
Figure 3-6 The generated mesh on the plate generated on the geometry section	30
Figure 3-7 ACP (Pre) setup program	31
Figure 3-8 The completed composite material made using ACP (Pre). The laminate is a 3 layer laminate with a thickness ratio of 0.7 and all fibre orientations 45°	32
Figure 3-9 The analysis setup page for a composite plate. Showing the added UDL of 1Pa and a fixed support and that the required results are a total deformation of the plate under eigenvalue buckling.....	33

Figure 3-10 The final results of the plate. Since the load multiplier in this case is 40109 that means the dimensional buckling stress is also 40109. To find the non-dimensional buckling stress equation 15 is used	34
Figure 4-1 Laminate boundary conditions	35
Figure 4-2 Layer properties of Laminated nanocomposite in the boundary condition tests	36
Figure 4-3 The effects of different boundary conditions on the buckling stress for CFRL under uniaxial and biaxial loading.....	37
Figure 4-4 The effects of different boundary conditions on the buckling stress for GFRL under uniaxial and biaxial loading.....	37
Figure 4-5 layer properties of Laminated nanocomposite in the effect of fibre orientation on buckling stress tests	39
Figure 4-6 Non-Dimensional Buckling stress (N_0) vs surface layers fibre orientation for a nanocomposite reinforced with carbon fibre uniaxially loaded	40
Figure 4-7 Non-Dimensional Buckling stress (N_0) vs surface layers fibre orientation for a nanocomposite reinforced with glass fibre uniaxially loaded	41
Figure 4-8 Non-Dimensional Buckling stress (N_0) vs surface layers fibre orientation for a nanocomposite reinforced with Carbon fibre biaxially loaded.....	41
Figure 4-9 Non-Dimensional Buckling stress (N_0) vs surface layers fibre orientation for a nanocomposite reinforced with glass fibre biaxially loaded.	42
Figure 4-10 Non-dimensional Buckling stress (N_0) vs thickness ratio for different middle layer fibre orientations.....	42
Figure 4-11 stacking sequences used in the analysis of the effect on stacking sequences on buckling stress including fibre angles and the order in which the layers are added.	44
Figure 4-12 layer properties of Laminated nanocomposite in the number of layers tests	45
Figure 4-13 Non-Dimensional Buckling stress (N_0) vs number of layers for a nanocomposite reinforced with glass fibre and Carbon fibre	47
Figure 4-14 Number of layers v N_0 for a uniaxial loading.....	47
Figure 4-15 Number of layers v N_0 for biaxial loading.....	48
Figure 4-16 Number of layers v N_0 for uniaxial loading.....	48
Figure 4-17 Number of layers v N_0 for biaxial loading.....	49
Figure 4-18 Layer properties of Laminated nanocomposite in the thickness ratio tests.....	50
Figure 4-19 Non-Dimensional Buckling stress (N_0) vs Thickness ratio for a nanocomposite reinforced with carbon fibre	51
Figure 4-20 Non-Dimensional Buckling stress (N_0) vs Thickness ratio for a nanocomposite reinforced with glass fibre	52
Figure 4-21 Layer properties of Laminated nanocomposite in the aspect ratio tests.....	53

Figure 4-22 Non-Dimensional Buckling stress (N_0) vs Aspect ratio for a nanocomposite reinforced with glass fibre and Carbon fibre	54
Figure 4-23 Layer properties of Laminated nanocomposite in the boundary condition tests ..	56
Figure 4-24 Non-Dimensional Buckling stress (N_0) vs Weight Fraction (W_{GPL}) for a nanocomposite reinforced with Carbon fibre with 3 layers with a thickness ratio of 0.2 and equal fibre orientations (45°)	58
Figure 4-25 Non-Dimensional Buckling stress (N_0) vs Weight Fraction (W_{GPL}) for a nanocomposite reinforced with glass fibre with 3 layers with a thickness ratio of 0.2 and equal fibre orientations (45°)	58
Figure 4-26 Non-Dimensional Buckling stress (N_0) vs Weight Fraction (W_{GPL}) for a nanocomposite reinforced with Carbon fibre with 10 layers with equal thickness and equal fibre orientations (45°)	59
Figure 4-27 Non-Dimensional Buckling stress (N_0) vs Weight Fraction (W_{GPL}) for a nanocomposite reinforced with glass fibre with 10 layers with equal thickness and equal fibre orientations (45°)	59
Figure 4-28 Non-Dimensional Buckling stress (N_0) vs Weight Fraction (W_{GPL}) for a nanocomposite reinforced with Carbon fibre with 10 layers with equal thickness and equal fibre orientations (90°)	60
Figure 4-29 Non-Dimensional Buckling stress (N_0) vs Weight Fraction (W_{GPL}) for a nanocomposite reinforced with glass fibre with 10 layers with equal thickness and equal fibre orientations (90°)	60
Figure 4-30 Layer properties of Laminated nanocomposite in the fibre volume tests.....	62
Figure 4-31 Non-Dimensional Buckling stress (N_0) vs Volume Content (V_{GPL}) for a nanocomposite reinforced with carbon fibre with 3 layers with thickness ratio of 0.2 and equal fibre orientations of 45°	63
Figure 4-32 Non-Dimensional Buckling stress (N_0) vs Volume Content (V_{GPL}) for a nanocomposite reinforced with glass fibre with 3 layers with thickness ratio of 0.2 and equal fibre orientations of 45°	64
Figure 4-33 Non-Dimensional Buckling stress (N_0) vs Volume Content (V_{GPL}) for a nanocomposite reinforced with Carbon fibre with 10 layers with equal thickness and equal fibre orientations of 45°	64
Figure 4-34 Non-Dimensional Buckling stress (N_0) vs Volume Content (V_{GPL}) for a nanocomposite reinforced with glass fibre with 10 layers with equal thickness and equal fibre orientations of 45°	65
Figure 4-35 Non-Dimensional Buckling stress (N_0) vs Volume Content (V_{GPL}) for a nanocomposite reinforced with Carbon fibre with 10 layers with equal thickness and equal fibre orientation of 90°	65
Figure 4-36 Non-Dimensional Buckling stress (N_0) vs Volume Content (V_{GPL}) for a nanocomposite reinforced with glass fibre with 10 layers with equal thickness and equal fibre orientation of 90°	66

LIST OF TABLES

Table 2-1 Properties of different reinforcement and filler materials (Chung & Chung, 2012).	12
Table 3-1 Properties of graphene nanoplatelets nanofill, polymer matrix, carbon fibre and glass fibre. These properties were obtained from (Radebe, et al., 2019).	24
Table 4-1 The thickness of the layers of a 3 layer composite laminate for different thickness ratios.	51
Table 4-2 The dimension of the width and height of the laminate for different aspect ratios. (a) is the width and (b) is the height.....	54
Table A-1 Glass fibre material properties when V_F is kept constant at 0.1, while W_{GPL} is varied.	75
Table A-2 Glass fibre material properties when V_F is kept constant at 0.2, while W_{GPL} is varied.	76
Table A-3 Glass fibre material properties when V_F is kept constant at 0.3, while W_{GPL} is varied.	77
Table A-4 Glass fibre material properties when V_F is kept constant at 0.4, while W_{GPL} is varied.	78
Table A-5 Glass fibre material properties when V_F is kept constant at 0.5, while W_{GPL} is varied.	79
Table A-6 Glass fibre material properties when W_{GPL} is kept constant at 0.02, while V_F is varied.	80
Table A-7 Glass fibre material properties when W_{GPL} is kept constant at 0.04, while V_F is varied.	80
Table A-8 Glass fibre material properties when W_{GPL} is kept constant at 0.06, while V_F is varied	81
Table A-9 Glass fibre material properties when W_{GPL} is kept constant at 0.08, while V_F is varied	81
Table A-10 Glass fibre material properties when W_{GPL} is kept constant at 0.02, while V_F is varied	82
Table A-11 Carbon fibre material properties when V_F is kept constant at 0.1, while W_{GPL} is varied.	83
Table A-12 Carbon fibre material properties when V_F is kept constant at 0.2, while W_{GPL} is varied.	84
Table A-13 Carbon fibre material properties when V_F is kept constant at 0.3, while W_{GPL} is varied.	85
Table A-14 Carbon fibre material properties when V_F is kept constant at 0.4, while W_{GPL} is varied.	86

Table A-15 Carbon fibre material properties when V_F is kept constant at 0.5, while W_{GPL} is varied.	87
Table A-16 Carbon fibre material properties when W_{GPL} is kept constant at 0.02, while V_F is varied.	88
Table A - 17 Carbon fibre material properties when W_{GPL} is kept constant at 0.04, while V_F is varied.	88
Table A-18 Carbon fibre material properties when W_{GPL} is kept constant at 0.06, while V_F is varied.	89
Table A-19 Carbon fibre material properties when W_{GPL} is kept constant at 0.08, while V_F is varied.	89
Table A-20 Carbon fibre material properties when W_{GPL} is kept constant at 0.10, while V_F is varied.	90

CHAPTER 1

INTRODUCTION

1.1 Introduction to study

Since the beginning of time, man has endeavoured to improve the materials used for different tasks. These materials range from those used in construction to those used for weaponry. The first tools made by humans were made of stone and have since evolved to the materials used today. Composite materials are used extensively in the 21st century. Reinforced concrete, composite wood and reinforced plastics are examples of composite materials used every day. Composite materials are preferred to other materials because of their high strength, low weight and relatively low cost. Wood (2008) named composite materials as one of the top ten advances made in material science in the past 50 years. Part of the list of top advances in material science are nanotechnology, carbon fibre and carbon nanotubes (CNTs). Nanocomposite materials are a sub-category of composite materials which make use of reinforcement with one or more dimensions in the nanoscale. Nanocomposite materials have excellent properties and have the potential of being used in many industries. The ability to design and manufacture nanocomposite materials in an efficient manner while reducing the cost would be an important stepping stone to the next era of material science.

1.2 Research goals and objectives

The goal of this dissertation is to highlight the structural response of nanocomposite laminates, by analysing their buckling resistance using finite element analysis. A graphene and fibre reinforced nanocomposite laminate (GFRNL) is numerically tested for buckling resistance using ANSYS. The objective of this dissertation is to determine the optimal performance of a GFRNL against buckling, when the following parameters are investigated: fibre orientation, number of layers, stacking sequence, thickness ratio, aspect ratio, graphene weight fraction, fibre volume content and boundary conditions. The analysis of the GFRNL makes use of classical laminate plate theory. Therefore, the effects of shear deformation are ignored and it is assumed that the laminate is in a state of plane stress and the layers are bonded perfectly together.

CHAPTER 2

LITERATURE REVIEW

2.1 Introduction

A large amount of research has been done in the field of nanocomposite materials. This dissertation will focus on polymer matrix nanocomposites and laminated composites. Furthermore, literature showing the effect of fibre content, fibre orientation, boundary conditions, aspect ratio and stacking sequences on the buckling stress of a composite laminate will be reviewed.

2.2 Literature review

2.2.1 Composites, nanocomposite and laminated composites

Berthelot & Frederick (1999) define a composite material as “*A combination of two or more different materials that are mixed in an effort to blend the best properties of both.*” The goal of combining materials in order to make a composite is to obtain a material that has performance characteristics that are greater than the component materials. Composite materials consist of one or more discontinuous phases, which are called “*reinforcement*” and one continuous phase called a “*matrix*”. In general, the reinforcement material, which is usually in the form of fibres, is designed to provide the stiffness and strength to the composite and the matrix material is designed to bind the fibres together, distribute the load and add to the overall mechanical properties of the composite. There are a wide variety of materials that can be used as reinforcement material. However, for the matrix, usually one of three materials is used: a polymer, ceramic or metal. Composites can be classified by either their matrix or reinforcement. The matrix classifications are polymer-matrix composites (PMC), ceramic-matrix composites (CMC) and metal-matrix composites (MMC). The reinforcement classifications are fibre-reinforced composites, particle composites, structural composites (Idowu, et al., 2015). The different classifications and sub-classifications of composites based on matrix and reinforcement material are shown in figure 2-1 and 2-2 respectively. Compared to other materials, composite materials have high strength to weight ratio, good electrical and thermal properties, and are relatively easy to fabricate. Thus, composite materials are widely used in multiple industries such as the automobile, defence and aerospace.

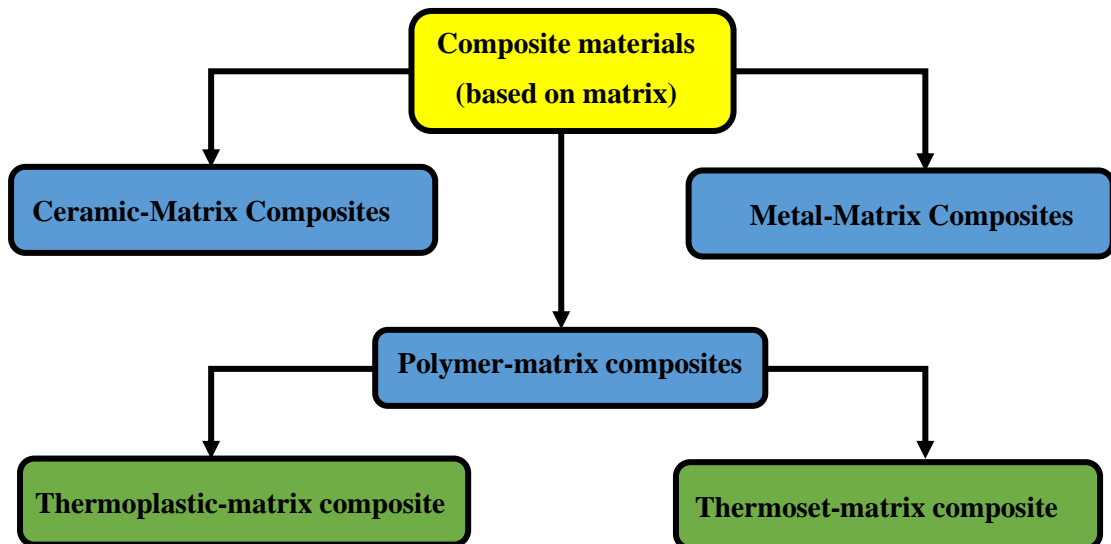


Figure 2-1 Composite material classifications based on matrix material with further sub-categories (Idowu, et al., 2015).

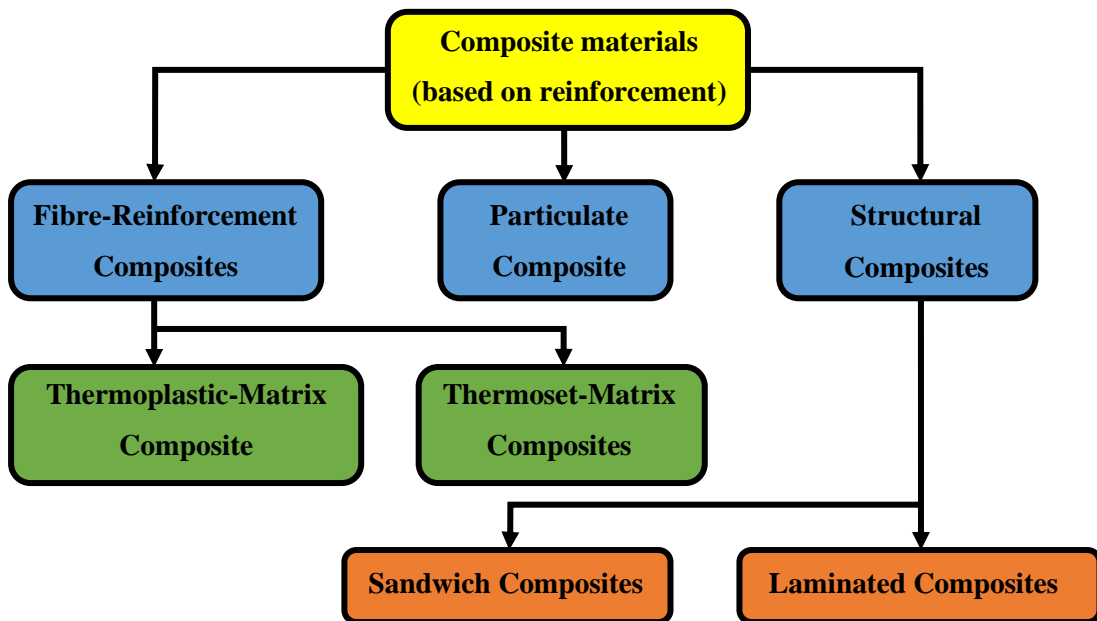


Figure 2-2 Composite material classifications based on reinforcement material, including further sub-categories (Idowu, et al., 2015).

Nanocomposites are composite materials where the reinforcement has at least one or more dimensions in the nanoscale (1 nm is equivalent to 10^{-9} m). Nanocomposites possess unique material properties compared to traditional composite materials, such as electrical conductivity and colloidal stability (Camargo, et al., 2009). Some researchers such as Pandya (2013) classify nanocomposites into two categories, polymer and non-polymer based nanocomposite. Other researchers such as Camargo (2009) choose to classify nanocomposites according to the matrix.

In this classification, a nanocomposite material is classified as Ceramic Matrix Nanocomposite (CMNC), Metal Matrix Nanocomposite (MMNC) or Polymer Matrix Nanocomposite (PMNC). The mechanical, thermal, flammability and barrier properties of a polymer matrix can be enhanced by adding some nanofillers to it (de Oliveira & Beatrice, 2018). Nanofillers are additives in solid form which have at least one dimension in nanoscale and they vary from isotropic to highly anisotropic.

Laminated composites consist of several layers of fibre-reinforced composites that are bonded together in order to achieve the required mechanical properties. Each layer can have similar or different material properties. There are many important parameters of a laminated composite, including stacking sequence, fibre orientation, geometry and fibre content. Finding the optimum values for these parameters, in order to achieve the highest natural frequency and buckling load is one of the biggest issues in laminated composite design (Suna, 2014). Thus, several studies similar to the one presented in this dissertation investigate the optimal properties of a laminated composite materials.

2.2.2 Reinforcement and nanofiller material

The different types of nanofillers used to reinforce polymer nanocomposites can be classified by their dimensions. A nanocomposite has been previously defined as a composite material where at least one component has one or more dimension(s) in the nanoscale. When the nanofiller has one dimension in the nanoscale, it is named a one dimensional nanofiller and when a PMNC has this type of nanofiller it is named a polymer-layered nanocomposite. An example of a polymer-layered nanocomposite is graphene reinforced PMNC. When the nanofiller has two dimensions in the nanoscale, it is named a two dimensional nanofiller. This type of nanofiller is usually formed by whiskers or Carbon nanotubes (CNTs). When the nanofiller has all three dimensions in nanoscale, it is named an isodimensional nanoparticle or three dimensional nanofiller. Figure 2-3 shows a visual representation of the classifications of nanofillers (Akpan, et al., 2019). As can be seen in figure 2-3 (a), one dimensional nanofillers is usually in the shape of sheets. With the thickness of the sheet being less than 100nm ($D < 100\text{nm}$). In figure 2-3 (b) it can be seen that two dimensional nanofillers are usually in the shape of tubes, fibres, or filaments. The diameter of a two dimensional nanofiller is less than 100nm in all directions (D_1 and $D_2 < 100\text{nm}$). A three dimension nanofiller is usually a equiaxed particles with all three dimensions less than 100nm (D_1, D_2 and $D_3 < 100\text{nm}$).

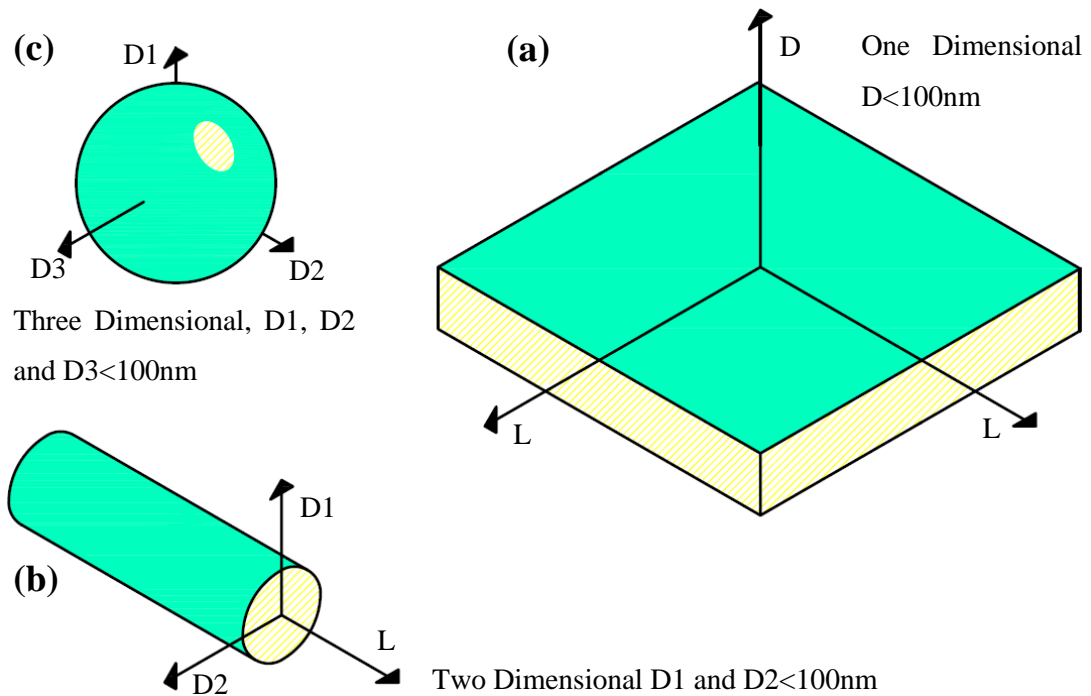


Figure 2-3 The three classifications of nanofillers; (a) one dimensional nanofiller, (b) two dimensional nanofiller and (c) three dimensional nanofiller (Akpan, et al., 2019).

Graphene can be described as a single thin layer of graphite. Graphite is an allotrope of carbon, meaning it is one of many ways carbon atoms can be arranged. Graphene and diamond are also examples of allotropes of carbon. The material properties of graphene are excellent. In particular, graphene has a Young's modulus of approximately 1 TPa and a strength of approximately 130 GPa, making it one of the stiffest and strongest materials used today (Kilic, et al., 2018). Due to graphene's pure graphitic composition it has an outstanding thermal conductivity of approximately 5000 Wm.K and electric conductivity of approximately 10 Sm (Changgu, et al., 2008). These properties have made graphene very attractive for use in many applications. Du & Cheng (2012) state that graphene is a potential nanofiller that can improve the properties of composites dramatically. However, similar to CNTs, there are technical issues that need to be overcome in order for this material to be used more widely. The technical issues include mass fabrication, structural response of graphene to matrix interface and dispersion of graphene in matrix (Kilic, et al., 2018).

Carbon nanotubes (CNTs) are another very common nanocomposite reinforcement and polymer nanofiller. There has been increased interest in CNT research due to its high strength and stiffness. CNTs can be thought of as a sheet of graphene rolled into a tube. CNTs can be single walled (SWCNTs) or double walled (DWCNTs). CNTs have been used extensively on composite materials due to the fact that it has been found that the addition of CNTs to composite

materials results in the enhancement of material properties (Vodenitcharova & Zhang, 2005). There has been debate on the effectiveness of CNTs on polymer based composites. Lau (2002) found that a CNT/epoxy beam can have lower flexural strength compared to a pure epoxy beam when there is a weak bond between the CNTs and the surrounding polymer matrix. However, other researchers, like Vodenitcharova (2005) and Barber (2003) argue that this is not a big issue since CNTs and polymer matrices can form strong interfaces. Moreover, there are other methods to overcome this problem. Apart from adding nanotubes to a polymer matrix, researchers have also used other forms of matrices. Zhang (2000) coated an electron beam deposit with various metals in order to obtain a continuous metal nanowire or a high performance metal. Zhang (2000) found that titanium had a strong bond with CNTs, whereas gold and aluminium produced a weak bond. CNTs are the most commonly studied carbon based nanomaterial. This is due to the aforementioned properties and that CNTs possess excellent electrical, thermal and electronic transport properties (Kilic, et al., 2018). However due to poor dispersion and the high cost of CNTs, it is sometimes not feasible to use CNTs in composite materials.

Graphene nanoplatelets (GnPs) are a carbon based filler and have emerged as one of the most attractive polymer nanofillers. Due to their large aspect ratio, surface area and their relative ease of adding to a host matrix. Moreover GnPs have excellent properties and a significantly lower price compared to CNTs (Kilic, et al., 2018). When good dispersion of the nanoplatelets is achieved, less amounts of nanofillers are required for an efficient enhancement of mechanical properties, thus further reducing the cost of using GnPs.

In recent years, there has been an increase in the application of carbon fibre reinforced composites. Carbon fibre reinforced composites have high strength, high toughness and low weight. Graphene and carbon fibre both contain carbon but the difference between graphene and carbon fibre is that graphene contains only carbon atoms whereas carbon fibre contains carbon atoms along with other atoms such as oxygen and nitrogen. Rezaei (2008) showed that an increase in carbon fibre content in a polymer composite resulted in an increase in strength, stiffness and hardness. Carbon fibre reinforced materials have dominated in the advanced composite materials space and have been used extensively in industries such as automobiles, aerospace and sporting goods among others (Chung & Chung, 2012). Table 2-1 shows the properties of different fibre materials that can be used as nanofill to matrix or reinforcement to composite.

Table 2-1 Properties of different reinforcement and filler materials (Chung & Chung, 2012).

Materials	Density (g/cm ³)	Tensile strength (GPa)	Modulus of Elasticity (GPa)	Ductility (%)	Melting temp (°C)	Specific modulus (10 ⁶ m)	Specific strength (10 ⁴ m)
E-glass	2.55	3.4	72.4	4.7	<1 725	2.90	14
S-glass	2.50	4.5	86.9	5.2	<1 725	3.56	18
Carbon (high-strength)	1.50	5.7	280	2.0	3700	18.8	19
Carbon (high modulus)	1.50	1.9	530	0.36	3700	36.3	13
Graphite whiskers	7.2	8.90	240	3.7	1890	3.40	12

2.2.3 Fibre volume content

The volume content, also known as the volume ratio, is the percentage of the volume of fibre in the composite material (Derek, 1981). For an existing composite, the fibre volume content can be calculated using equation 1. This equation is based on the mixture of densities rule. The known densities of the composite fibre and matrix are used to determine the volume content (Chung, 2017).

$$\rho_c = v_f \rho_f + (1 - v_f) \rho_m \quad (1)$$

Where: ρ_c = density of composite

ρ_f = density of fibre

ρ_m = density of matrix

v_f = volume content of fibre

The amount of volume content in a composite material affects the buckling load of a composite. Battawi (2018) studied the effect of different fibre contents on the buckling load of a composite beam. He discovered that when the volume content is gradually increased, the buckling load initially increases and decreases after a certain point. Battawi (2018) states that the reason for the results being this way is because of the brittle behaviour caused by incremental increases in fibre content. The bar graph representing the results found by Battawi for different slenderness ratios is shown in figure 2-4.

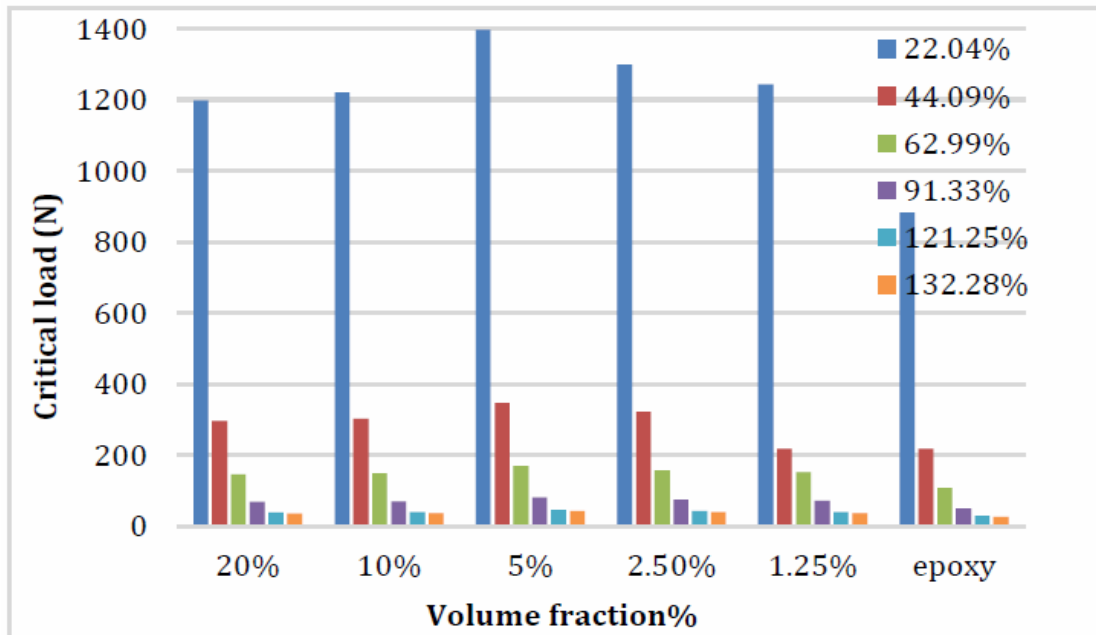


Figure 2-4 Volume fraction vs critical load by Battawi (2008) for different slenderness ratios of beam length.

Chiad (2018) examined the effect of fibre and powder on the buckling load of a composite material. He determined that fibre was a better reinforcement compared to powder reinforcement. Moreover, he determined that as the fibre content of a composite material is increased the buckling load increased as well. Tegaw (2018) found similar results to Chiad. Tegaw (2018) studied the effect of fibre volume fraction, ply orientation and aspect ratio on the buckling behaviour of a laminate. He determined that for a given fibre orientation the buckling load increases with the increase in fibre volume fraction. Battawi's results, as shown in figure 2-4, are different from (Tegaw, 2018) and (Chiad, et al., 2018) results due to the shape of the material being different. Battawi (2018) tested a circular composite beam, whereas Tegaw (2018) and Chiad (2018) tested laminated plates. Therefore, since in this dissertation a nanocomposite laminate will be tested, results similar to those obtained by Tegaw (2018) and Chiad (2018) are expected.

2.2.4 Boundary conditions

Carleton (2016) defines a boundary condition as a place on a structure where there is a known force or displacement at the beginning of an analysis. Boundary conditions are usually expressed in degrees of freedom (DoF). A degree of freedom is defined as a set of independent displacements or rotations that define the position of a mass with respect to its original position. A point in two dimensions (2D) can have up to three DoF. Meaning the point can move

vertically, horizontally or rotate about the out of plane axis. A point in three dimensions (3D) can have up to six DoF, meaning it can move in the X, Y and Z direction; and rotate about the X, Y and Z axis. Figure 2-5 shows all the DoF experienced by a point in 3D.

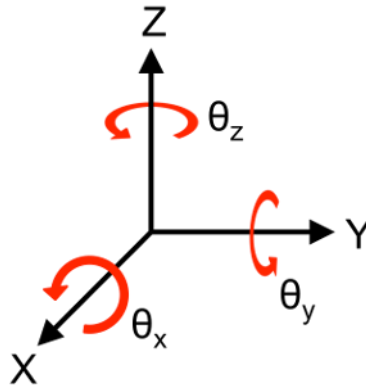


Figure 2-5 Degrees of freedom experienced by a point in 3D (Carleton, 2016).

A restraint that prevents the movement of a structure in one or more degrees of freedom is called a support. There are three common types of supports: a roller support, a pinned support and a fixed support. A roller support allows movement parallel to the roller plane and rotation about a point, thus it has two DoF. A pinned or simply supported support allows movement around a point. Thus, a pinned support has only one DoF. A fixed or clamped support cannot move or rotate in any direction. Thus, a fixed support has no DoF.

The boundary condition of a laminate is an important factor in determining the critical buckling load. Moreover, boundary conditions play a crucial role in determining other factors such as aspect ratio, modulus ratio etc. Suleiman (2019) studied the effects of boundary conditions on buckling load for a laminated composite. The laminate is under biaxial loading. He observed that a clamped boundary condition had a higher critical buckling load compared to a simply supported boundary. Moreover, he observed that the critical buckling load increased with the increase in the number of nodes on the laminate. Suleiman (2019) explains that the reason the buckling load of a laminate with clamped boundary condition is higher than that of a laminate with simply supported boundary conditions is due to the higher rigidity of the clamped boundary condition.

The equation used to calculate the critical buckling load of a column subjected to a longitudinal compressive load is Euler's critical buckling load equation (equation 2). One of the variables in this equation is L, which is the unsupported length of the column. L is dependent on the boundary conditions of a column. Figure 2-6 shows the effective length factors used for columns. As can be seen in figure 2-6 a column with two fixed support has the lowest recommended effective length compared to other types of supports. Thus, this results in the

fixed-fixed column having a higher critical buckling load compare to the pinned-pinned column. Another important point from figure 2-6 is that a cantilever column has the highest recommended effective length, thus a cantilever column will always have the least buckling load compared to other boundary conditions.

$$P_{cr} = \frac{\pi^2 EI}{L^2} \tag{2}$$

Where: P_{cr} = Critical buckling

E = Modulus of Elasticity

I = Moment of Inertia

L = Effective Length Factor


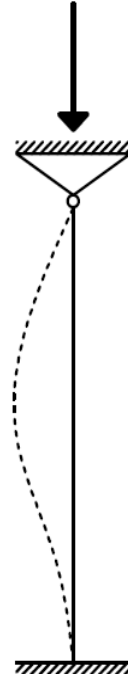
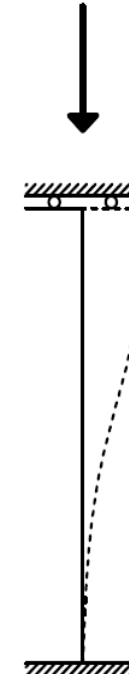
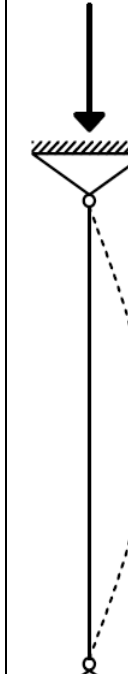

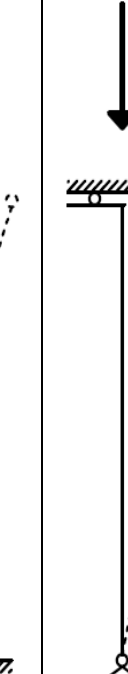
Buckling shape of column						
	Fixed – Fixed Column	Pinned – Fixed Column	Roller – Fixed Column	Pinned – Pinned Column	Cantilever column	Pinned – Roller Column
Theoretical value	0.5	0.7	1.0	1.0	2.0	2.0
Recommended design value	0.6	0.8	1.2	1.0	2.1	2.0

Figure 2-6 Theoretical and recommended effect length factors (Halkyard, 2005).

2.2.5 Layer fibre orientation

The fibre orientation is the direction in which the fibres of a composite are aligned. Fibre orientation is measured in degrees. The reason it is beneficial to arrange the fibres of a composite in one direction is that when fibres are dispersed the effectiveness of the reinforcement material decreases and the optimum strength and stiffness is achieved when the fibres are parallel to the loading (Callister, 2007). Fibre orientations can be optimized for different load cases in order to achieve the best results (Khandan, et al., 2012). However, due to manufacturing difficulties, the fibre orientations usually used are discrete values, which are 0° , 90° , 45° , -45° (Allaire & Delgado, 2016).

Hamani (2013) studied the effect of fibre orientation on the buckling load of a laminate with circular notches. The research focused more on the effect of the size of notches than on the buckling load. However, from the results discovered by Hamani (2013) a theme can be observed. The effect of the fibre orientation on the buckling load is that when the fibre orientation is increased from 0° to 90° the buckling load increases. The minimum buckling load corresponds to an angle of 0° and the maximum buckling load corresponds to an angle of 90° . This applies to all fibre orientation vs buckling load diagrams in this study. Figure 2-7 shows an example of the results obtained by Hamani (2013). Note that in this study, the fibre orientation of 0° is perpendicular to the applied load and the fibre orientation of 90° is parallel in the applied load

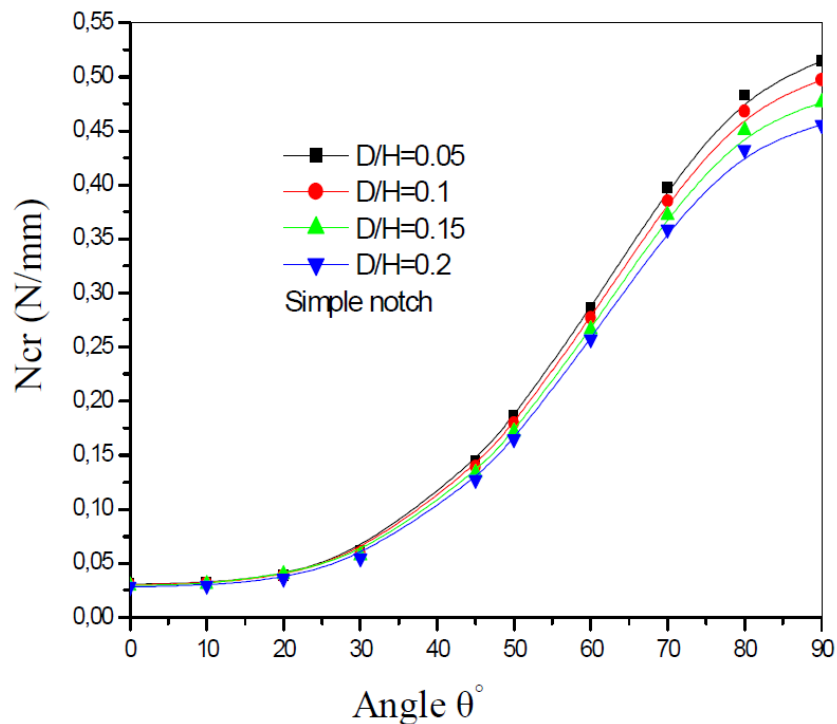


Figure 2-7 Results obtained by Hamani (2013) on fibre angle vs buckling load.

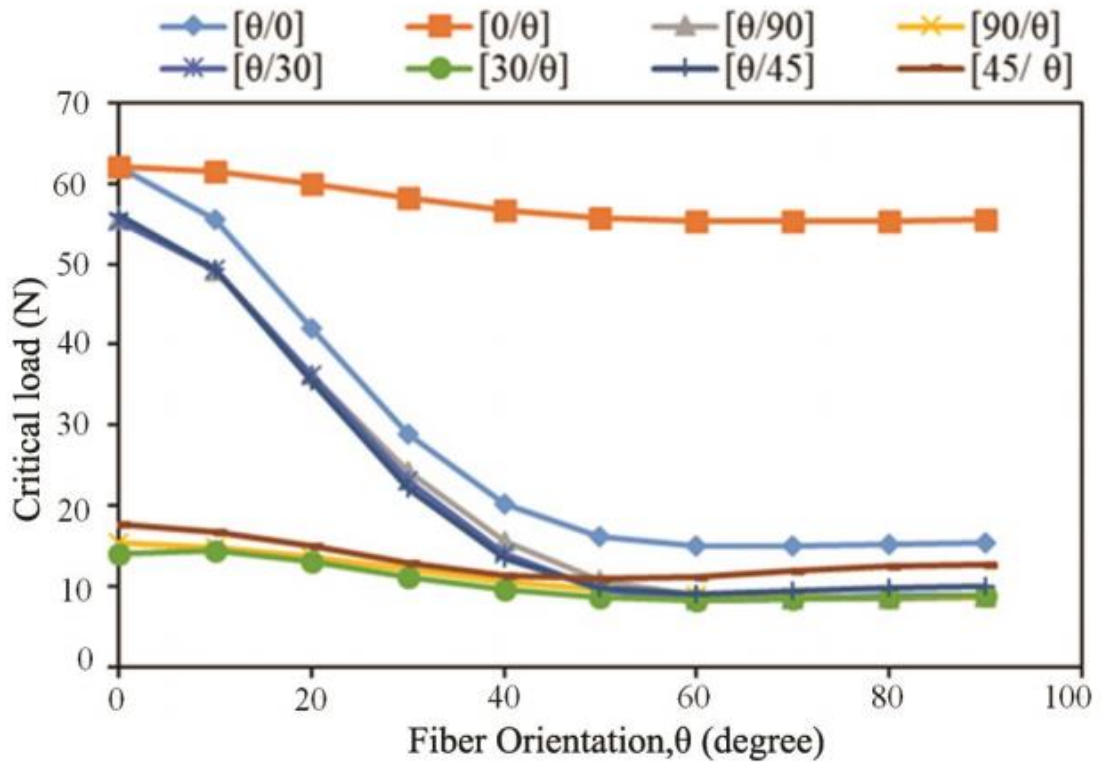


Figure 2-8 Results obtained by Dhuban (2017) on fibre angle vs buckling load.

Dhuban (2017) studied the effects of fibre orientation on the buckling of a simply supported plate subjected to an axial compression load. He determined that the fibre orientation of the middle layers in a three layer laminate has little effect on the critical buckling load. He also determined that the outer layers have a greater effect on the buckling load of the laminate. Figure 2-9 shows the stresses acting on a plate when it experiences bending or buckling. The outer layers experience tension and compression (Mao, et al., 2008). Thus, the stronger the outer layers are, the more resistant to buckling the laminate will be. The shape of the graph obtained by Dhuban (2017) is similar to the one obtained by Hamani (2013), see figure 2-8. However, the difference in the graphs is that as the fibre orientation increases the buckling load increases for Hamani (2013) and the buckling load decreases for Dhuban (2017). Therefore, in the case of this dissertation, the expected result is that the shape of the fibre orientation vs buckling graph will be in a bell curve shape. Moreover, the middle layer of the laminated composite will have little to no effect on the buckling load of the laminate and the optimum fibre orientation will be one where buckling load is parallel to the fibre orientation.

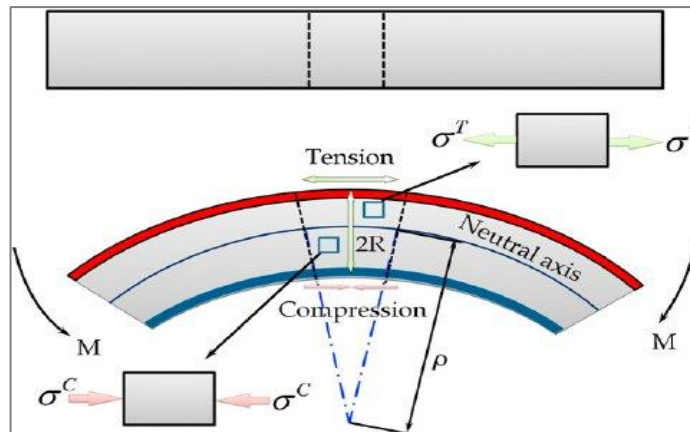


Figure 2-9 Stresses acting on a plate under bending (Mao, et al., 2008).

2.2.6 Aspect ratio

Aspect ratio is the width to the height of a rectangle. Therefore, a square will have an aspect ratio of 1 since the width and height are equal. Changing the aspect ratio of a laminate affects the buckling load of a laminate. Narayana (2013) studied the effects of aspect ratio on the buckling load of a sixteen layered graphene reinforced laminated composite, with rectangular cut-outs, using Finite element analysis (FEA). His results show that the buckling loads decreased as the aspect ratio of the plate increased. Suleiman (2019) also examined the effect of the aspect ratio on the critical buckling load of a thin rectangular laminated composite under biaxial loading. He determined that the buckling load increased with the increase in aspect ratio. When the aspect ratio is changed the cross section of the laminate is changed, and thus the moment of inertia is also changed. The moment of inertia plays a critical role in calculating the critical buckling of a plate, see equation 2. Thus, this is another important factor that decides whether the buckling load increases or decreases.

2.2.7 Composite laminate material stacking sequence

The stacking sequence of a laminate is the order in which the layers of a laminate are ordered. The stacking sequence is based on the fibre orientations of the layers. The different classifications of stacking sequences are symmetric laminates, anti-symmetric laminates, balanced laminates, angle ply laminates, cross ply laminates, specially orthotropic laminates and quasi-isometric laminates (Herakovich, 1998). The laminates examined in this dissertation are cross ply laminates, angle-ply laminates, symmetric ply laminates and anti-symmetric ply laminates.

A symmetric ply laminate is a laminate with plies with equal fibre orientations, thicknesses and materials above and below the midplane of the laminate. Figure 2-10 (a) show a symmetric ply

laminate with layers $[30/45/0]_s$. A anti-symmetric ply laminate is a laminate where the plies have equal material and thickness above and below the midplane, however, the fibre orientations of the layers are opposite to each other above and below the midplane, figure 2-10 (b) shows an anti-symmetric ply laminate with layers $[-90/45/-30/30/-45/90]$. A cross ply laminate is a laminate composed of layers with only alternating 90° and 0° fibre orientations. Figure 2-10 (c) shows a cross ply laminate with layers $[0/90/0/90/0/90]$. An angle ply laminate is a laminate with equal material and thickness but the fibres are orientated at $+\theta$ and $-\theta$. Figure 2-10 (d) shows an example of an angle ply laminates with layers $[45/-45/90/-90/30/-30]$.

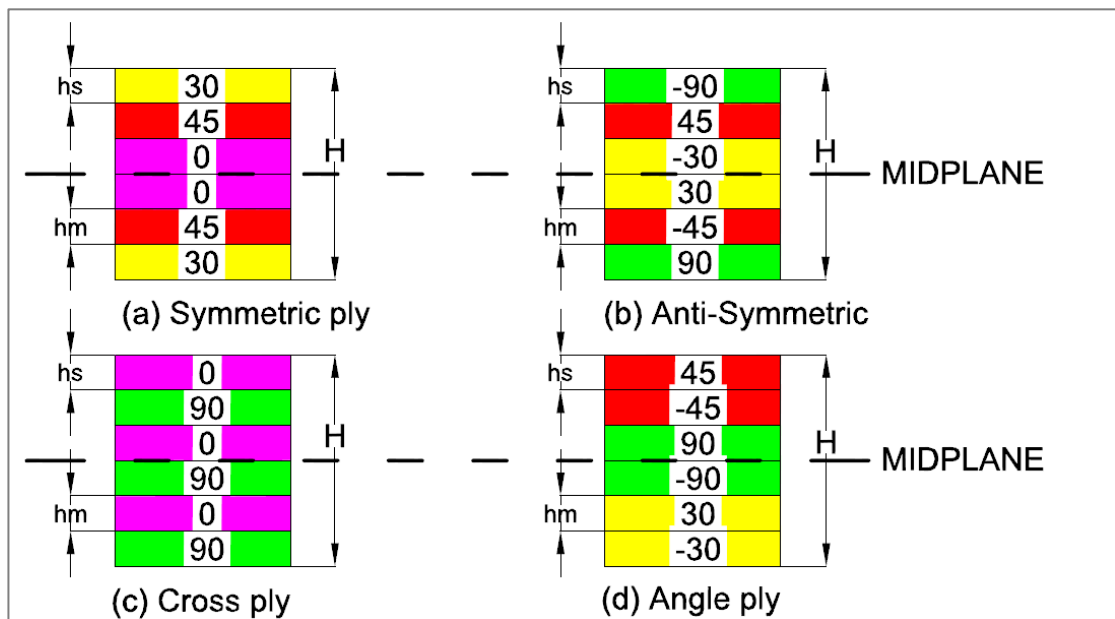


Figure 2-10 Different types of stacking sequences. (a) Symmetric ply laminate, (b) Anti-symmetric laminate, (c) Cross ply laminate and (d) Angle ply laminate.

Heidari-Rarani (2014) studied the buckling behaviour of a thin laminated composite with different stacking sequence. The stacking sequences used are a cross ply laminate and angle ply laminate. The laminate is under a SFSF boundary condition and the plate is uniaxially loaded. The results revealed that under these conditions there is very little difference in the buckling load for different stacking orders. The difference in the results is lower than 3.2% which is statistically insignificant. Dhuban (2017) studied the effect of stacking sequence on the buckling load however the stacking sequences he used are not relevant to this dissertation. Dhuban (2017) did however determine that stacking sequence $[0_2C/0B/\pm 45]_s$ was the best combination of hybrid stacking sequences.

2.2.8 Nanocomposite studies and other findings

Several studies have been conducted on nanocomposite materials. A large amount of studies focusing on polymer nanocomposites reinforced with CNTs or GnPs. Different investigations have employed different equipment and techniques of evaluating the properties of the nanocomposite. Many researchers use physical experiments such as atomic force microscopy and others use simulations to predict the properties of the nanocomposite material.

A larger amount of research has been conducted to see how to achieve the best properties out of a nanocomposite material. Jun (2018) discovered that the thermal stability, tensile strength and tensile modulus of a GnP composite was enhanced by 11.2%, 33% and 59.1% respectively at different temperatures. Moreover, Jun (2018) discovered that nanofillers of large sheets are beneficial when it comes to electrical conductivity and smaller sized nanofillers significantly improved the thermal and mechanical properties of the GnP composite. Mészáros (2014) determined that the presence of graphene in nanocomposites enhanced the elastic recovery of the matrix, thus reducing the plastic deformation of the nanocomposite.

Dai (2014) determined that the Young's modulus of a nanocomposite increases with the increase in aspect ratio, fibre volume content, elastic properties of a graphene/polymer interface layer and decreasing the degree of intercalation. The tensile strength increases with the increase in fibre volume content and decreasing the degree of intercalation. Moreover, Dai (2014) concluded that the fibre orientation of the laminate layers has a significant impact on the strength and Young's modulus on the nanocomposite laminate. When the nanocomposite laminate layers are randomly arranged the Young's modulus and strength is much lower compared to when the layers are aligned. Since Euler's buckling formula is as shown in equation 2. An increase in Young's modulus while all the other variables remain constant, results in an increase in the critical buckling load of the laminate.

Parashar (2012) studied the buckling stability of a graphene/polymer nanocomposite using multiscale modelling techniques. he discovered the buckling strength increased by 26% with only 6% filler volume fraction. Song (2018) determined that the buckling and bending characteristics of the laminate are significantly influenced by the fibre orientation, weight fraction, geometry and size of the graphene nanofillers.

figure 2-9 show the stresses acting on a plate when experiences bending or buckling. the outer layers experience tension and compression (Mao, et al., 2008). Thus the stronger the outer layers are the more resistant to buckling the laminate will be.

2.3 Literature review summary

The literature that has been reviewed in this dissertation shows that the following results should be expected:

- The buckling load of the laminate will increase initially as the fibre volume content is increased and decrease after a certain fibre volume is reached.
- The laminate with all fixed boundary condition (CCCC) will have the highest buckling load compared to other boundary conditions. And the laminate with the cantilever boundary condition (CFFF) will have the lowest buckling load compared to all other boundary conditions.
- The graph of fibre orientation vs non-dimensional buckling load (N_0) will be a bell curve. Therefore, there will be a range where the buckling load is increasing and there will be a range where the buckling load is decreasing. Moreover there will be angles corresponding to the maximum and minimum buckling load.
- As the aspect ratio increases the buckling load will also increase.

For the other parameters that are to be examined in this dissertation no final conclusion of the results to be expected could be discerned from the literature.

CHAPTER 3

MODELS

3.1 Problem formulation

In this chapter the geometry, boundary conditions and loading of the laminate examined in this dissertation are discussed. The laminate is subjected to uniaxial and biaxial loading. The laminate has n number of layers. The layers of the laminate are divided into two groups, surface layers and middle layer(s). The surface layers have a thickness of h_s , and since there are two surface layers, each layer has a thickness of $h_s/2$. The middle layers have a thickness of h_m . In cases where there are multiple middle layers, the thickness of the middle layers is h_m/n_m , where n_m is the number of middle layers. The fibre orientations of the laminates are denoted by θ_s and θ_m , where θ_s and θ_m denote the fibre orientation of the surface and middle layers respectively. The thickness ratio, denoted by α , is the thickness of the surface layers (h_s) divided by the total thickness of the laminate (H). Thickness ratio is determined by equation 3. The aspect ratio is the width to the height of the laminate and is calculated using equation 4. Figure 3-1 shows the general layout of the laminate.

$$\alpha = \frac{h_s}{H} \quad (3)$$

$$\text{aspect ratio} = \frac{\text{Width}}{\text{height}} = \frac{a}{b} \quad (4)$$

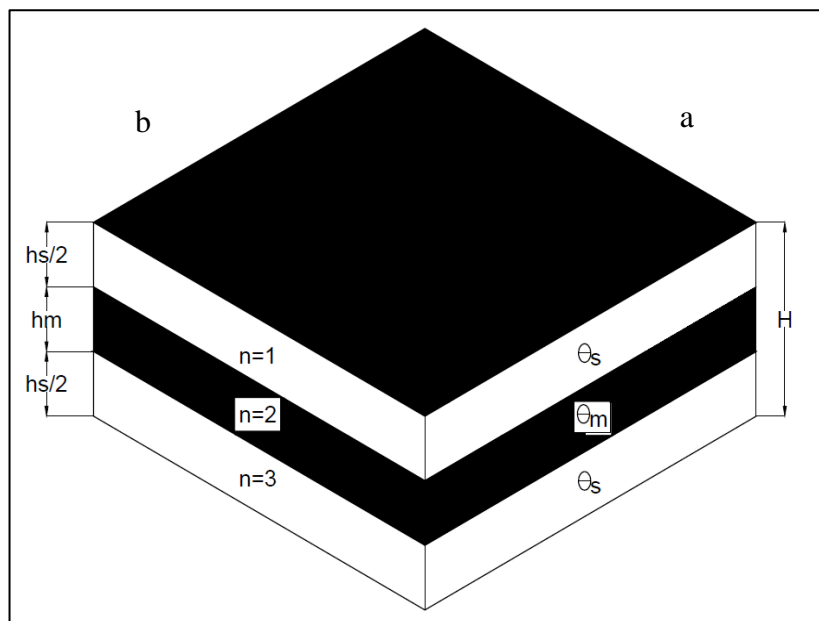


Figure 3-1 A 3 layer composite laminate, used in multiples analysis in this paper.

3.2 Micromechanical modelling

The effective mechanical properties of a unidirectional composite material are fundamental to the analysis and design of a fibre composite structure. Physical experiments can be used to determine these properties. However, physical experiments can be very costly and the materials required for the experiment may not be readily available. Micromechanical equations are used to overcome this problem. Micromechanical equations are used for predicting the properties of a composite material by using the properties of the constituent materials (fibre and matrix). Chamis (1983) studies further micromechanical equations used to determine different properties of a composite such as geometric properties, mechanical properties, thermal properties and hygral properties. In this dissertation, micromechanical equations are initially used to determine the properties of the polymer matrix nanofilled with GnPs. The micromechanical equations are then used to determine the properties of the GFRNL. See appendix A for the properties of GFRNL when different properties are used.

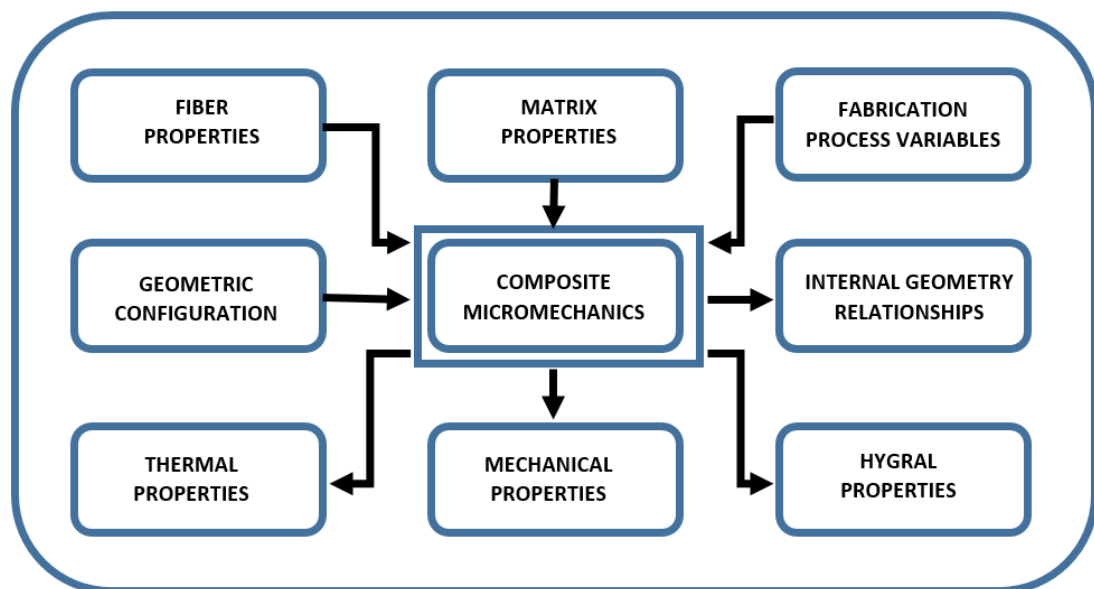


Figure 3-2 Schematic diagram of how composite micromechanical equations get the different results. The diagram shows the inputs and outputs of the micromechanical equations (Chamis, 1983).

Figure 3-2 is a schematic diagram showing how the different properties of a composite material are determined using micromechanical equations. The inputs consist of the properties of the matrix and fibre material, the geometric configuration of the composite and the fabrication process variables. There are various outputs that can be obtained from the micromechanical equations, as can be seen in figure 3-2. The properties relevant to this dissertation are mechanical properties.

The material being studied in this dissertation is a laminated composite made up of nanocomposite plies. The nanocomposite plies are made up of a graphene reinforced polymer matrix and reinforced with carbon or glass fibres. Thus, two sets of micromechanical equations are used. One set of micromechanical equations is used to determine the properties of the graphene reinforced polymer matrix and the other set of micromechanical equations is used to determine the properties of the graphene and fibre reinforced composite. The fibre and matrix material properties used in this dissertation as the input data for the micromechanical equations are shown in table 3-1. The geometric configuration of the laminate is discussed in chapter 3.1.

Table 3-1 Properties of graphene nanoplatelets nanofill, polymer matrix, carbon fibre and glass fibre. These properties were obtained from (Radebe, et al., 2019).

	Graphene Reinforced Polymer Matrix		Carbon Fibre	Glass Fibre
	Graphene Nanoplatelets	Polymer Matrix		
Young's modulus (Pa)	1,010 x 10 ¹²	3,5 x 10 ⁹	E ₁₁ = 263 x 10 ⁹	E ₁₁ = 72.4 x 10 ⁹
			E ₂₂ = 19 x 10 ⁹	E ₁₁ = 72.4 x 10 ⁹
Density (Kg/m ³)	1060	1200	1550	2.55x10 ⁻⁶
Poissons ratio	0,186	0.35	0.2	0.2
Shear modulus (Pa)	425.8 x 10 ⁹	1.30 x 10 ⁹	27.6 x 10 ⁹	30.17 x 10 ⁹

3.2.1 Graphene reinforced polymer matrix

In this section, the effective values for Young's modulus, Poisson's ratio and shear modulus of a polymer matrix reinforced with GnPs nanofill is determined. In the following equations the subscripts GPL, GM and M denote graphene nanoplatelets, graphene reinforced matrix and unreinforced matrix respectively.

$$E_{GM} = \left(\frac{3}{8} \frac{1 + \xi_L \eta_L V_{GPL}}{1 - \eta_L V_{GPL}} + \frac{5}{8} \frac{1 + \xi_W \eta_W V_{GPL}}{1 - \eta_W V_{GPL}} \right) x E_M \quad (5)$$

Where: V_{GPL} is the volume content of the graphene nanoplatelets

ξ_L and ξ_W are calculated using equations 6 and 7

η_L and η_W and are calculated using equations 8 and 9

$$\xi_L = 2 \frac{l_{GPL}}{h_{GPL}} \quad (6)$$

$$\xi_w = 2 \frac{w_{GPL}}{h_{GPL}} \quad (7)$$

Where: l_{GPL} is the length of the graphene nanoplatelet

h_{GPL} is the thickness of the graphene nanoplatelet

w_{GPL} is the width of the graphene nanoplatelet

$$\eta_L = \frac{\left(\frac{E_{GPL}}{E_M}\right) - 1}{\left(\frac{E_{GPL}}{E_M}\right) + \xi_l} \quad (8)$$

$$\eta_w = \frac{\left(\frac{E_{GPL}}{E_M}\right) - 1}{\left(\frac{E_{GPL}}{E_M}\right) + \xi_w} \quad (9)$$

The following equation is used to determine volume fraction of graphene nanoplatelets.

$$V_{GPL} = \frac{W_{GPL}}{W_{GPL} + \left(\frac{\rho_{GPL}}{\rho_M}\right)(1 - W_{GPL})} \quad (10)$$

Where: W_{GPL} is the weight fraction of graphene nanoplatelets

ρ_{GPL} is the mass density of the nanocomposites

ρ_M is the mass density of the polymer matrix

The Poisson's ratio and shear modulus are calculated using the following equations

$$\nu_{GM} = \nu_{GPL}V_{GPL} + \nu_M(1 - V_{GPL}) \quad (11)$$

$$G_{GM} = \frac{E_{GM}}{2(1 + \nu_{GM})} \quad (12)$$

Where: ν_{GPL} is the Poisson's ratio of the graphene nanoplatelet

ν_M is the Poisson's ratio of the matrix

3.2.2 Graphene and Fibre Reinforced Nanocomposite laminate

In this section, the effective values for Young's modulus, Poisson's ratio and shear modulus of the GFRNL are determined. In the following equations the subscript F denote graphene fibre reinforcement.

$$E_{11} = E_{F11}V_F + E_{GM}(1 - V_F) \quad (13)$$

$$E_{22} = E_{GM} \left(\frac{E_{F22} + E_{GM} + (E_{F22} - E_{GM})V_F}{E_{F22} + E_{GM} - (E_{F22} - E_{GM})V_F} \right) \quad (14)$$

$$G_{12} = G_{GM} \left(\frac{G_{F12} + G_{GM} + (G_{F12} - G_{GM})V_F}{G_{F12} + G_{GM} - (G_{F12} - G_{GM})V_F} \right) \quad (15)$$

$$v_{12} = v_{F12}V_F + v_{GM}(1 - V_F) \quad (16)$$

The properties obtained using the micromechanical equations above will be the input data for the composite material on ANSYS.

3.3 ANSYS modelling

The composite laminate will be evaluated using ANSYS ACP (pre), Static structural and eigenvalue buckling analysis. To demonstrate how ANSYS is used to evaluate the laminate, a three plate laminate is analysed and each step is shown. The full project schematic used in the analysis of the laminate is shown in Figure 3-3 (a). As can be seen in figure 3-3 (b-e), the ANSYS programme has a component system (engineering data) and three analysis systems, ACP (Pre), static structural and eigenvalue buckling. These analysis systems share data. The engineering data is connected to the ACP (Pre) analysis system. The setup data in the ACP (Pre) is used in the static structural model. Static structural and eigenvalue buckling share a model and the solution. These analysis systems will be discussed further in this chapter.

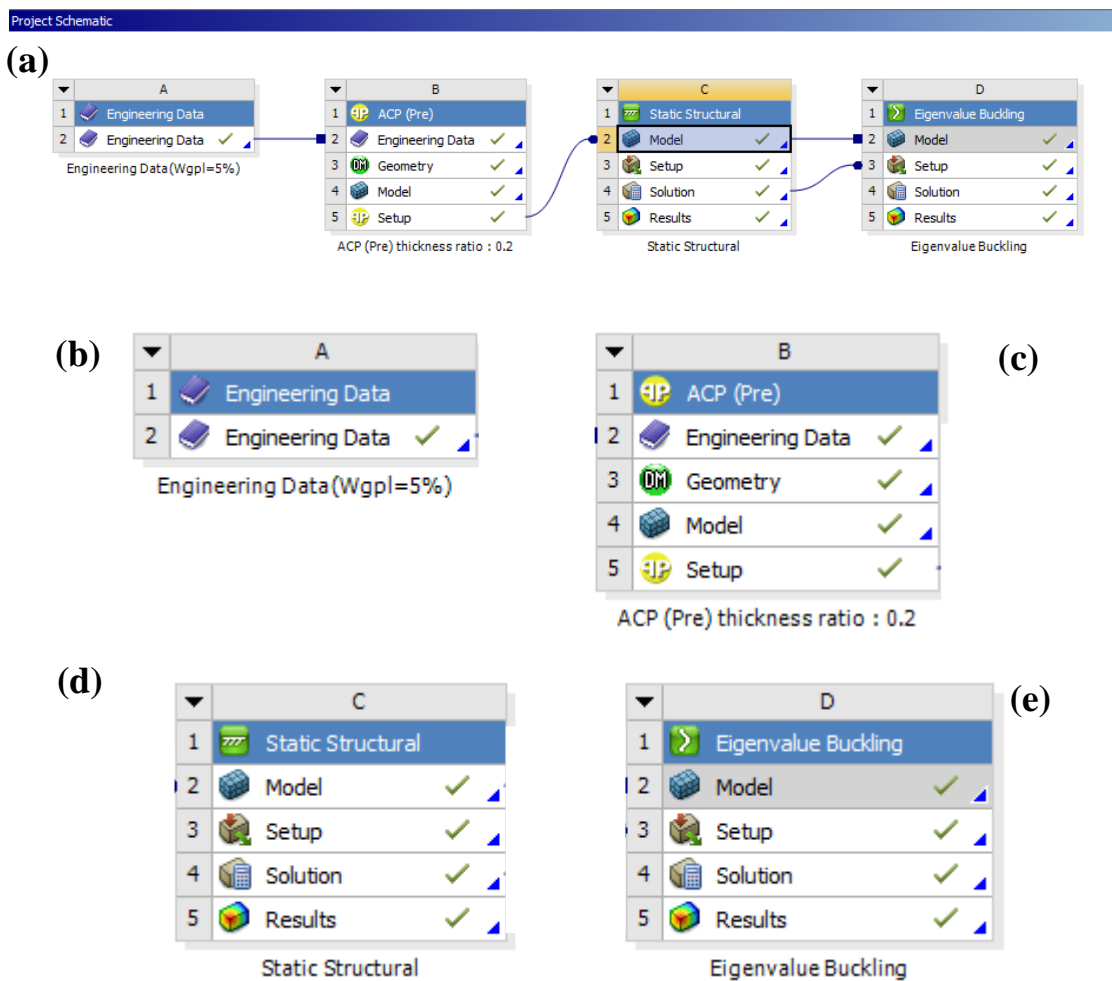


Figure 3-3 Project schematic in ANSYS used to analyse a laminate nanocomposite material and an enlarged image of the different analysis systems, (b) engineering data, (c) ACP (Pre), (d) Static structural and (e) Eigenvalue buckling.

3.3.1 Engineering data

Engineering data is entered separately in a component system. This is because there are multiple data points. Two new materials are created $GFRNL_{(MIDDLE\ LAYER)}$ and $GFRNL_{(SURFACE\ LAYER)}$, where GFRNL denotes Graphene and Fibre Reinforced Nanocomposite Laminate. The Orthotropic elasticity data for $GFRNL_{(MIDDLE\ LAYER)}$ and $GFRNL_{(SURFACE\ LAYER)}$ entered in this section was determined using micromechanical equations, the properties for the carbon fibre reinforced laminate (CFRL) and glass fibre reinforced laminate (GFRL) have been determined using micromechanical equations. In this example, the properties of CFRL are used. Young's Modulus in the X direction was determined using equation 13. Young's Modulus in the Y direction was determined using equation 14. The effects of the Young's modulus in the Z direction are negligible, therefore it was assumed to be 1000 Pa. The material Poisson's ratio is determined using equation 16. The shear Modulus is determined using equation 15 and is assumed to be equal in all directions. See figure 3-4.

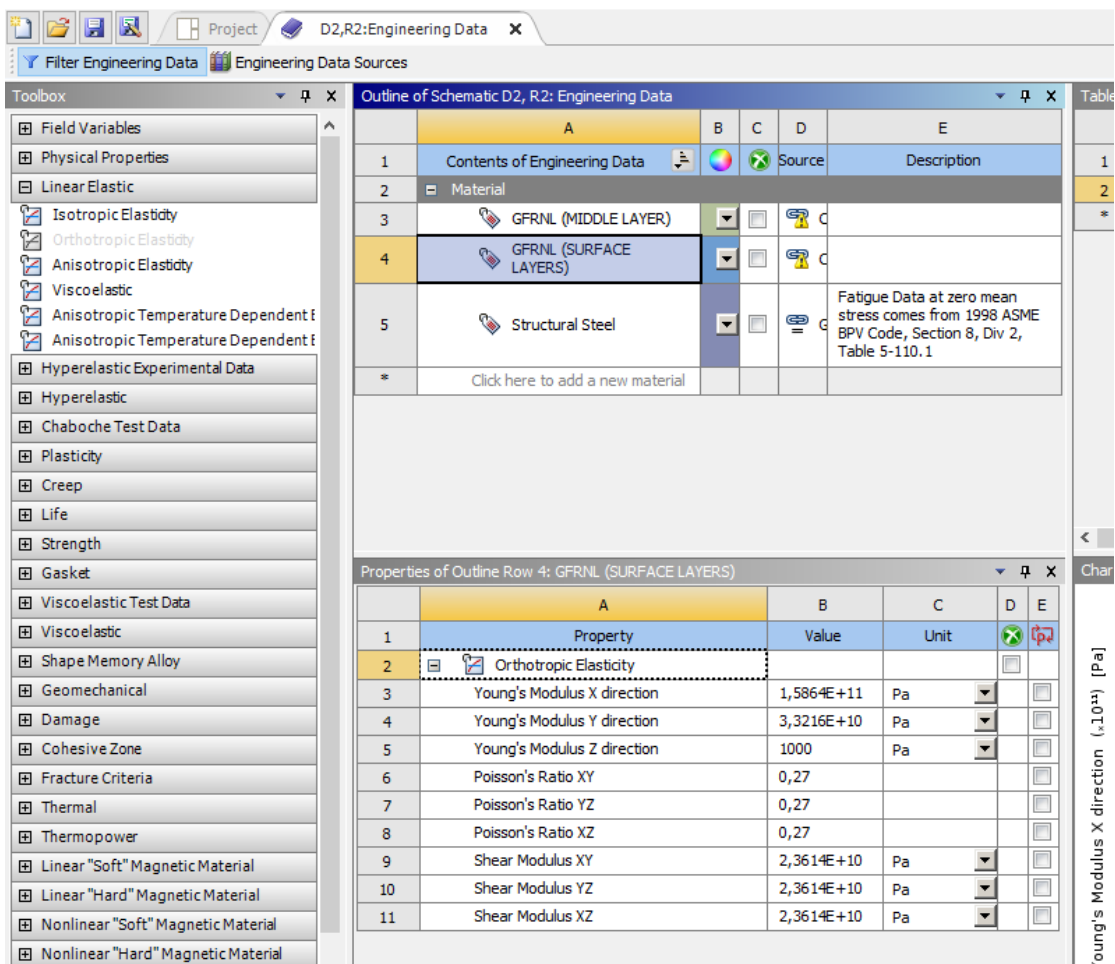


Figure 3-4 New materials created on ANSYS and the data entered for a surface layer with $W_{GPL} = 0.05$ and $V_F = 0.5$.

3.3.2 ACP (pre)

The different elements of ACP Pre analysis system are discussed in this section. Refer to figure 3-3 (c).

3.3.2.1 Engineering data

The engineering data is transferred from the engineering data component system already mentioned in chapter 3.3.1. As can be see figure 3-3 (a), there is a connection in the engineering data labelled Engineering data ($W_{GPL}=5\%$) and the engineering data in ACP (pre)

3.3.2.2 Geometry

Using design modeller, a 2d diagram of a 1m x 1m plate is drawn. At this point the plate has no thickness (figure 3-5).

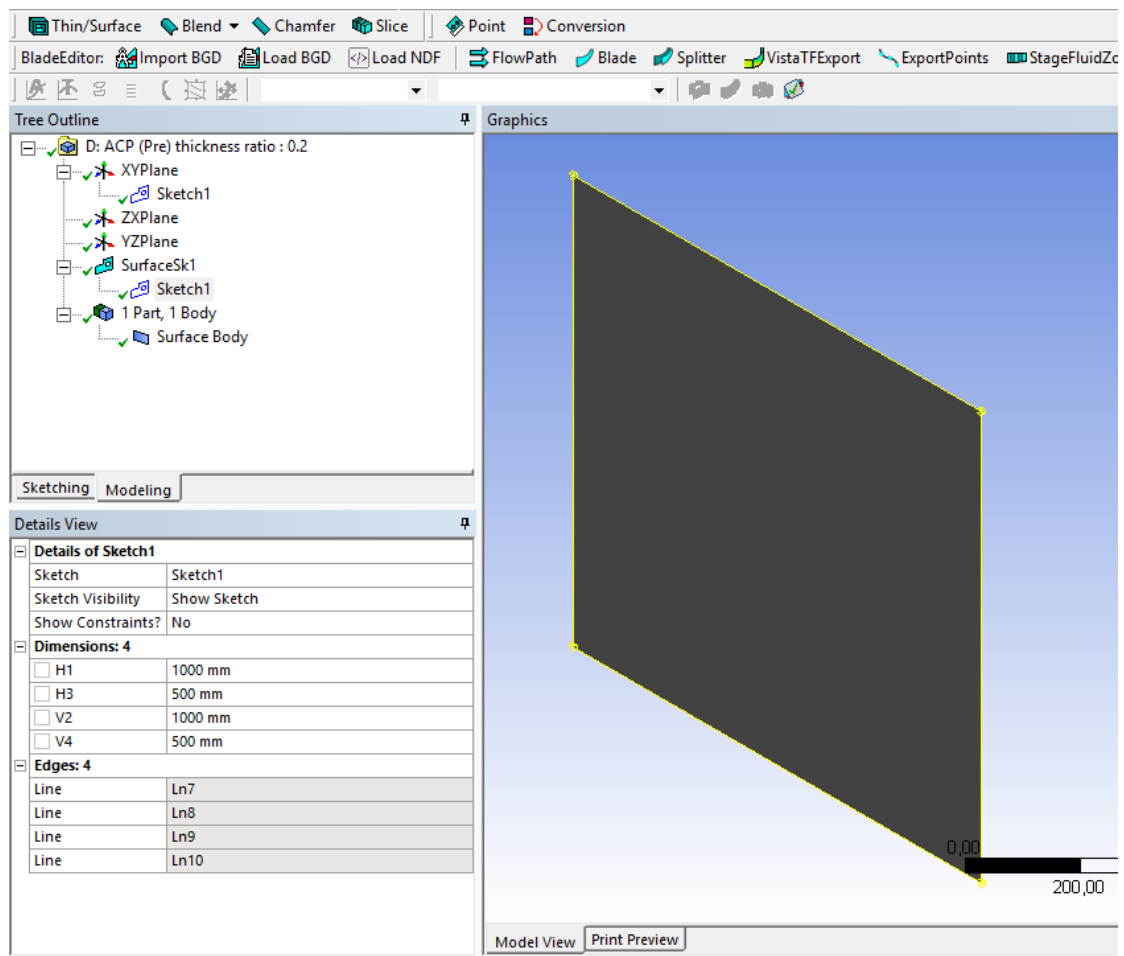


Figure 3-5 A 2d diagram of the plate created using design modeller. The dimensions of the plate is 1m x 1m.

3.3.2.3 Model

The model section is used to produce a mesh on the geometry. The size of the mesh generated in this example is 18mm (figure 3-6).

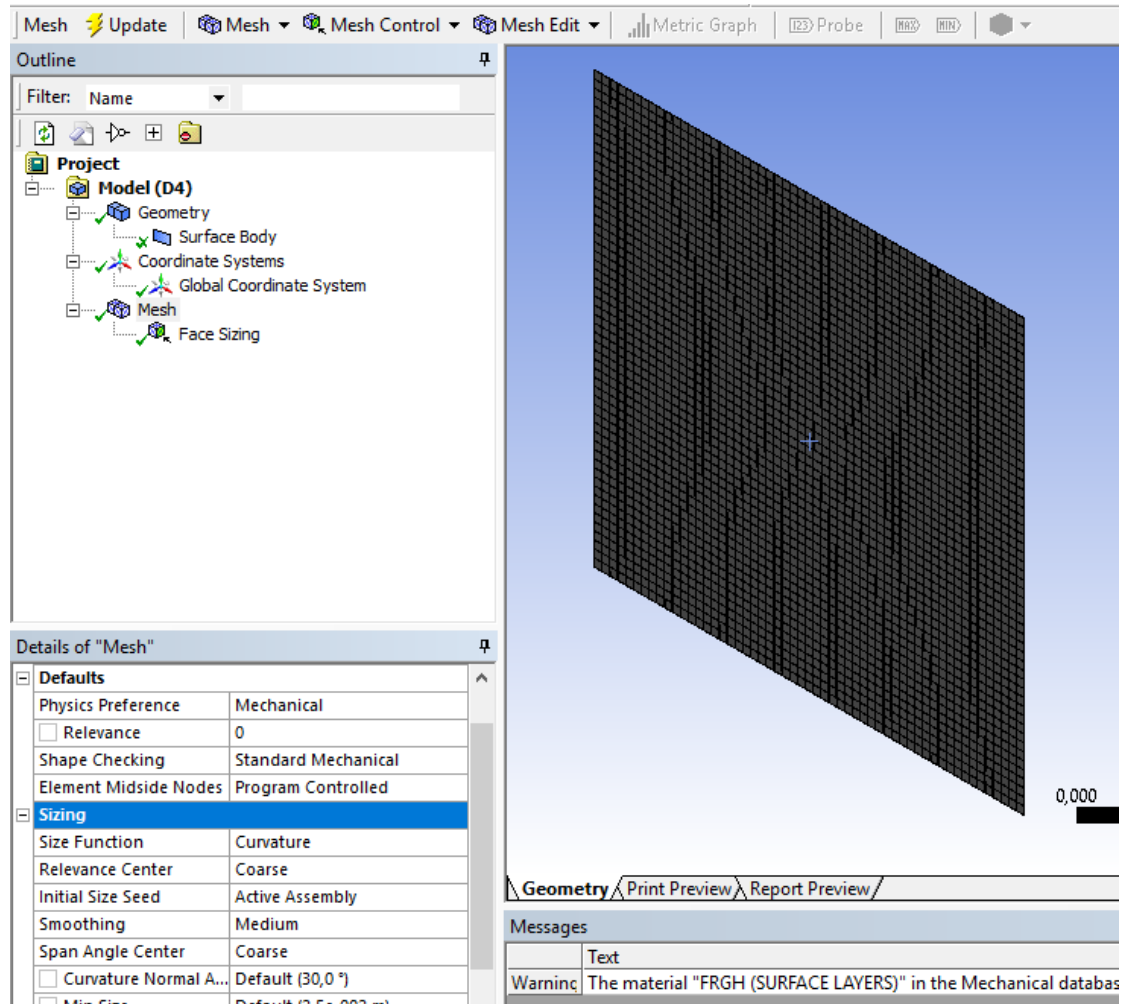


Figure 3-6 The generated mesh on the plate generated on the geometry section

3.3.2.4 ACP (Pre) setup

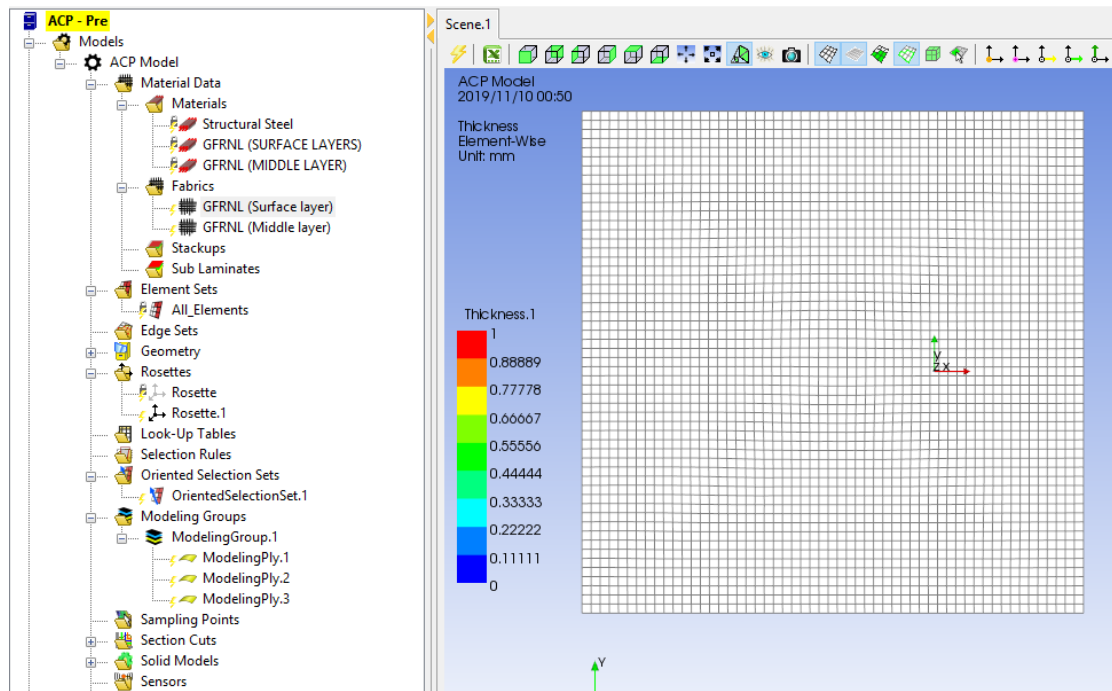


Figure 3-7 ACP (Pre) setup program

The ACP (Pre) setup program is shown in figure 3-7. The steps used to create the composite material are listed below:

- Two fabrics are created: GFRNL (Surface Layers) and GFRNL (middle Layer). When creating a fabric, the thickness of the layer is added. If the layer thicknesses are not equal, the thickness of the surface and middle layers depends on the thickness ratio.
- Create element set and select all elements.
- Create a rosette. A rosette is the reference angle at which all angles will be measured from.
- Create an orientated selection set or use the default one.
- Create a modelling group.
 - Under modelling group, create any number of laminate layers required and add the fibre orientations to the layers. The fibre orientation is dependent on the selected angle orientation and stacking sequence of the plies
- Create a solid model. Figure 3-8 shows the solid model created for a 3 layer laminate with a thickness ratio of 0.2 and all fibre orientations 45°.

Once the steps mentioned above are done, a composite material is completely constructed. The next step is to analyse the material. See figure 3-8, showing the completed composite laminate with 3 layers with properties $V_F=0.5$, $W_{GPL}=0.05$, $\theta_s=45^\circ$, $\theta_m=45^\circ$, $h_s/2=0.15\text{mm}$ and $h_m=1.2\text{mm}$.

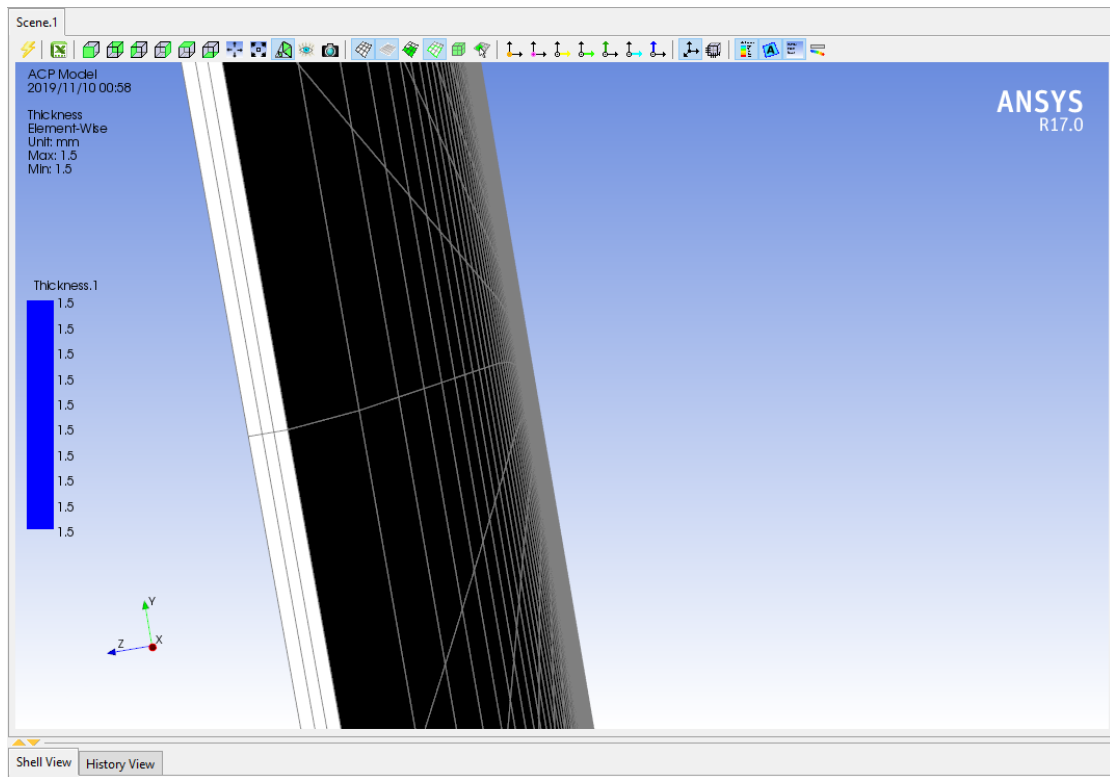


Figure 3-8 The completed composite material made using ACP (Pre). The laminate is a 3 layer laminate with a thickness ratio of 0.7 and all fibre orientations 45° .

3.3.3 Static structural and eigenvalue buckling

3.3.3.1 Model and Setup

The static structural model uses data from the ACP (Pre) setup. The Eigenvalue buckling model uses the same data as the static structural model. Figure 3-3 (a) shows that there is a line connecting ACP (Pre) setup with static structural Model and there is another line connecting the static structural model with the eigenvalue buckling model.

In the setup section the load and boundary conditions are added to the laminate. In this case a 1 Pa uniaxial uniformly distributed load (UDL)/stress is applied and CFFF boundary conditions are present. The types of results that one wants to obtain are stated at this point. The desired result for this example is a total deformation under eigenvalue buckling. Figure 3-9 shows the setup of the laminate.

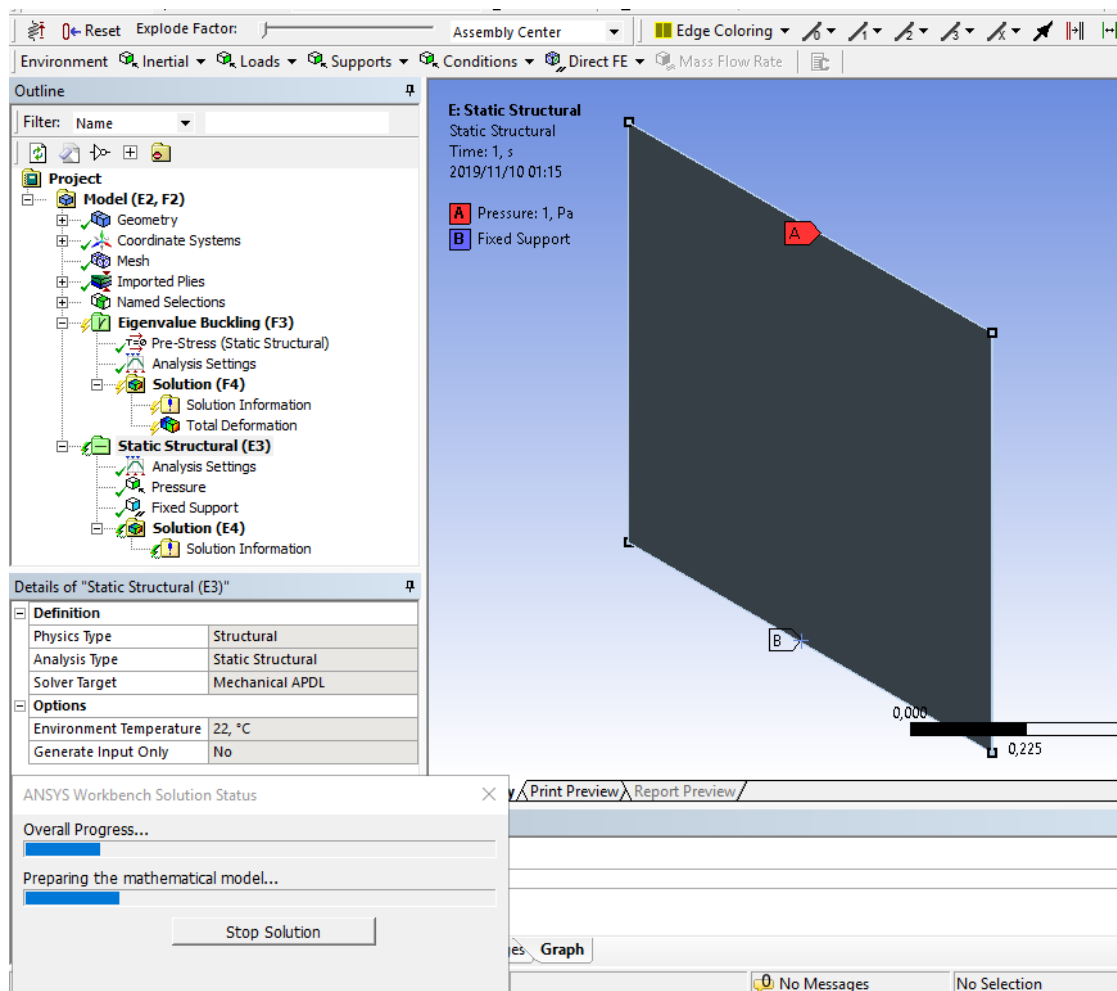


Figure 3-9 The analysis setup page for a composite plate. Showing the added UDL of 1Pa and a fixed support and that the required results are a total deformation of the plate under eigenvalue buckling.

3.3.3.2 Solution and Results

The next step after setting up the laminate is to click the solve button and ANSYS does all the calculations. The result that is achieved on ANSYS is a load multiplier. The buckling stress of the laminate is found by multiplying the stress/pressure used on the laminate with the load multiplier, as shown in equation 17. Since the stress used on the laminate is 1 Pa, the buckling stress is equal to the load multiplier. Thus, the resulting buckling pressure is in Pa. for this dissertation, a non-dimensional stress is used. To convert the stress from dimensional to non-dimensional equation 18 is used. Figure 3-10 shows the results on ANSYS.

$$N_x = L * \text{Load multiplier} \quad (17)$$

Where: N_x = Dimensional buckling stress

L = Stress

$$N_0 = \frac{b}{E_0 * H^3} N_x \quad (18)$$

Where: N_0 = Non-dimensional stress

E_0 = 1 GPa

H = Full thickness of the plate

b = height of plate

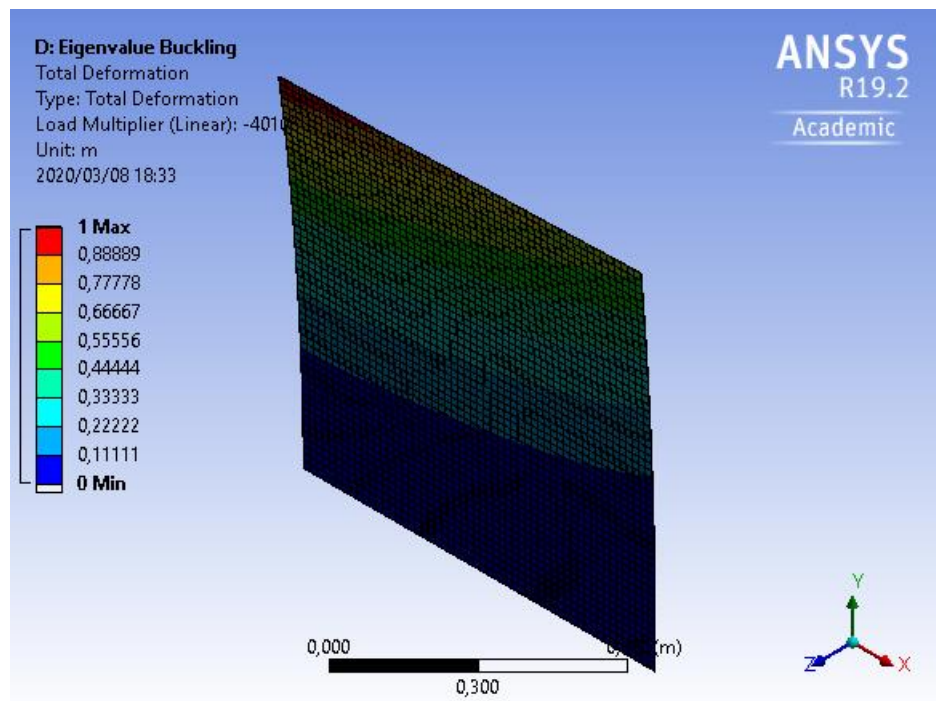


Figure 3-10 The final results of the plate. Since the load multiplier in this case is 40109 that means the dimensional buckling stress is also 40109. To find the non-dimensional buckling stress equation 15 is used

CHAPTER 4

RESULTS AND DISCUSSION

4.1. Effect of Boundary conditions on buckling stress

4.1.1 Results

The effect of different boundary conditions on a 3 ply GFRNL are discussed in this section. The laminate layer properties are $V_F=0.1$, $W_{GPL}=0.01$, $\theta_s = \theta_m=45^\circ$, $h_s/2=0.15\text{mm}$ and $h_m=1.2\text{mm}$, layer properties are shown in figure 4-2. The laminate is loading both uniaxially and biaxially. The boundary conditions used in the analysis are shown in figure 4-1. C stands for a clamped/fixed boundary, F stand for a free boundary and S stands for a simply supported/pinned boundary.

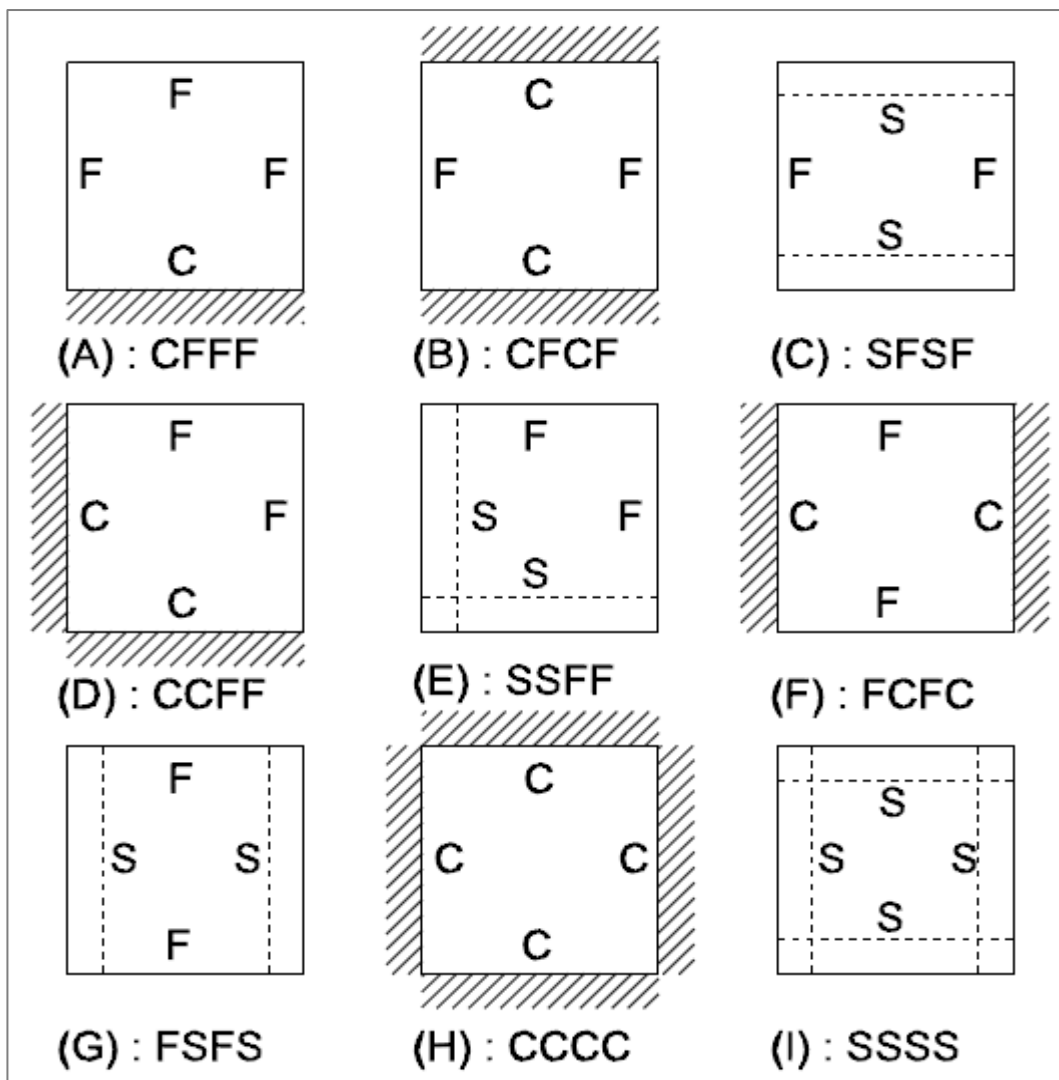


Figure 4-1 Laminates boundary conditions

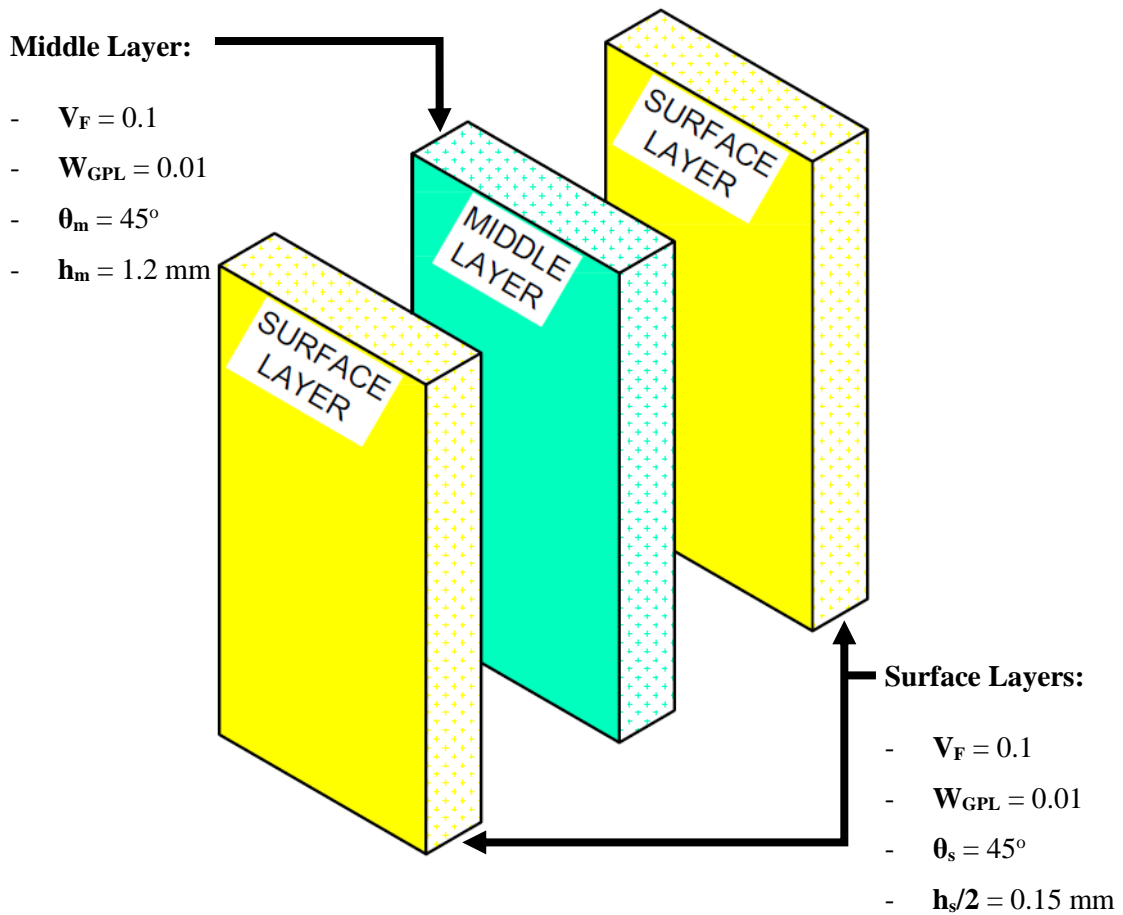


Figure 4-2 Layer properties of Laminated nanocomposite in the boundary condition tests

Figure 4-3 and 4-4 show the buckling stress of a GFRNL when loaded uniaxially and biaxially under different boundary conditions. Figure 4-3 shows results for a CFRL and figure 4-4 shows results for a GFRL. The results from the figures show that the boundary condition CFFF has the least buckling resistance and CCCC has the greatest buckling resistance. There are pairs of boundary conditions that are similar but differ in that they have a clamped or a simply supported boundary. Examples of these pairs are CFCF and SFSF (figure 4-1 b and c), where they are supported at the same edges but have different kinds of supports. These pairs are represented on figures 4-3 and 4-4 by red lines. For all these pairs, the boundary condition with the fixed support always has the higher buckling stress. CFCF has a greater buckling stress than SFSF and CCFF has a greater buckling stress than SSFF. The difference in buckling for a uniaxial and biaxial load is small. However, when the laminate is biaxially loaded it experiences a lower buckling stress compared to when it is uniaxially loaded. The difference in CFRL and GFRL is small; however, CFRL experiences a larger buckling stress.

4.1.1.1 Effect of boundary conditions on carbon fibre reinforced laminate

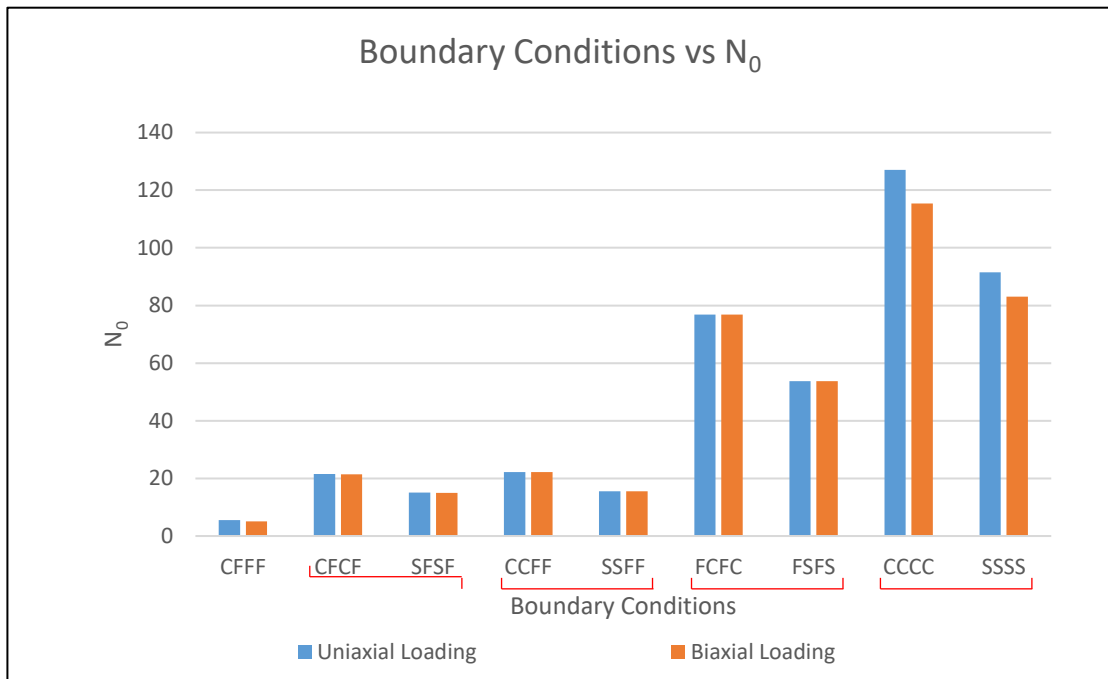


Figure 4-3 The effects of different boundary conditions on the buckling stress for CFRL under uniaxial and biaxial loading.

4.1.1.2 Effect of boundary conditions on glass fibre reinforced laminate

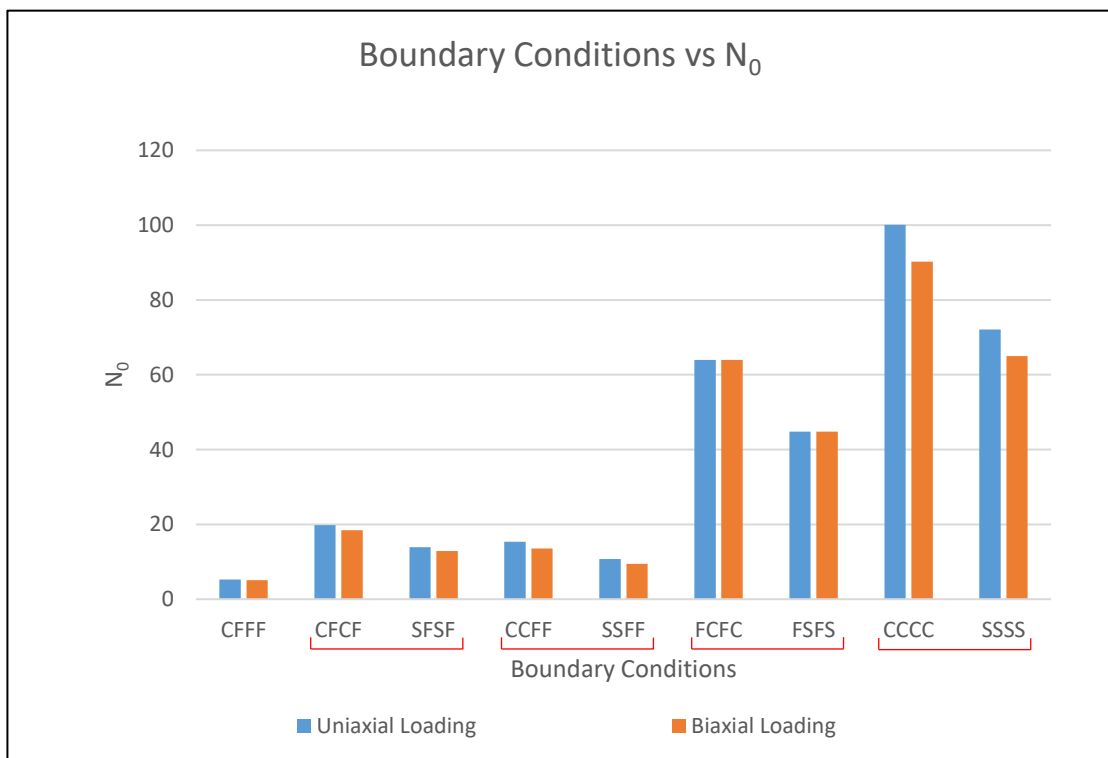


Figure 4-4 The effects of different boundary conditions on the buckling stress for GFRL under uniaxial and biaxial loading.

4.1.2 Discussion of Results

The order of boundary conditions from the one that produces the largest buckling stress to the one that produces the smallest buckling stress for both uniaxial and biaxial loading is: CCCC, SSSS, FCFC, FSFS, CFCF, CCFF, SFSF, SSFF and CFFF. The results show that CCCC has the highest buckling stress and CFFF has the least critical buckling stress. The boundary condition with the second least buckling stress is SSFF. This shows that the boundary conditions with clamped supports have larger critical buckling stress compared to the boundary conditions with simply supported boundary conditions.

The results obtained on the effects of boundary conditions were in accordance to what was expected. The effective length of a clamped plate is lower to the effective length of a simple supported plate (figure 2-6). Thus, it is expected that a laminate with a clamped boundary will experience a higher critical buckling stress. Moreover, a clamped boundary has less degrees of freedom compared to a simply supported boundary, causing the clamped support to be more rigid. Suleiman (2019) mentioned that due to their rigidity, clamped boundary conditions have a higher critical buckling stress compared to simply supported and cantilever boundary conditions. The results obtained in this section are in accordance to the results obtained by Suleiman (2019).

The effect of the biaxial load is very small compared to the uniaxial load, which is unexpected, considering that an additional load is added to the laminate. There are other factors that could cause the influence of a biaxial load to be low, like fibre orientation and magnitude of load. Moreover the additional load may cause other forms of failure, such as shear. The buckling obtained in CFRL are higher than the ones obtained for GFRL. This is expected, since carbon fibre has a higher Young's modulus compared to glass fibre. The Young's modulus is an important factor in the determination of the critical buckling stress.

4.2. Effect of Fibre Orientation on Buckling Stress

4.2.1 Results

The effect of fibre orientation on a three layer GFRNL are discussed in this section. It has been established in the previous chapter that the CFFF boundary condition has the least buckling stress. Thus, all analysis from here on will use this boundary condition since it will produce the worst-case scenario buckling stress. The GFRNL tested in this section is loaded uniaxially and biaxially. The surface layer properties are $V_F=0.5$, $W_{GPL}=0.05$ and $h_s/2=0.15$ mm and the middle layer properties are $V_F=0.1$, $W_{GPL}=0.01$ and $h_m=1.2$ mm.

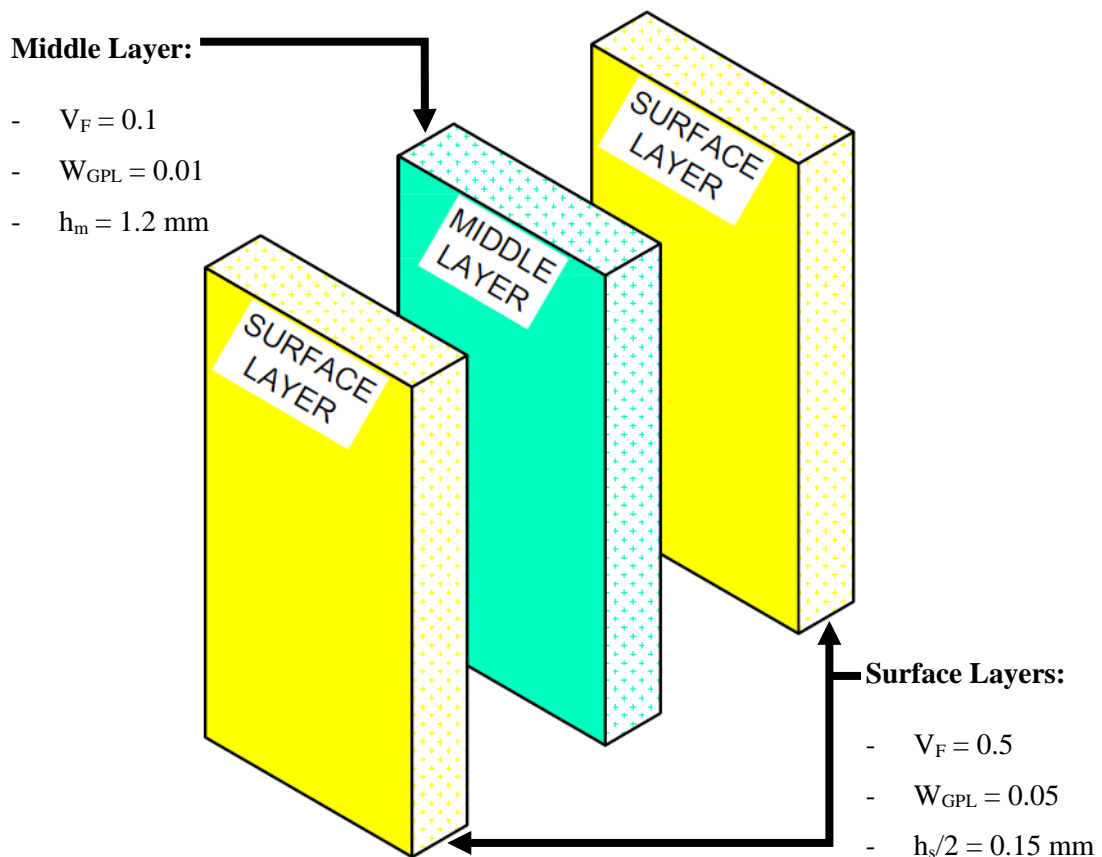


Figure 4-5 layer properties of Laminated nanocomposite in the effect of fibre orientation on buckling stress tests

The effect of changing the fibre orientation of the surface layers while keeping the middle layer constant when the laminate is loaded uniaxially is examined in figures 4-6 and 4-7. Figure 4-6 shows the results for a CFRL and figure 4-7 shows the results for a GFRL. The graph is a bell curve. In figure 4-6 when $\theta_s=0^\circ$ the buckling stress is at a minimum, whereas when $\theta_s=90^\circ$ the buckling stress is at a maximum. In figure 4-7, the graph for GFRL, the buckling stress initially dips slightly before increasing, thus $\theta_s=22^\circ$ corresponds to the minimum buckling stress and

similar to CFRL the maximum stress corresponds to $\theta_s=90^\circ$. The buckling stress for GFRL is greater than the buckling stress for CFRL when $\theta_s < 53^\circ$, this area is highlighted green. Beyond $\theta_s=53^\circ$, the buckling stress for CFRL is greater than GFRL. Significantly higher buckling stresses can be achieved for CFRL compared to GFRL. The maximum buckling stresses for CFRL and GFRL are 51 and 20,60 respectively. All the graphs in figure 4-6 are superimposed over one another. Therefore the middle layer fibre orientation has little effect on the buckling stress of the laminate. A similar result can be seen in figure 4-7. the graphs are very close to each other, therefore, the same conclusion can be made as in figure 4-6. The middle layer fibre orientation has little effect on the buckling stress of the laminate.

Figure 4-8 and 4-9 show the buckling stress of a GFRNL when loaded biaxially. Figure 4-8 shows results for a CFRL and figure 4-9 shows results for a GFRL. When the laminate is biaxially loaded the fibre orientations corresponding to the minimum and maximum buckling stresses change. For CFRL the maximum buckling stress has moved from $\theta_s=90^\circ$ to $\theta_s=105^\circ$ and for GFRL the maximum buckling stress has moved from $\theta_s=90^\circ$ to $\theta_s=100^\circ$. Figure 4-10 is a bar graph showing the effect of θ_m when the laminate has different thickness ratios. It can be seen in the figure that as the thickness ratio increases the effect of the middle layer on the buckling resistance of the laminate decreases.

4.2.1.1 Effect of fibre orientation on uniaxially loaded carbon and glass fibre reinforced nanocomposite

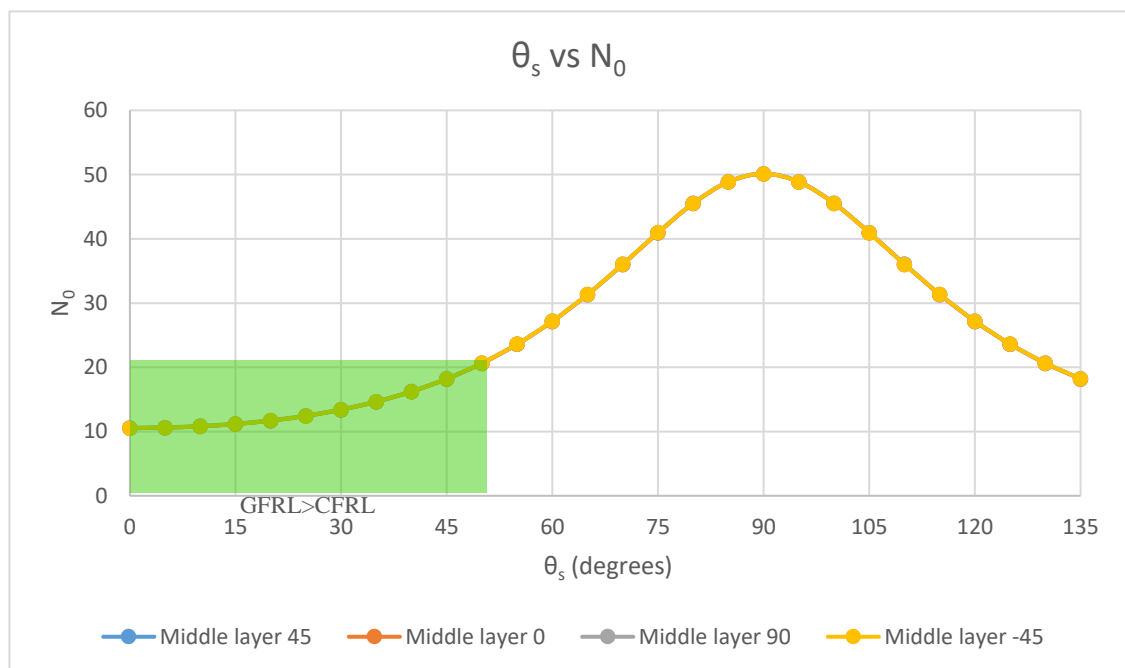


Figure 4-6 Non-Dimensional Buckling stress (N_0) vs surface layers fibre orientation for a nanocomposite reinforced with carbon fibre uniaxially loaded

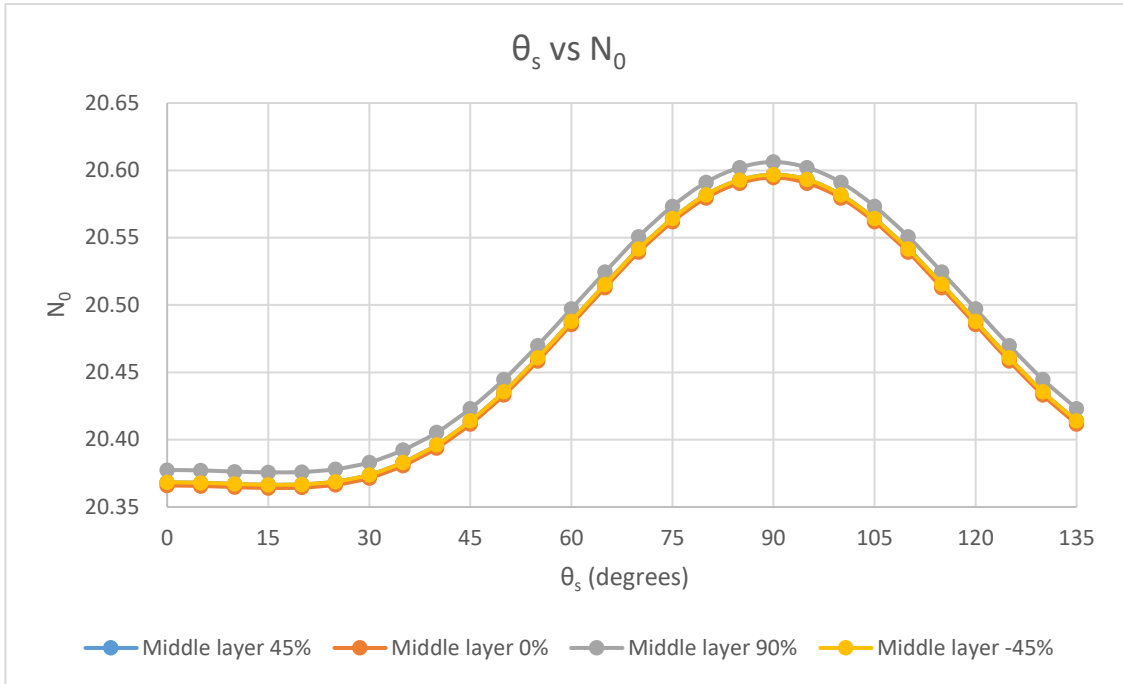


Figure 4-7 Non-Dimensional Buckling stress (N_0) vs surface layers fibre orientation for a nanocomposite reinforced with glass fibre uniaxially loaded

4.2.1.2 Effect of fibre orientation on biaxially loaded carbon and glass fibre reinforced nanocomposite

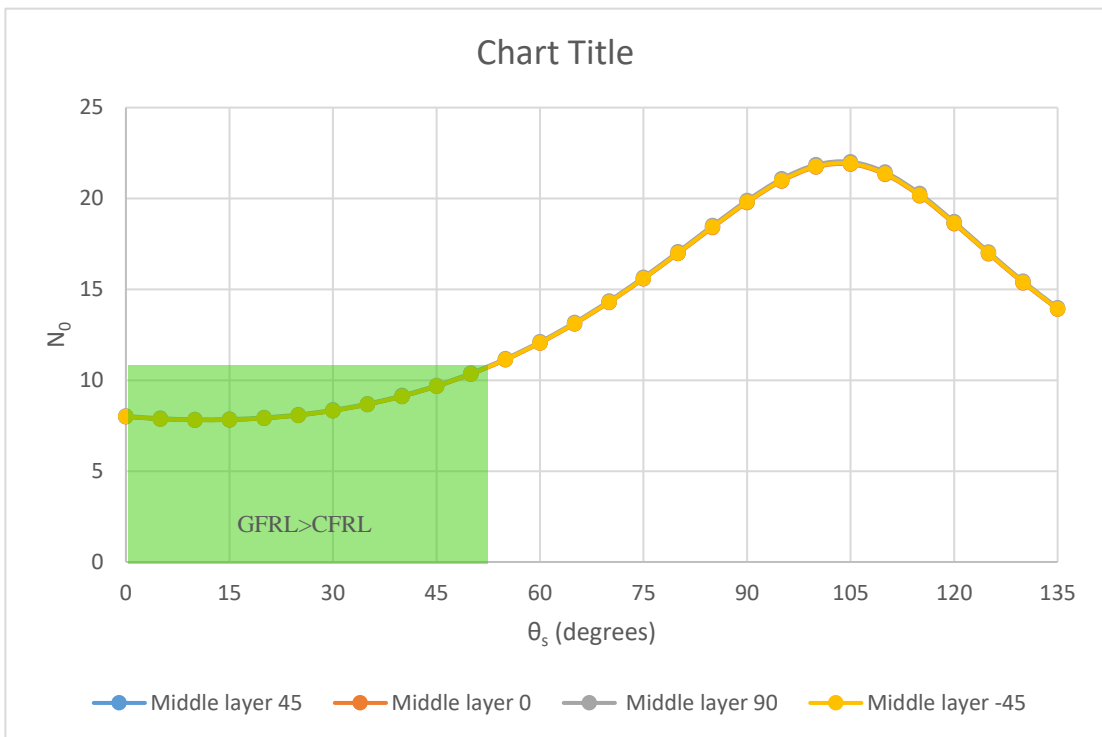


Figure 4-8 Non-Dimensional Buckling stress (N_0) vs surface layers fibre orientation for a nanocomposite reinforced with Carbon fibre biaxially loaded.

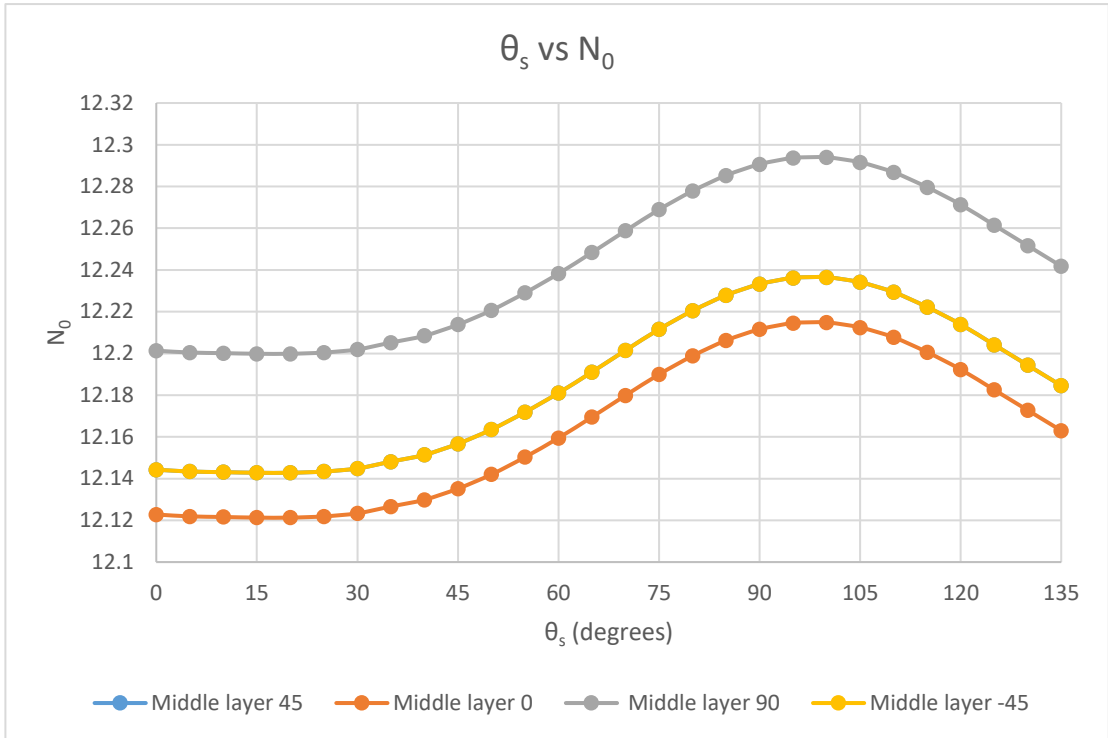


Figure 4-9 Non-Dimensional Buckling stress (N_0) vs surface layers fibre orientation for a nanocomposite reinforced with glass fibre biaxially loaded.

4.2.1.3 Effect of middle layer on buckling stress

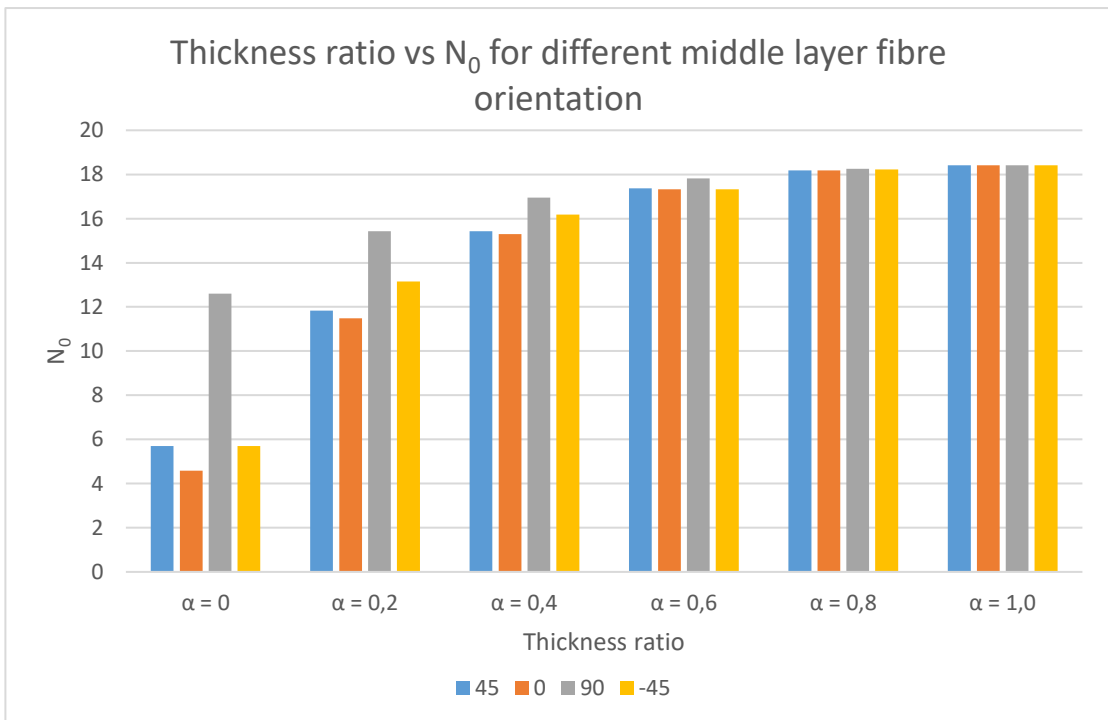


Figure 4-10 Non-dimensional Buckling stress (N_0) vs thickness ratio for different middle layer fibre orientations

4.2.2 Discussion of results

In figures 4-6 and 4-7 the maximum buckling stress corresponds to $\theta_s=90^\circ$ and the minimum buckling stress corresponds to $\theta_s=0^\circ$. It should be noted that the uniaxial load is parallel to the fibres when $\theta_s=90^\circ$ and is perpendicular to the fibres when $\theta_s=0^\circ$. Thus, it can be concluded that for a single compressive load, the buckling resistance is maximized when the load is parallel to the fibres and minimum when the load is perpendicular to the fibres. This aligns with Callister's (2007) assertion that for optimum strength the load should be aligned with the fibres of a composite. Figure 4-8 and 4-9 show that when a biaxial load was used the fibre orientations corresponding with the maximum and minimum stresses changed. This is expected, since the effective load is no longer parallel to the 90° fibre orientation. Moreover, this shows that different types of loads have an influence of the fibre orientation vs N_0 graph. Adding a load to the laminate shifted the graphs to the right.

The shape of the N_0 vs θ_s graph is similar to the graph found by Hosseini & Hadi (2014). The similarity is that both graphs form a bell curve. However, there is a difference in the fibre orientations corresponding to the maximum and minimum buckling stress. The difference in the results is possibly due to the methodologies of the studies. Hosseini & Hadi (2014) were studying the effects of delamination imperfections on the buckling load of a laminate. Moreover, there are other factors such as type of loading that affect the fibre orientation corresponding to the maximum buckling stress, as can be seen by the effects of adding a second load in figures 4-6 and 4-8. However, the result obtained in this dissertation is in accordance with the results obtained by Dhuban (2017). He stated that the surface layers of the laminate have a greater influence on the critical buckling load. Figure 4-10 goes further to show that the middle layer has a greater influence on the critical buckling stress as the thickness ratio decreases.

4.3. Effect of Number of Layers and Stacking Sequence on Buckling Stress

4.3.1 Results

The effect of the number of layers and stacking sequence of a GFRNL are discussed in this section. All layers have the same properties: $V_F = 0.1$, $W_{GPL} = 0.05$ and $\theta = 45^\circ$. The GFRNL is loaded both uniaxially and biaxially. The stacking sequences used in this section are cross ply, symmetric ply, anti-symmetric ply and angle ply laminates. Figure 4-11 shows the different stacking sequences used in this section including the order in which they are stacked. The angle ply, symmetric ply and anti-symmetric ply laminates are added by 2 layers every time the buckling stress is tested and the cross ply laminate is added by one layer every time the buckling stress is tested.

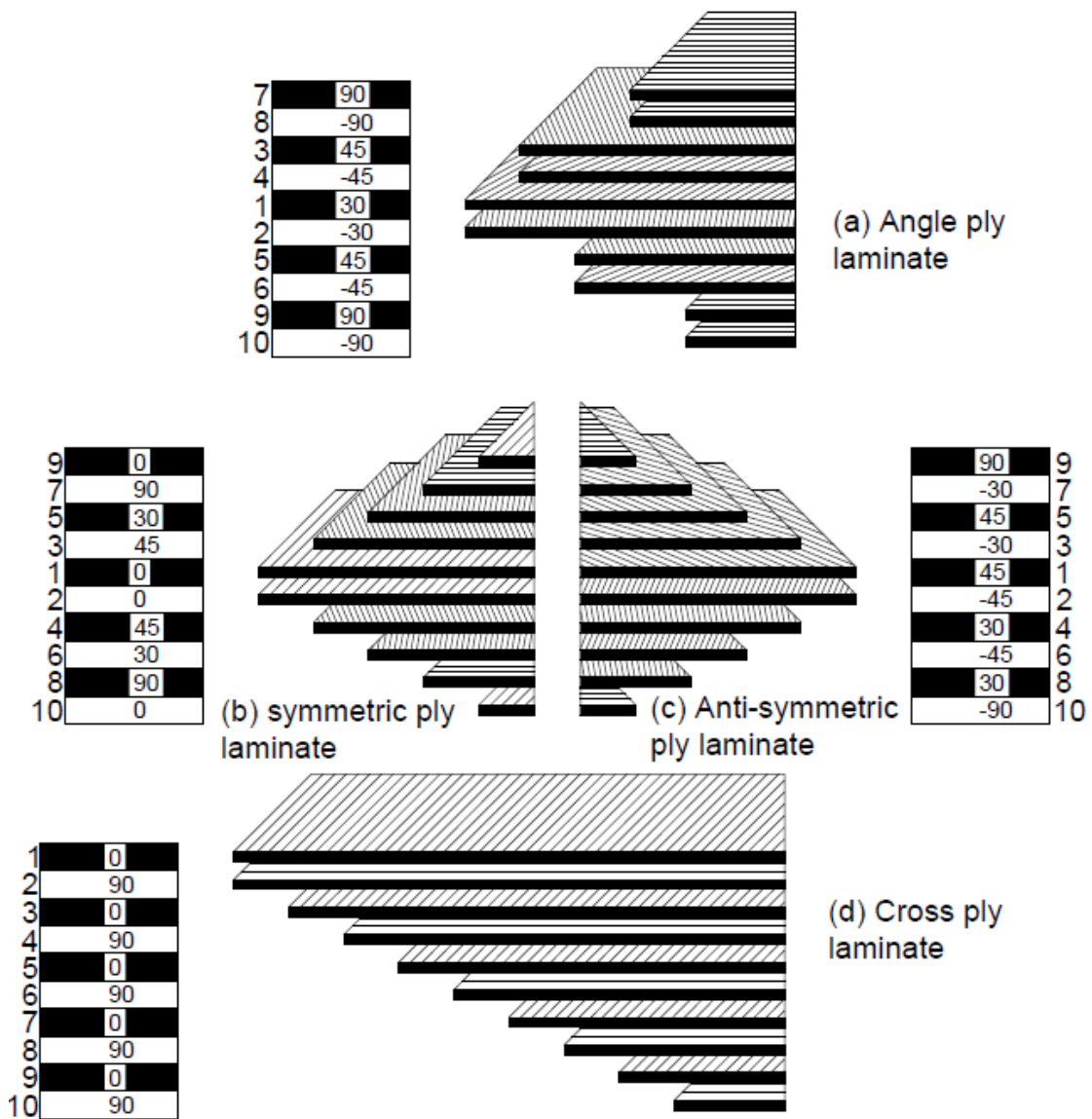


Figure 4-11 stacking sequences used in the analysis of the effect on stacking sequences on buckling stress including fibre angles and the order in which the layers are added.

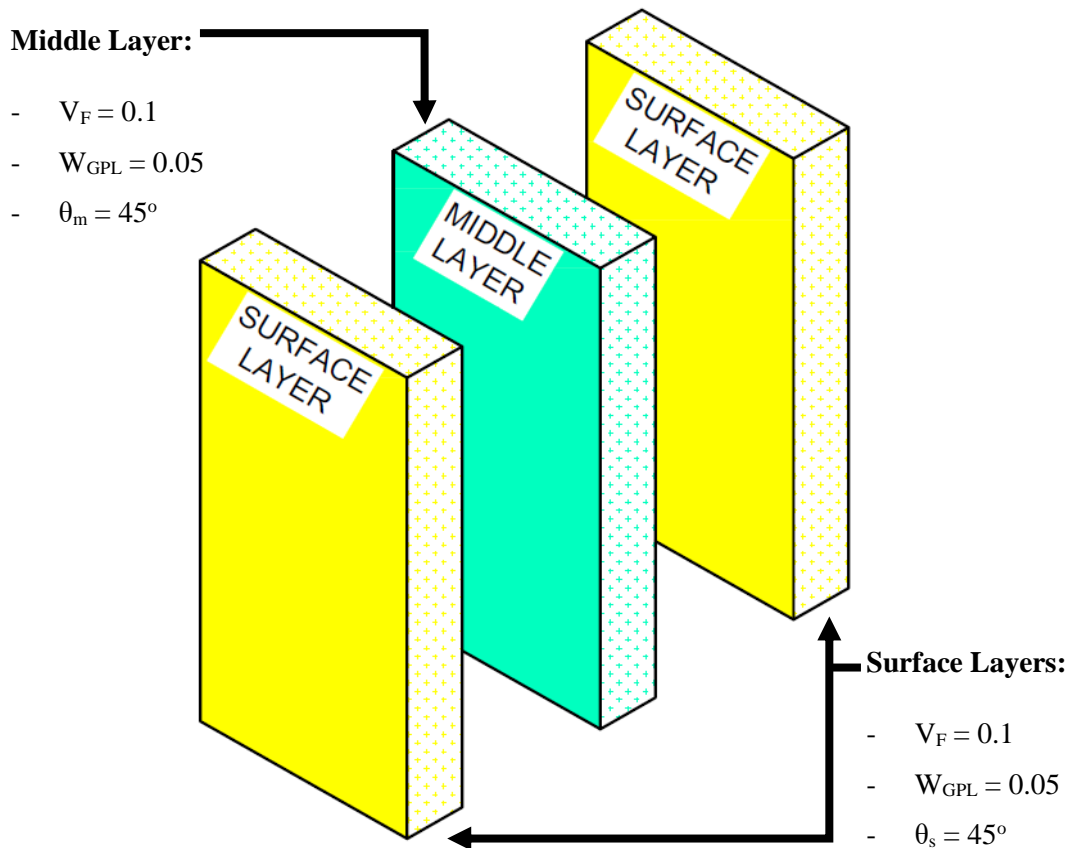


Figure 4-12 layer properties of Laminated nanocomposite in the number of layers tests

Figure 4-13 shows the graph of number of layers vs N_0 . $H=1.5\text{mm}$ and is kept constant while all layers of the laminate are equal in thickness. Meaning that in a case with 4 layers, the layer thicknesses will be $H/n = 1.5/4 = 0.375$ mm. Figure 4-13 shows that the buckling stress decreases as the number of layers increase for both CFRNL and GFRL. Figure 4-14 to 4-17 shows the effect of stacking sequence on the buckling stress. Figures 4-14 and 4-15 show the effect of the stacking sequence on an uniaxially loaded CFRNL and figures 4-16 and 4-17 show the effect of stacking sequence on a biaxially loaded CFRNL. The properties of the layers are $V_F = 0.5$ and $W_{GPL} = 0.05$. θ and α are dependent on the stacking sequence and number of layers respectively.

Figure 4-14 and 4-15 show the effect of stacking sequence on the buckling stress when the laminate is uniaxially loaded. These graphs show how the cross ply, angle ply, symmetric and anti-symmetric laminate affect the critical buckling stress. The cross ply laminate has plies with alternating fibre orientations of 90° and 0° . The graph has a wave shape meaning the local maximum buckling stress (crest) alternates with a local minimum buckling stress (trough). The crest corresponds to the addition of a layer with $\theta=90^\circ$ and the trough corresponds to the

addition of a layer with $\theta=0^\circ$. The cross ply laminate graph has the same shape for CFRL and GFRL when the laminate is uniaxially loaded. The buckling stress corresponding to an addition of layers with 90° , or the crests of the graph, have an approximately constant buckling stress and the layers corresponding to the addition of layers with 0° , or the trough of the graph, increase slightly every time a 0° ply is added.

Similar to the cross ply laminate, the symmetric ply laminate also has a wave like shape. However, the symmetric ply laminate has a greater wavelength than the cross ply laminate. The pair of angles added to the laminate affects the magnitude of the crest and the trough. As can be seen in figures 4-14 and 4-15, when a pair of layers (layer 3 and 4) with $\theta=45^\circ$ are added the crest of the graph increase slightly, however, when a pair of layers (layer 7 and 8) with $\theta=90^\circ$ are added the crest of the graph increased significantly. The anti-symmetric graph has the same graph condition as the symmetric laminate. The angle ply laminate increases as the number of layers increases.

Figure 4-16 and 4-17 show the effect of the stacking sequence when the laminate is subjected to biaxial loading. All the graphs in these figures have the same shape as in figure 4-11. Meaning the buckling stress decreases as the number of layers increases. The graphs are superimposed over each other, meaning there is very little difference in the buckling stresses caused by different stacking sequences.

4.3.1.1 Effect of number of layers on buckling stress, when fibre orientation is constant

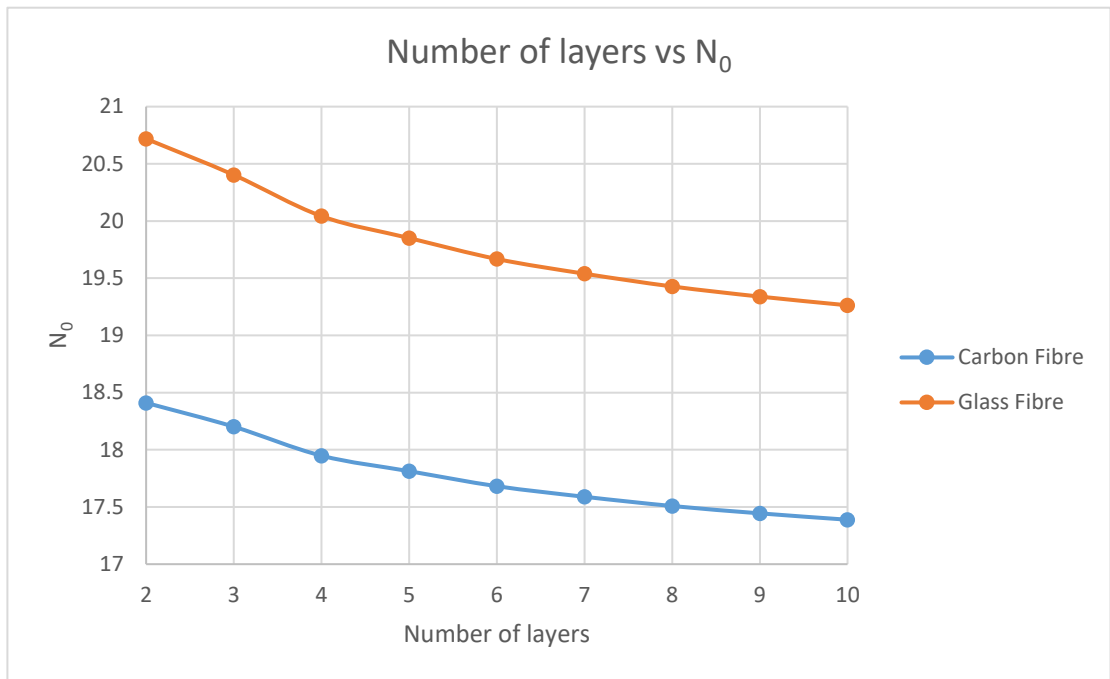


Figure 4-13 Non-Dimensional Buckling stress (N_0) vs number of layers for a nanocomposite reinforced with glass fibre and Carbon fibre

4.3.1.2 Effect of stacking sequence on uniaxial and biaxially loaded plate reinforced with carbon fibre

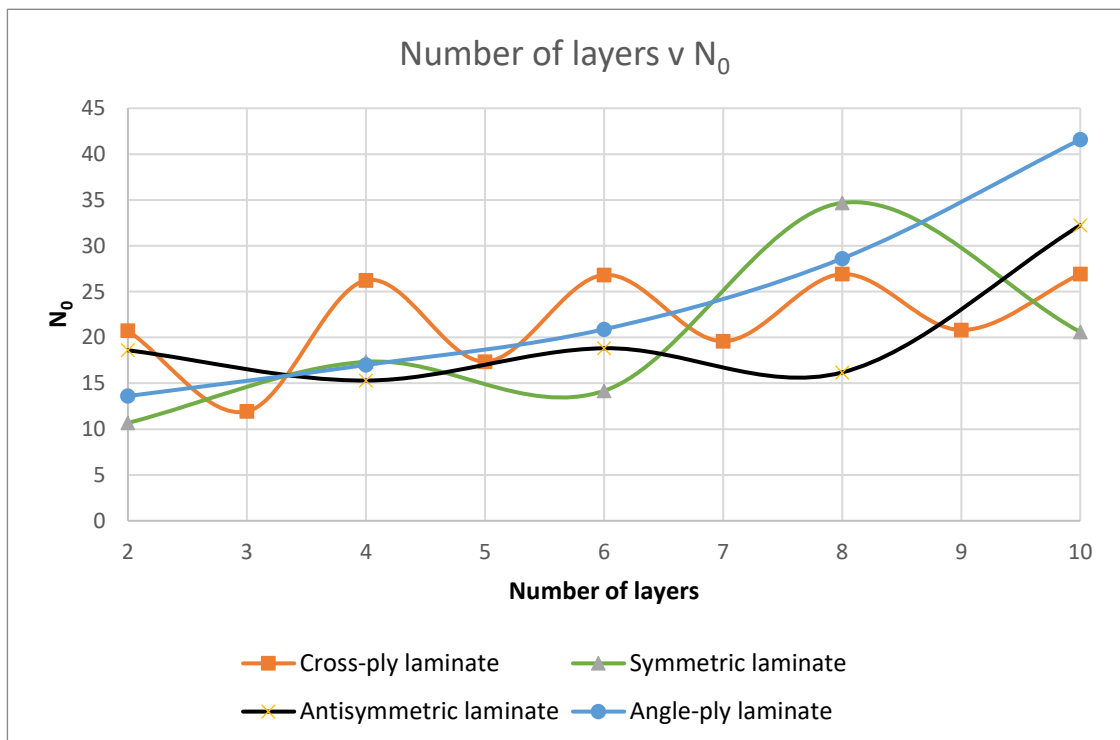


Figure 4-14 Number of layers v N_0 for a uniaxial loading

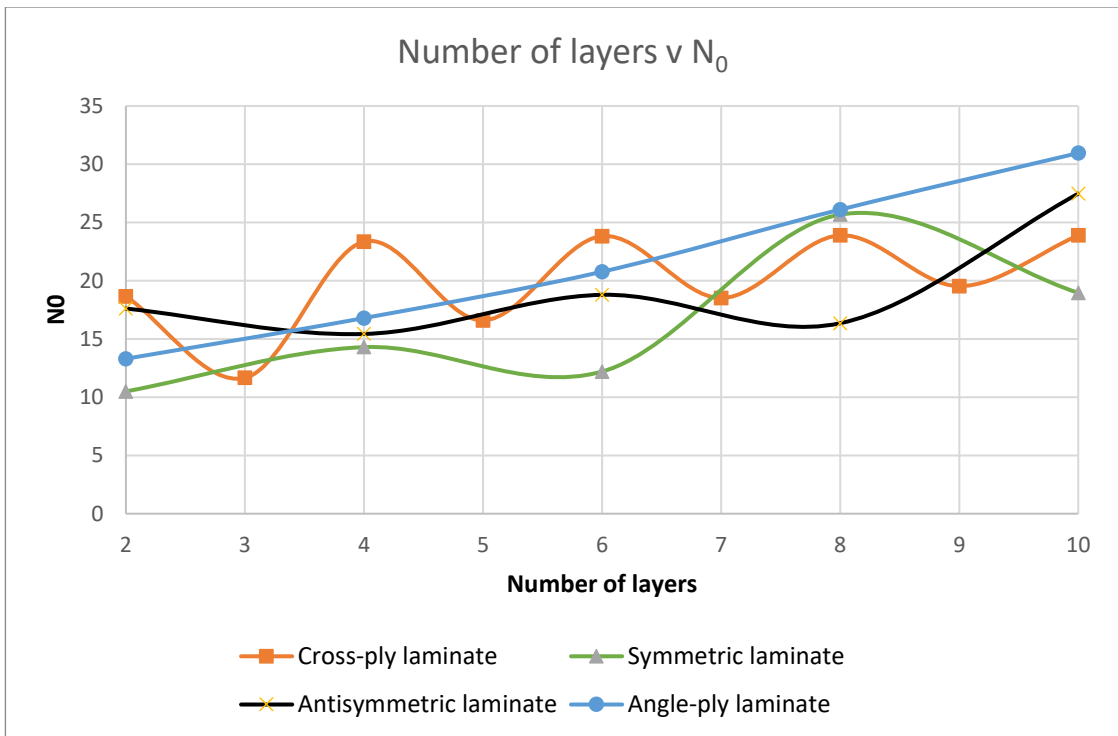


Figure 4-15 Number of layers v N_0 for biaxial loading

4.3.1.3 Effect of stacking sequence on uniaxial and biaxially loaded plate reinforced with glass fibre

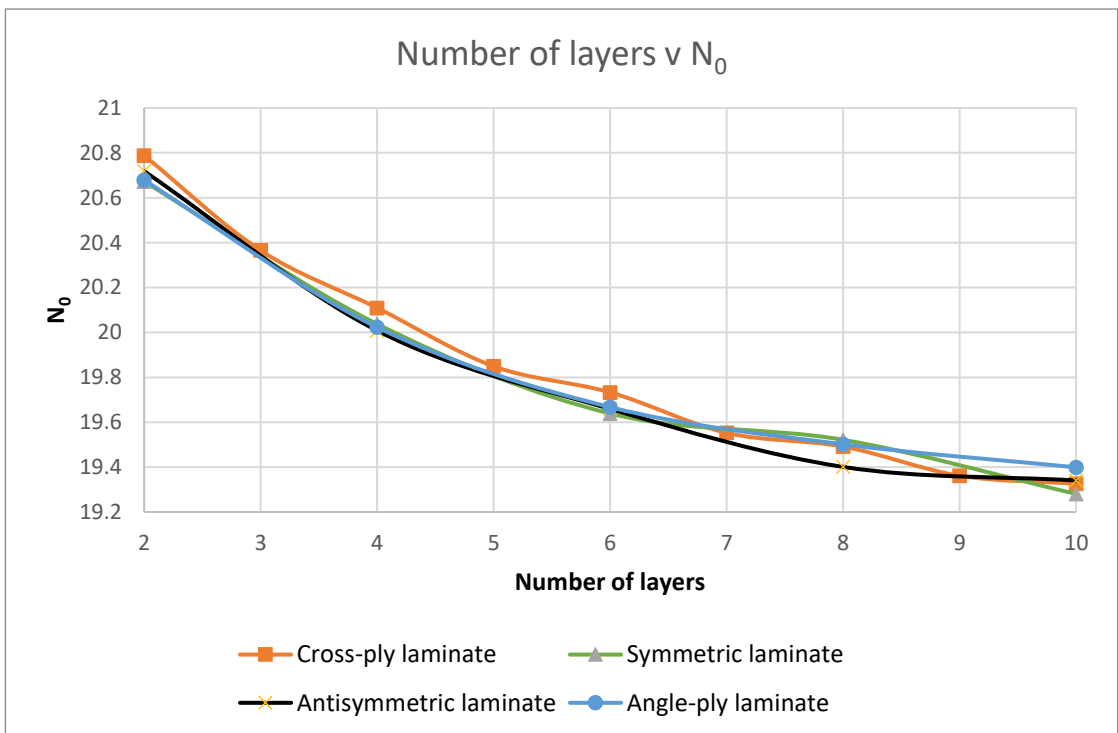


Figure 4-16 Number of layers v N_0 for uniaxial loading

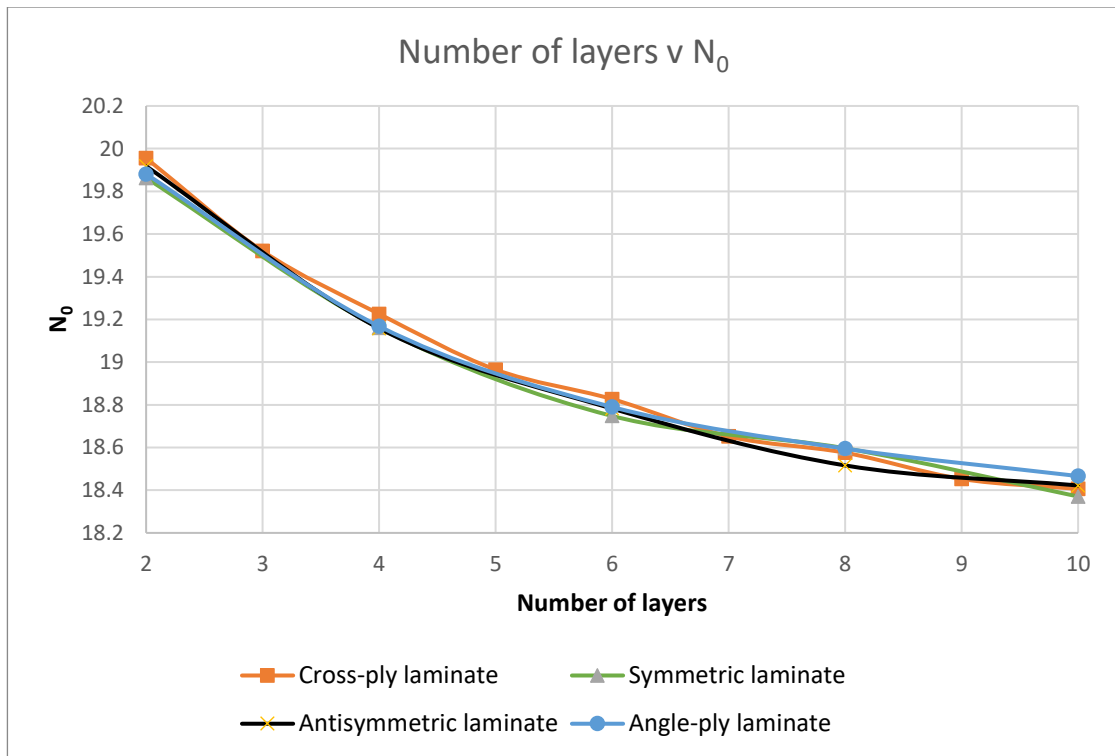


Figure 4-17 Number of layers v N_0 for biaxial loading

4.3.2 Discussion of results

According to figure 4-13, for a laminate with plies of equal fibre orientations, when the number of layers of a laminate are increased the critical buckling stress decreases. From this result, it can be additionally concluded that as the thickness ratio of the laminate is decreased, the buckling stress decreases. This conclusion can be made because adding layers of equal thickness while keeping H constant results in a decrease in thickness ratio.

There is a significant difference in the graphs when it comes to different types of loading. For uniaxial loading, the buckling stress is either constant or increasing as the number of layers increase. Whereas, for biaxial loading the buckling stress is decreasing as the number of layers is increased. The results for biaxial loading are more in line with the expected results, since they are similar to the results obtained in figure 4-13. To understand this difference, additional research would have to be conducted to see the response of different stacking sequences when subjected to different types of loading conditions. Results obtained on figure 4-16 and 4-17, for biaxial loading, are in accordance with the results obtained by Heidari-Rarani (2014). The results obtained for different stacking sequences are very similar.

4.4. Effect of Thickness Ratio on Buckling Stress.

4.4.1 Results

The effect of the thickness ratio on the critical buckling stress of a GFRNL is discussed in this section. The surface layer properties are $V_F=0.5$, $W_{GPL}=0.05$, $\theta_s=45^\circ$. The properties of the middle layer are $V_F=0.1$, $W_{GPL}=0.01$, $\theta_m=45^\circ$. The thickness ratio of the GFRNL is changed while the overall thickness and the properties of the plies are kept constant. The thickness ratio is determined using equation 3. The surface and middle layer thicknesses corresponding to different thickness ratios are shown in table 5-1.

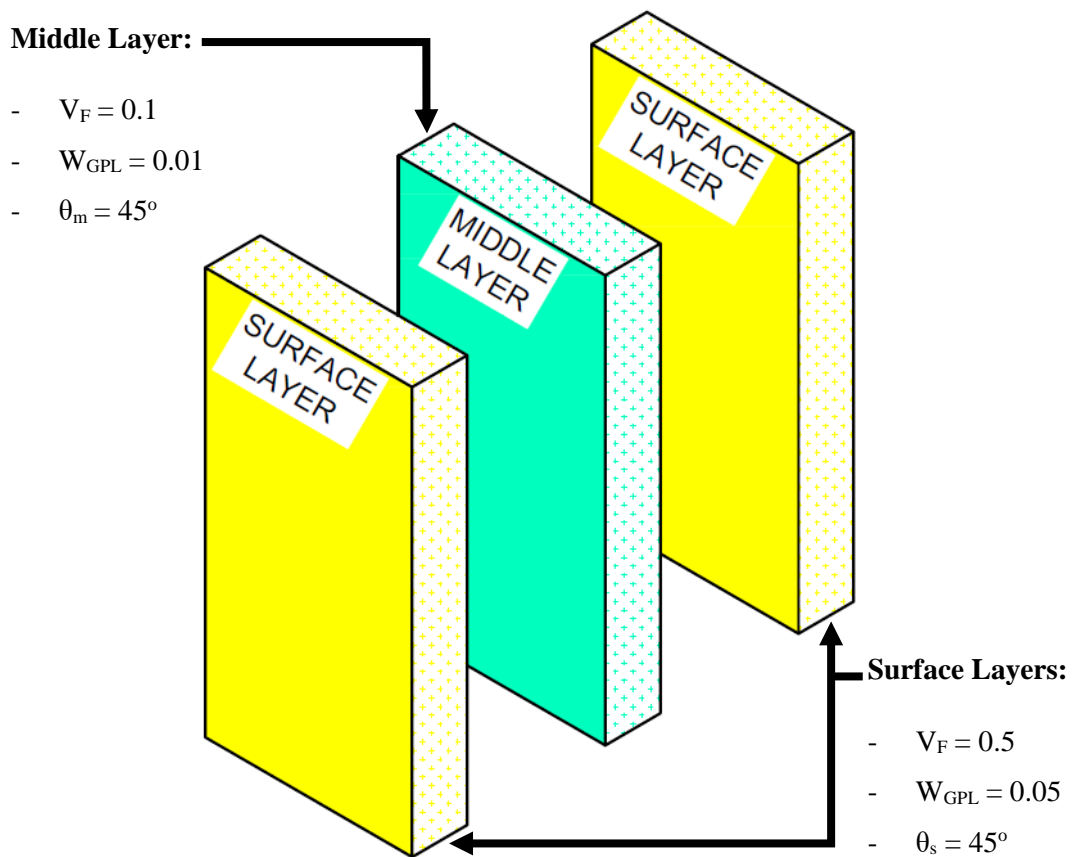


Figure 4-18 Layer properties of Laminated nanocomposite in the thickness ratio tests

Table 4-1 The thickness of the layers of a 3 layer composite laminate for different thickness ratios.

Thickness ratio (α)	H (mm)	h_s (mm)	$h_s/2$ (mm)	h_m (mm)
0	1.5	0	0	1.5
0.1	1.5	0.15	0.075	1.35
0.2	1.5	0.3	0.15	1.2
0.3	1.5	0.45	0.225	1.05
0.4	1.5	0.6	0.3	0.9
0.5	1.5	0.75	0.375	0.75
0.6	1.5	0.9	0.45	0.6
0.7	1.5	1.05	0.525	0.45
0.8	1.5	1.2	0.6	0.3
0.9	1.5	1.35	0.675	0.15
1	1.5	1.5	0.75	0

Figures 4-19 and 4-20 show that as the thickness ratio (α) is increased the buckling stress increases. The rate at which the buckling stress increases as α is changed, decreases as α gets larger. Beyond $\alpha=0.7$ the increase in buckling stress becomes insignificant for both CFRL and GFRL. The effect of different V_F 's, when the laminate is reinforced with carbon fibres (CFRL), is very low. As can be seen in figure 4-19 the different graphs are superimposed over each other. The effect of different V_F 's when the laminate is reinforced with glass fibre (GFRL) is more visible, as can be seen in figure 4-20.

4.4.1.1 Effect of Thickness ratio on nanocomposite plate reinforced with carbon fibre

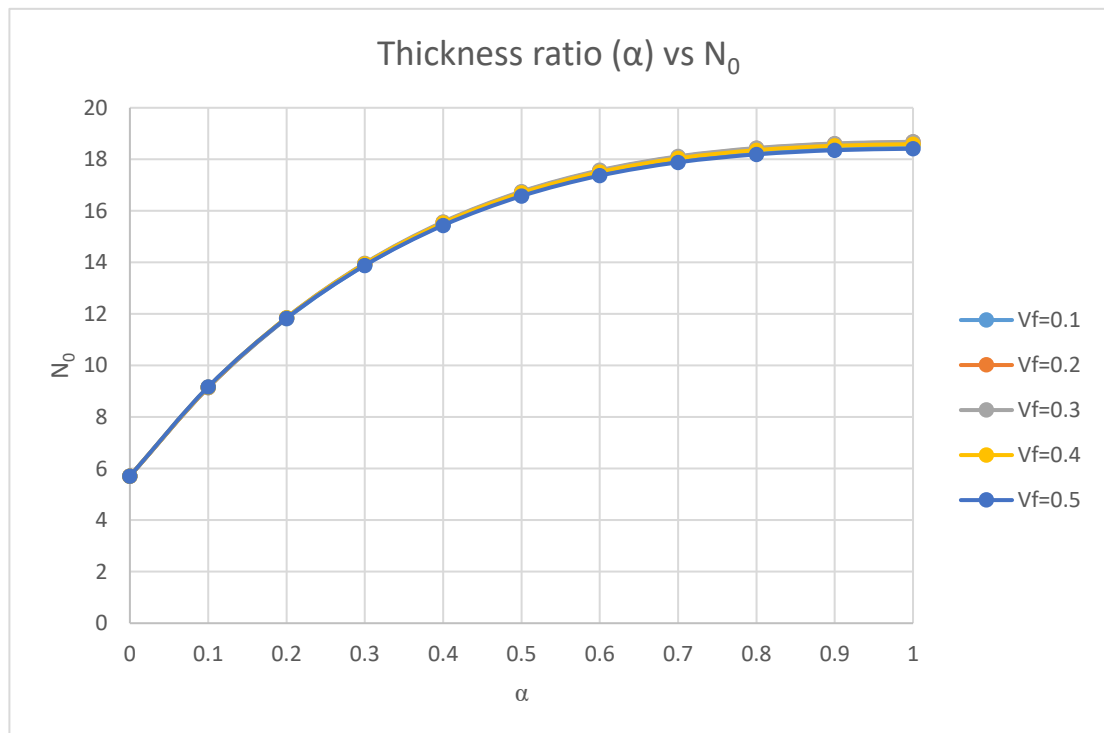


Figure 4-19 Non-Dimensional Buckling stress (N_0) vs Thickness ratio for a nanocomposite reinforced with carbon fibre

4.4.1.2 Effect of Thickness ratio on nanocomposite plate reinforced with glass fibre

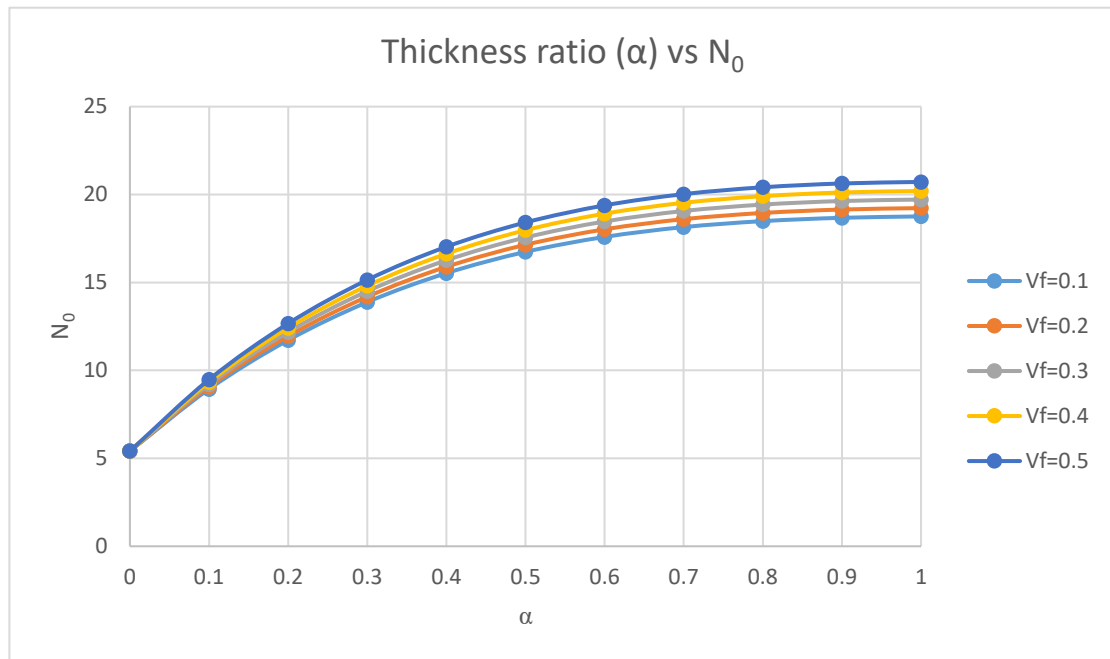


Figure 4-20 Non-Dimensional Buckling stress (N_0) vs Thickness ratio for a nanocomposite reinforced with glass fibre

4.4.2 Discussion of results

Figures 4-19 and 4-20 show that as the thickness ratio increase the buckling stress increases. This is in agreement with a conclusion made on the previous section, where the effect of adding plies to the composite is tested. However, the rate at which the buckling stress increases, decreases as the thickness ratio increases. It can be seen that beyond $\alpha=0.7$ the increase in buckling stress is very little, so much so that the graph is almost flat at this point.

The results obtained are in accordance to what was expected. Reddy (2013) found similar results when it comes to thickness ratio. He found that when the thickness ratio is increases the buckling stress increases as well. The V_F of the material has a very little effect on the critical buckling stress of the laminate.

As can be seen in equation 3 when the thickness ratio is increased, the surface layers of the material get thicker. Moreover, as can be seen in figure 2-9, as the laminate experiences bending, the surface layers experience a tensile and compressive force while the middle layer experiences a shear force (Mao, et al., 2008). Thus, the reason for the buckling stress increasing, as the thickness ratio increases, is that the surface layers get larger in thickness. The surface layers experience the tensile and compressive forces. Thus, if these layers are larger, the laminate resists these forces better.

4.5. Effect of Aspect Ratio on Buckling Stress

4.5.1 Results

The effect of the aspect ratio on a 3 layer GFRNL are discussed in this section. The surface layer properties are $V_F=0.1$, $W_{GPL}=0.05$, $\theta_s=45^\circ$ and $h_s/2=0.15\text{mm}$. The middle layer properties are $V_F=0.1$, $W_{GPL}=0.01$, $\theta_m=45^\circ$ and $h_m=1.2\text{mm}$. The aspect ratio is the ratio of the width/height. In order to achieve different aspect ratios, the height of the laminate is kept constant while the width of the laminate is varied. Since the height of the laminate is 1m, the aspect ratio is equal to the width of the laminate. See table 4-2 for the dimensions used for the laminate when testing the critical buckling stress of different aspect ratios.

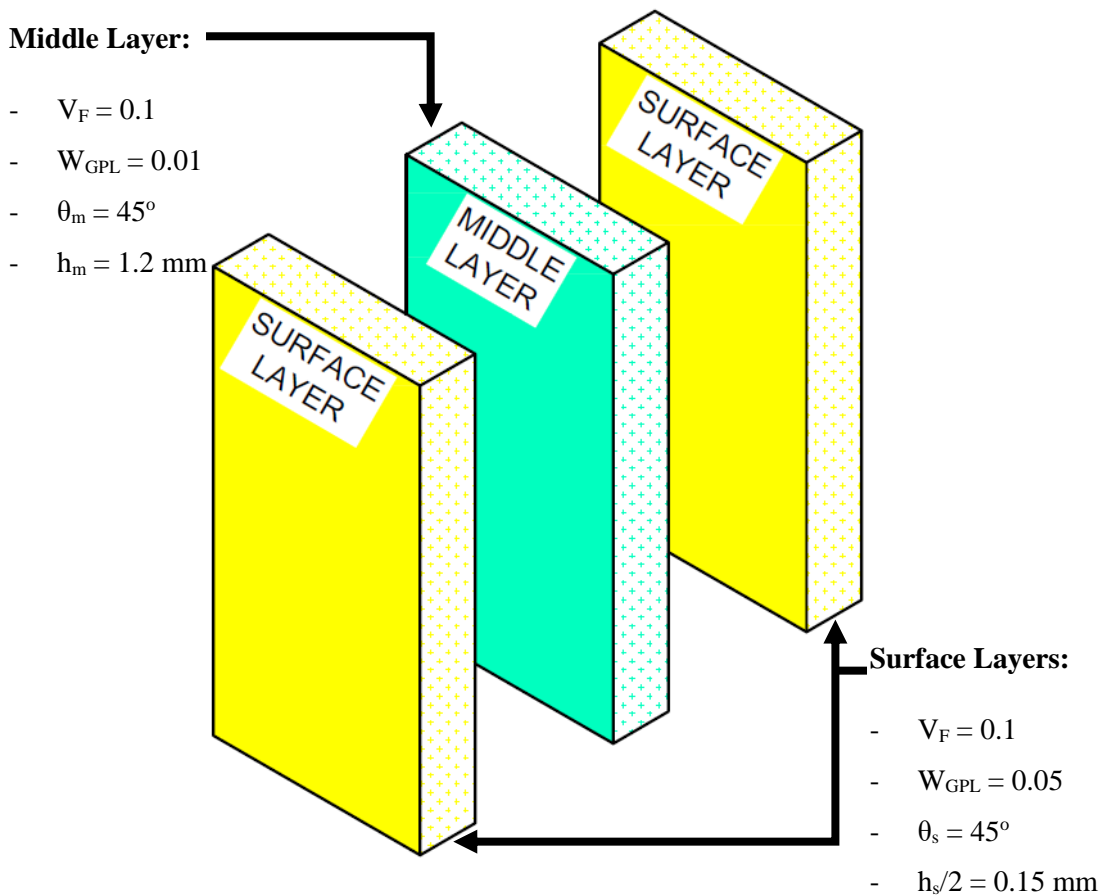


Figure 4-21 Layer properties of Laminated nanocomposite in the aspect ratio tests

Figure 4-22 shows that as when the aspect ratio is increased the buckling stress increases as well. The graphs for CFRL and GFRL are parallel to each other, thus the rate of increase of buckling stress is not dependent on the reinforcement material used. The rate at which the buckling is increasing is not constant, there are part where the buckling stress increases more than others. For instance the buckling stress increases much more from aspect ratio 0.25 to 0.5 compared to aspect ratios 0.75 and 1. However the difference is minor.

Table 4-2 The dimension of the width and height of the laminate for different aspect ratios. (a) is the width and (b) is the height.

Aspect Ratio	b (m)	a (m)
2	1	2
1.75	1	1.75
1.5	1	1.5
1.25	1	1.25
1	1	1
0.75	1	0.75
0.5	1	0.5
0.25	1	0.25

4.5.1.1 Effect of aspect ratio on both carbon and glass fibre reinforced nanocomposite

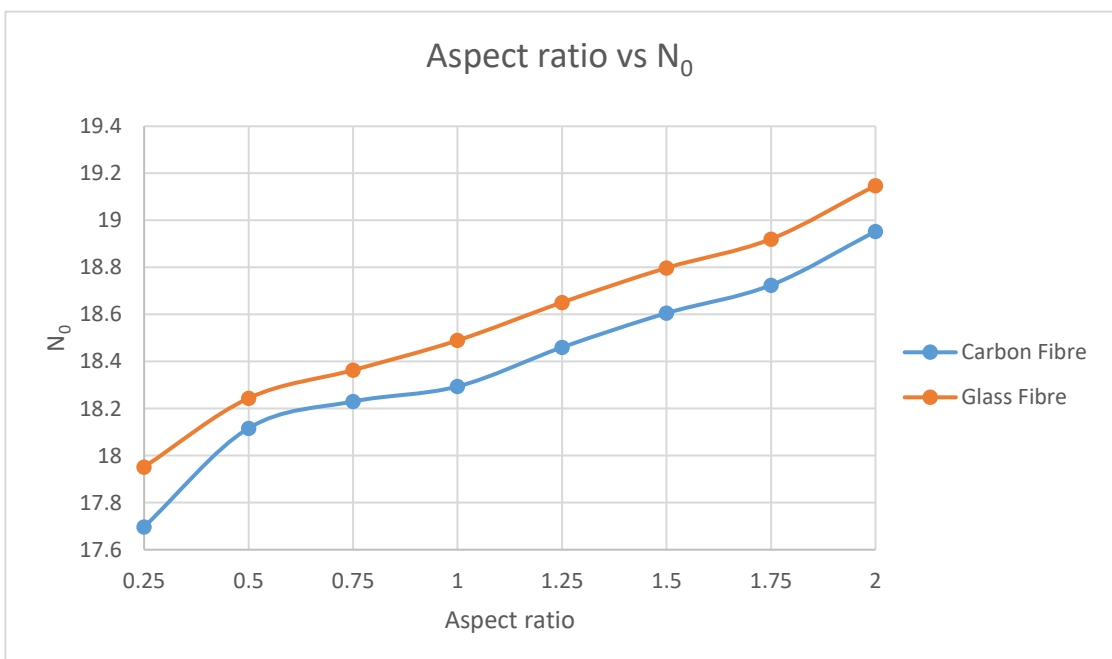


Figure 4-22 Non-Dimensional Buckling stress (N_0) vs Aspect ratio for a nanocomposite reinforced with glass fibre and Carbon fibre

4.5.2 Discussion of results

As the aspect ratio gets larger the laminate gets wider, since in this case the height is kept constant and the width is changed. Thus, as the plate gets wider and the area on which the load is placed gets bigger the buckling stress increases. This is due to the moment of inertia. When the moment of inertia becomes larger, the laminate becomes stiffer and the buckling stress increases, see Euler's buckling load equation 2. The result determined here are in line with the results determined by Suleiman (2019). Which is what was expected since his research was similar to the one done in this dissertation, when compared to Narayana's (2013) results discussed in the literature review. Which are contradictory to the one found in this dissertation.

4.6. Effect of Weight Fraction (W_{GPL}) on Buckling Stress

4.6.1 Results

The effect of the weight fraction of graphene nanoplatelets (W_{GPL}) on the buckling stress of the laminate is tested in this section. This is achieved by keeping the properties of the middle layer(s) constant while changing the values of W_{GPL} of the surface layers. The laminate is tested when it has 3 plies. Additionally the laminate is tested on how it reacts when additional plies are added and when the fibre orientation is increased. The laminate is initially tested with 3 layers with $\theta_s = \theta_m = 45^\circ$. Next, the laminate is tested when it has 10 layers and the fibre orientation remains the same. Lastly, the fibre orientation of the middle and surface layers is increased to 90° . The properties of the middle layer are kept constant at $V_F = 0.1$ and $W_{GPL} = 0.01$.

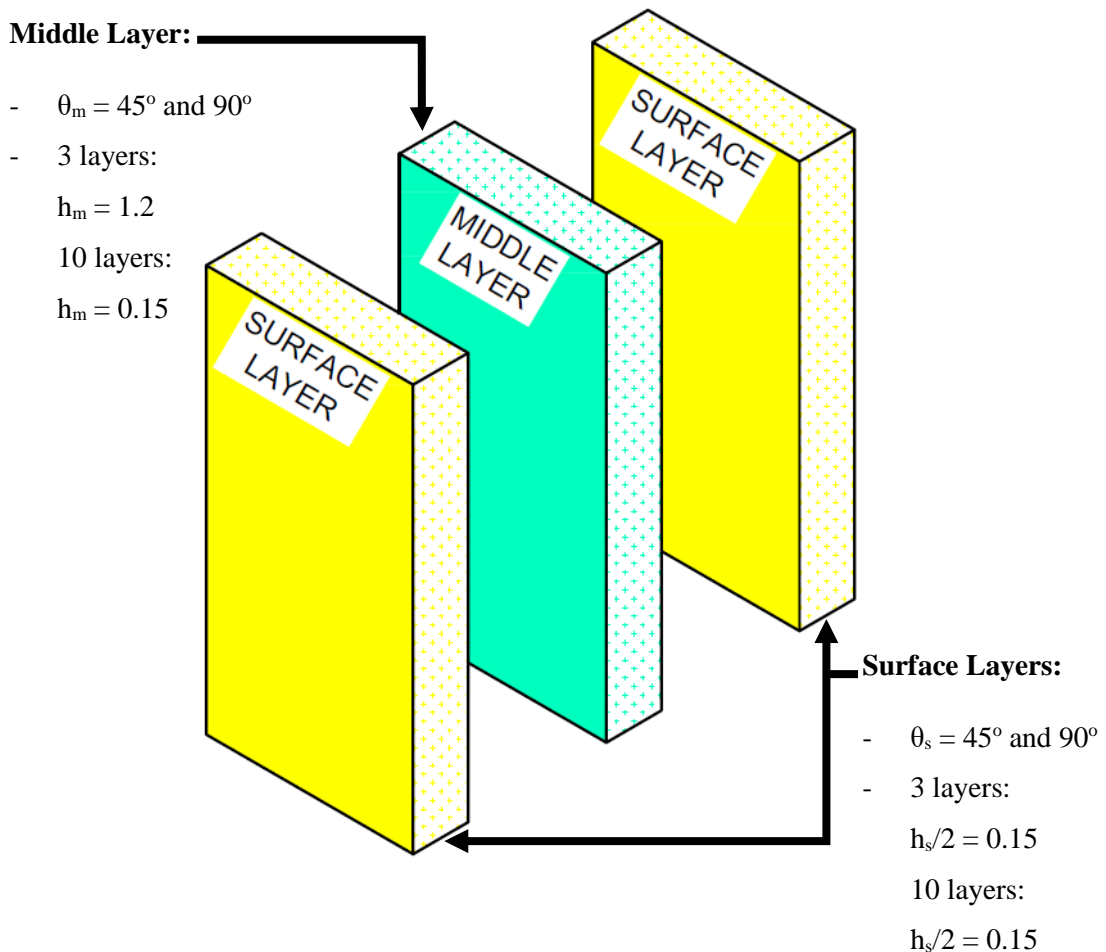


Figure 4-23 Layer properties of Laminated nanocomposite in the boundary condition tests

Figures 4-24 and 4-25 show the effect of increasing the W_{GPL} of the GFRNL for CFRL and GFRL respectively. In both graphs, the GFRNL with the highest V_F starts with the highest buckling stress. However, as W_{GPL} is increased the graphs reach a cross-over point, where the composite with the highest V_F starts having the lowest buckling stress and vice versa. The cross-over point for both graphs is at a W_{GPL} of around 0.05 and it corresponds to a buckling stress of approximately $N_0 = 12.5$.

Figure 4-26 and 4-27 show the effect of W_{GPL} on the GFRNL when the plies are increased from 3 to 10 while keeping all other properties the same. There is little difference caused to CFRL graph when this change is made. The cross-over point is still at the same place, see figure 4-26. However, for GFRL there is a more significant difference. The cross-over point moves from $W_{GPL} = 0.05$ to $W_{GPL} = 0.07$ and the buckling stress corresponding to the cross-over point slightly increases from $N_0 = 12.5$ to $N_0 = 14$, see figure 4-27.

When in addition to increasing the number of layers the fibre orientation is increased to 90° , which has been shown to correspond to the maximum buckling stress, the buckling stress increases for all V_F 's when CFRL is tested, as seen in figure 4-28. The cross-over point is shifted significantly, so much so that it is no longer visible in figure 4-28. The effects for GFRL are less profound compared to CFRL. The buckling stress and cross-over point have moved slightly.

4.6.1.1 Effect of W_{GPL} on 3 layer nanocomposite with 45° fibre orientation, reinforced with glass and carbon fibre

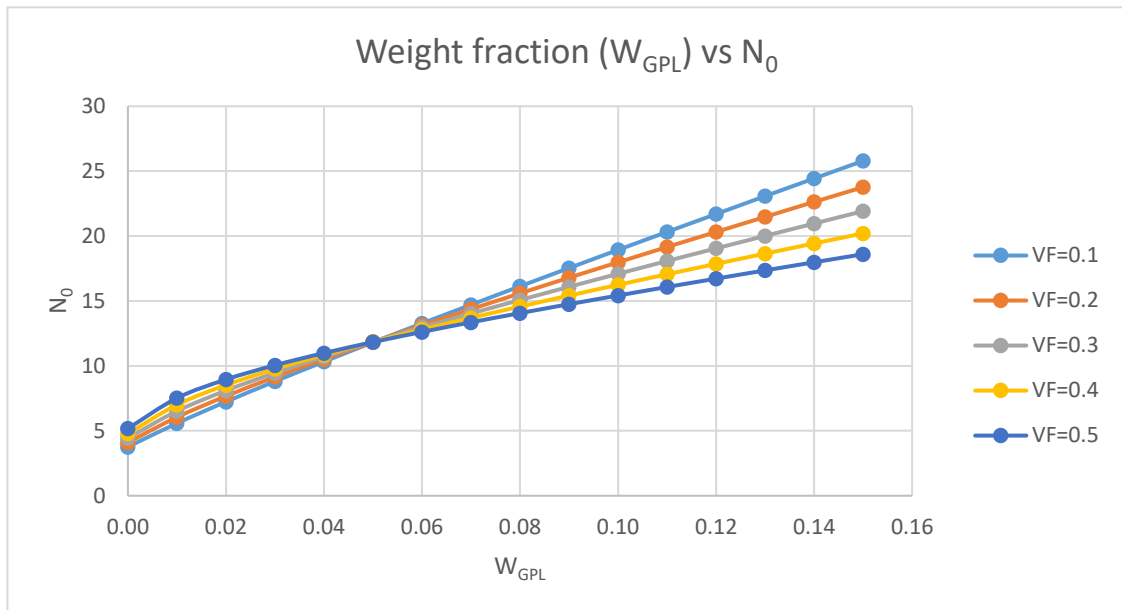


Figure 4-24 Non-Dimensional Buckling stress (N_0) vs Weight Fraction (W_{GPL}) for a nanocomposite reinforced with Carbon fibre with 3 layers with a thickness ratio of 0.2 and equal fibre orientations (45°)

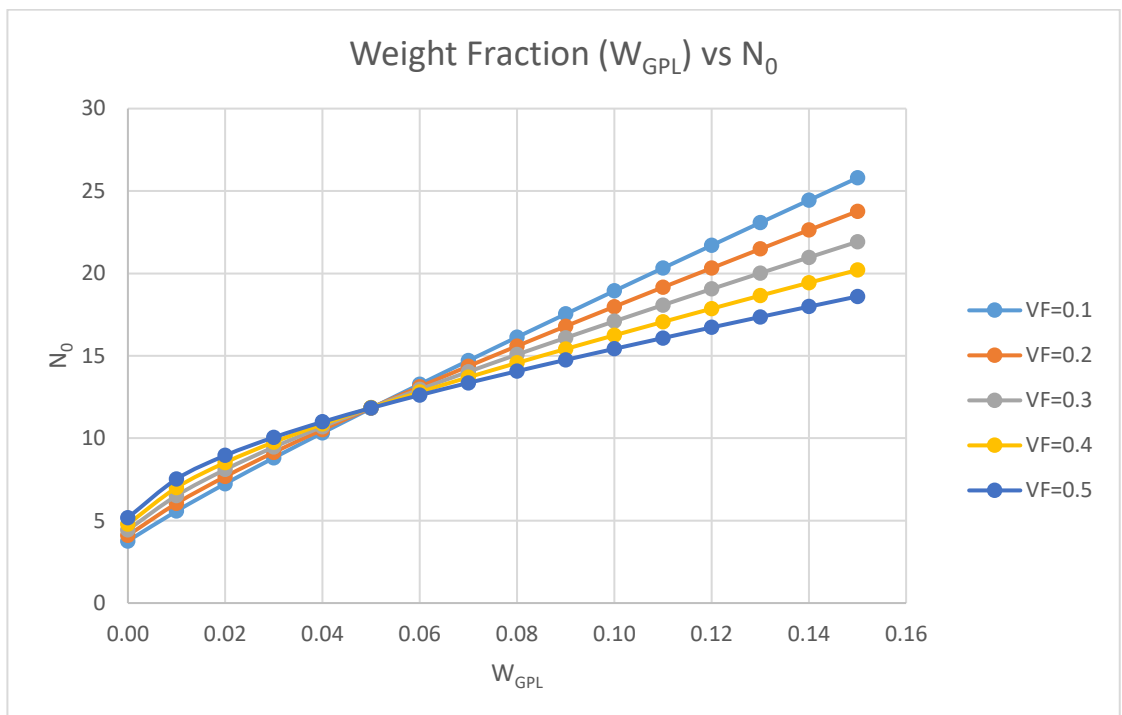


Figure 4-25 Non-Dimensional Buckling stress (N_0) vs Weight Fraction (W_{GPL}) for a nanocomposite reinforced with glass fibre with 3 layers with a thickness ratio of 0.2 and equal fibre orientations (45°)

4.6.1.2 Effect of W_{GPL} on 10 layer nanocomposite with 45° fibre orientation, reinforced with glass and carbon fibre

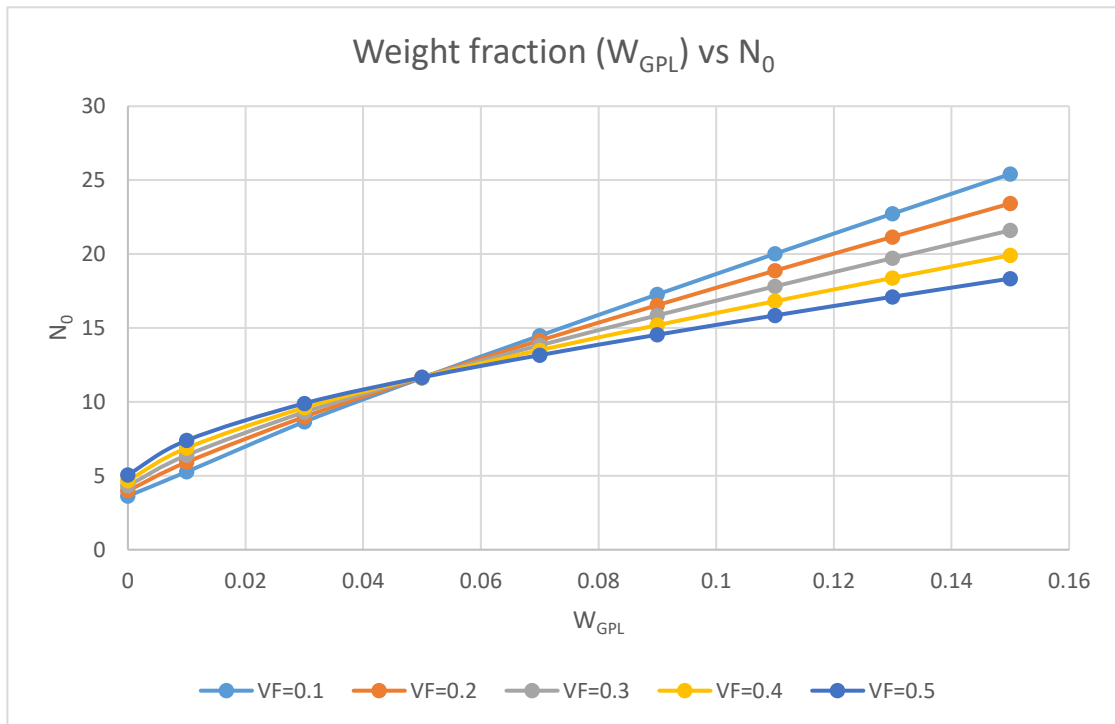


Figure 4-26 Non-Dimensional Buckling stress (N_0) vs Weight Fraction (W_{GPL}) for a nanocomposite reinforced with Carbon fibre with 10 layers with equal thickness and equal fibre orientations (45°)

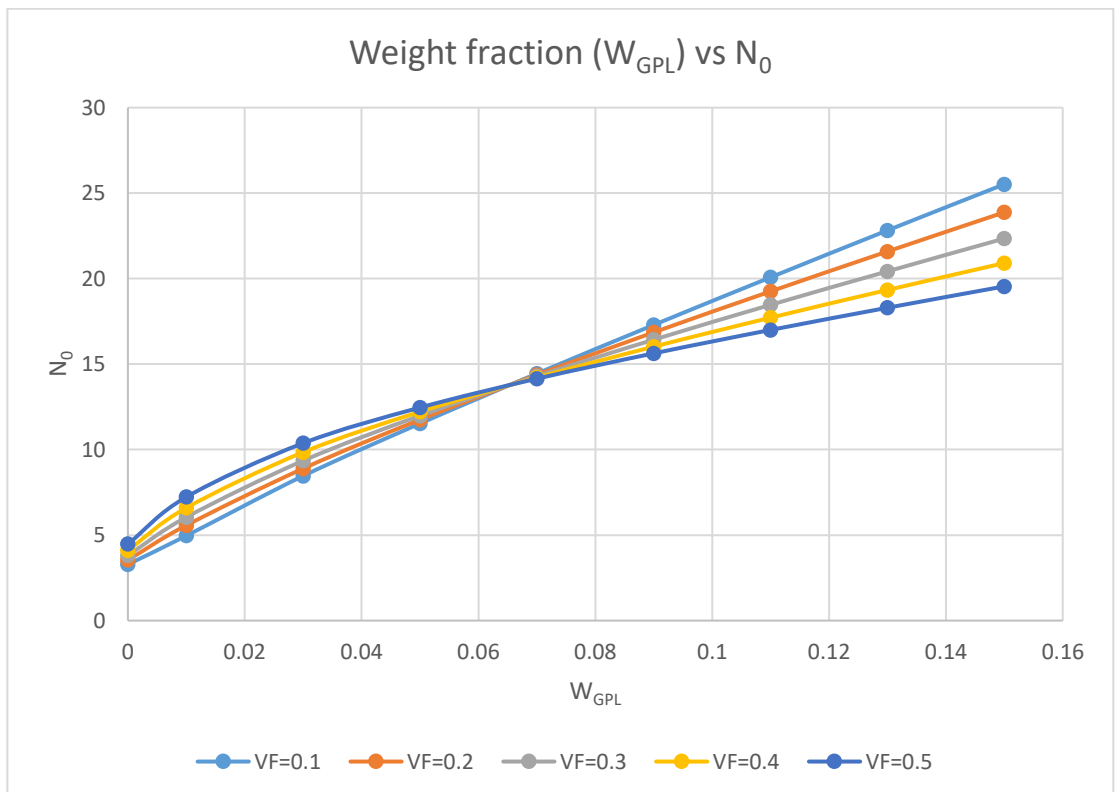


Figure 4-27 Non-Dimensional Buckling stress (N_0) vs Weight Fraction (W_{GPL}) for a nanocomposite reinforced with glass fibre with 10 layers with equal thickness and equal fibre orientations (45°)

4.6.1.3 Effect of W_{GPL} on 10 layer nanocomposite with 90° fibre orientation, reinforced with glass and carbon fibre

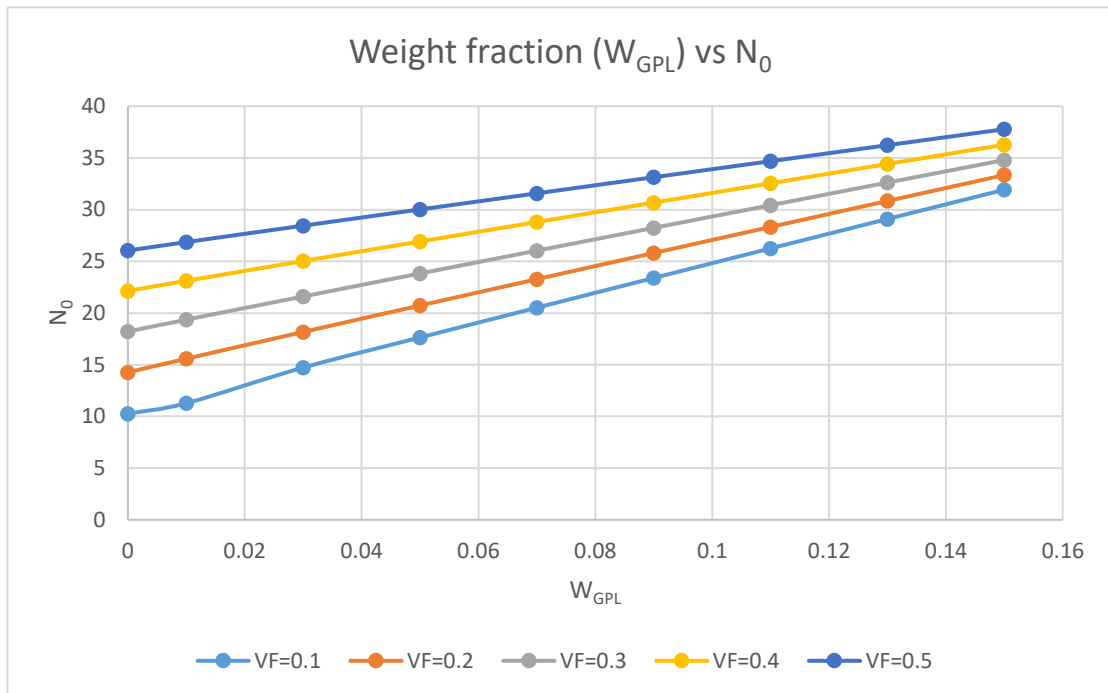


Figure 4-28 Non-Dimensional Buckling stress (N_0) vs Weight Fraction (W_{GPL}) for a nanocomposite reinforced with Carbon fibre with 10 layers with equal thickness and equal fibre orientations (90°)

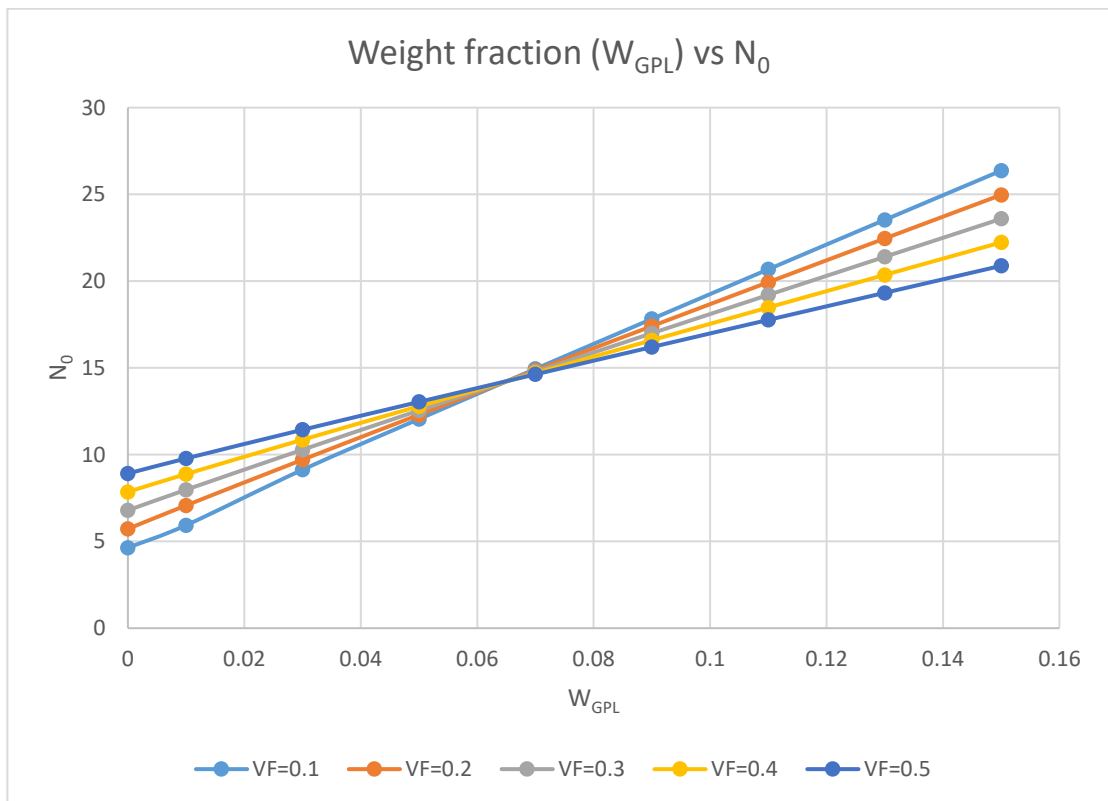


Figure 4-29 Non-Dimensional Buckling stress (N_0) vs Weight Fraction (W_{GPL}) for a nanocomposite reinforced with glass fibre with 10 layers with equal thickness and equal fibre orientations (90°)

4.6.2 Discussion of results

The effect of increasing both the number of layers and fibre orientation of the plies has a more significant impact on CFRL than on GFRL. It has been established in chapter 4.2 that for a fibre orientation less than 53° the GFRP buckling stress is slightly higher than that of CFRL, however when the fibre orientation is greater than 53° the buckling stress for CFRL can be significantly higher than that of GFRL. In this case, the fibre orientation has been changed from 45° to 90° . The effect on CFRL is that the buckling stresses are more than 3 times higher and the cross-over point has significantly changed. In fact, the cross-over point is no longer visible in the graph, see figure 4-28. For GFRL there is a difference but it is not as large as the one experienced by CFRL. The buckling stresses have increased slightly for GFRL; however, the cross-over point has barely been affected by the increase in fibre orientation, see figure 4-27. Thus, the conclusion can be made that as W_{GPL} increases the buckling stress increases. However the rate of increase depends on V_F and fibre orientation of layers.

4.7. Effect of Fibre Volume Content on Buckling Stress

4.7.1 Results

The effect of the fibre volume content (V_F) on the buckling stress of the laminate is tested in this section. This is achieved by keeping the properties of the middle layer(s) constant while changing the values of V_F of the surface layers. The laminate is tested when it has 3 layers. Additionally the laminate is tested on how it reacts when additional layers are added and when the fibre orientation is increased. The laminate is initially tested with 3 layers with $\theta_s = \theta_m = 45^\circ$. Next, the laminate is tested when it has 10 layers and the fibre orientations remains the same. Lastly, the fibre orientation is increased to 90° . The properties of the middle layer are kept constant at $V_F = 0.1$ and $W_{GPL} = 0.01$.

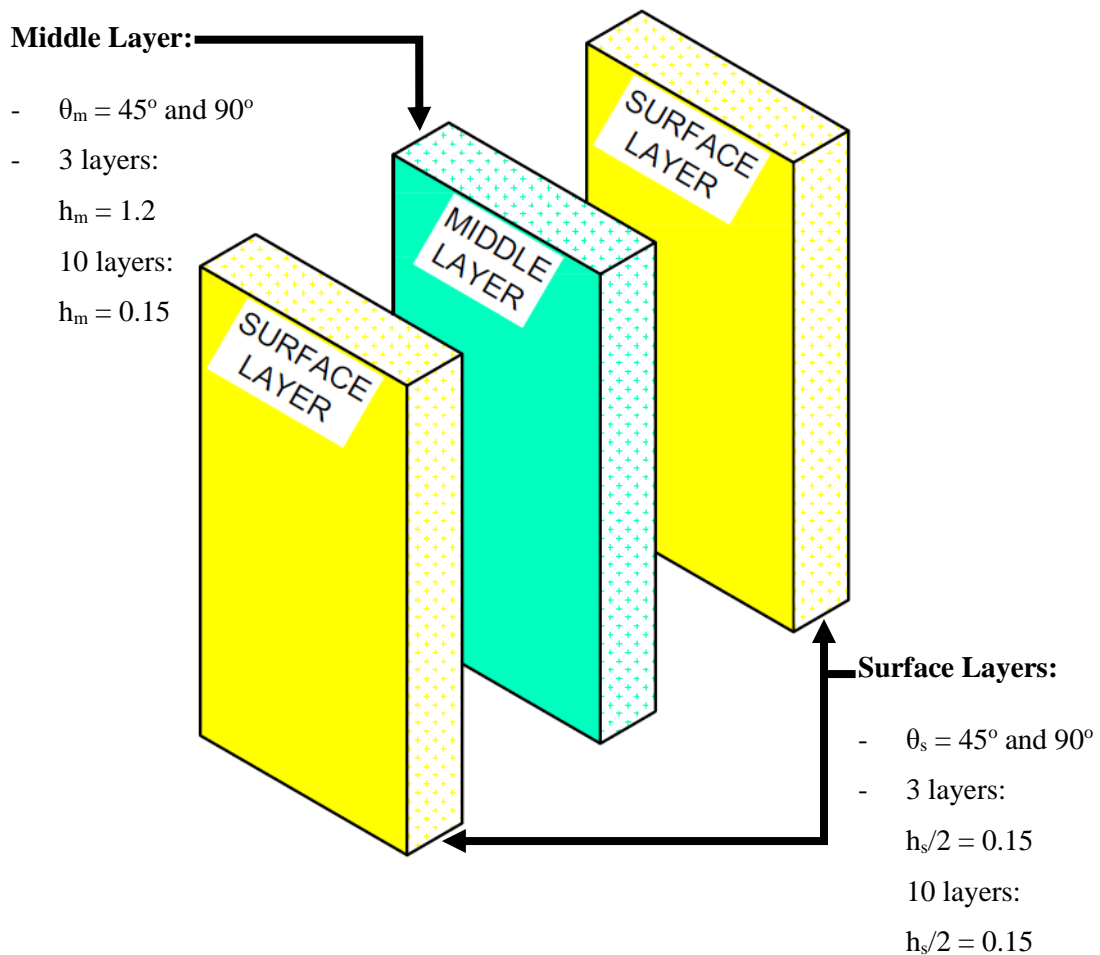


Figure 4-30 Layer properties of Laminated nanocomposite in the fibre volume tests

In figure 4-31 and 4-32, the material with the highest W_{GPL} start with the highest buckling stress. However, the buckling stress decreases for laminates with $W_{GPL} > 0.06$ as V_F is increase for both CFRL and GFRL. Moreover, the materials with $W_{GPL} < 0.06$ have an increasing buckling stress as V_F is increased. Thus, materials with high W_{GPL} decrease in buckling resistance as V_F is increase and materials with a low W_{GPL} increase in buckling resistance as V_F is increased.

Increasing the number of plies in the laminate does not have a significant effect on the critical buckling stress for both CFRL and GFRL, as can be seen when comparing figure 4-31 and figure 4-33. However, increasing the fibre orientation of the plies has a large impact on CFRL. In figure 4-35, the buckling stress of all the laminates increases as V_F increases and the buckling stresses are higher for CFRL than for GFRL.

4.7.1.1 Effect of Fibre Volume on 3 layer nanocomposite with 45° fibre orientation, reinforced with glass and carbon fibre

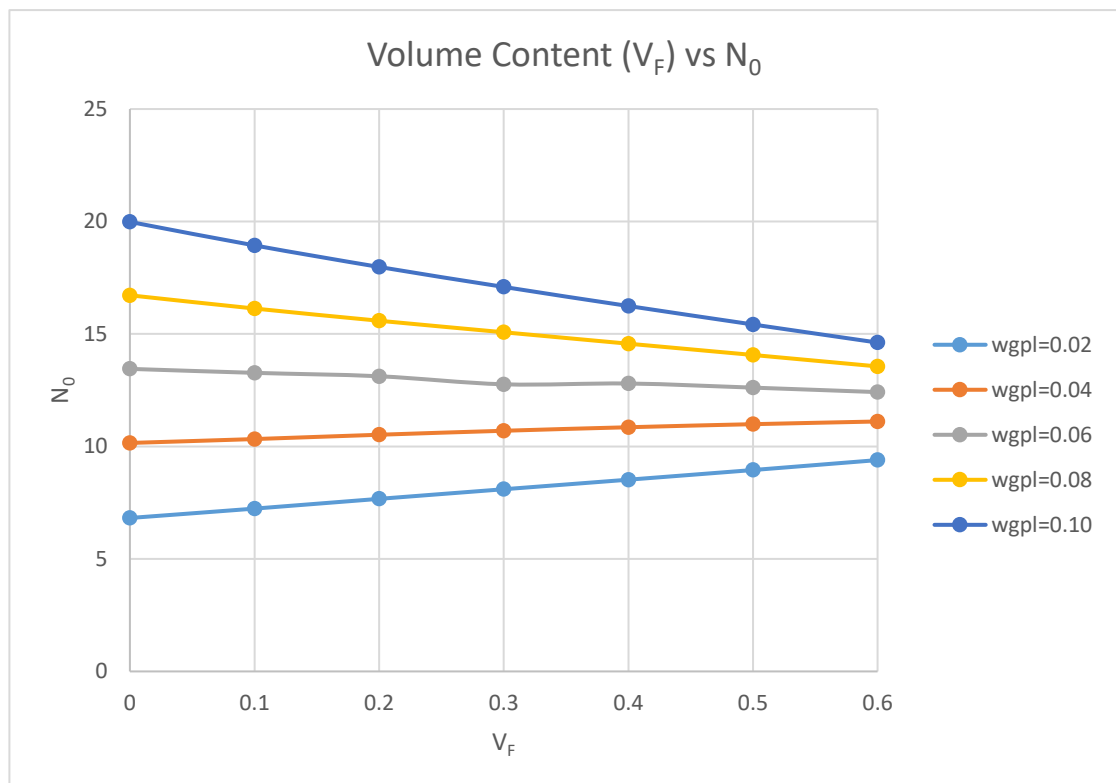


Figure 4-31 Non-Dimensional Buckling stress (N_0) vs Volume Content (V_{GPL}) for a nanocomposite reinforced with carbon fibre with 3 layers with thickness ratio of 0.2 and equal fibre orientations of 45°

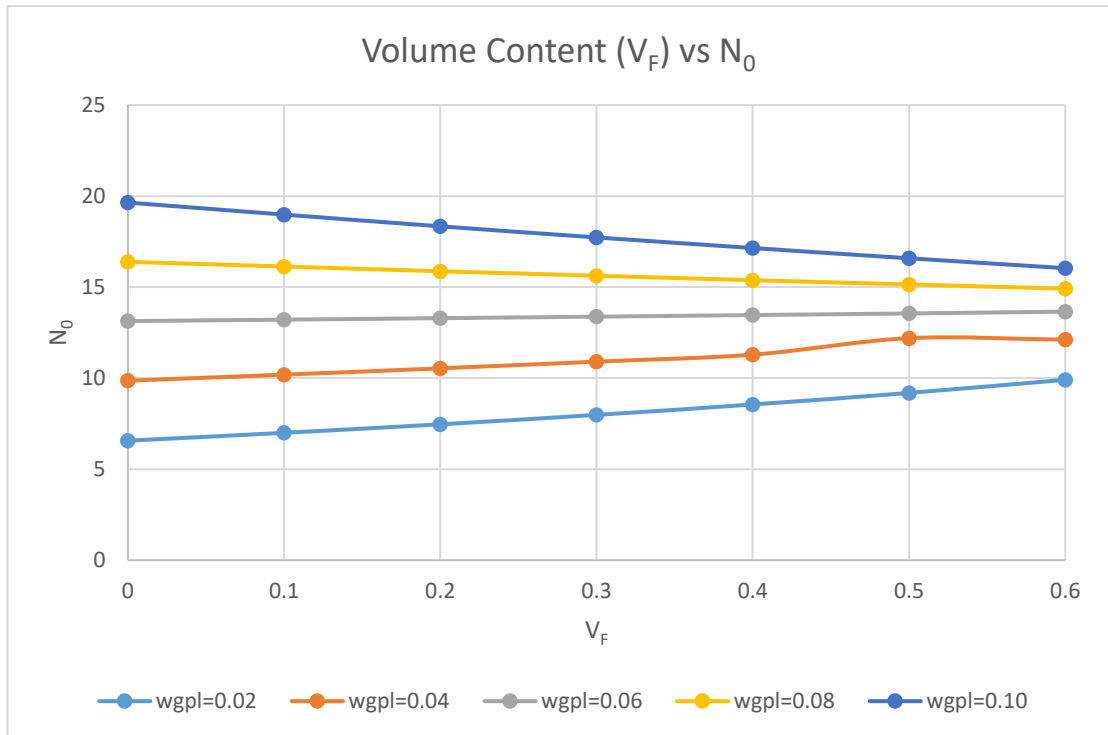


Figure 4-32 Non-Dimensional Buckling stress (N_0) vs Volume Content (VGPL) for a nanocomposite reinforced with glass fibre with 3 layers with thickness ratio of 0.2 and equal fibre orientations of 45°

4.7.1.2 Effect of Fibre Volume on 10 layer nanocomposite with 45° fibre orientation, reinforced with glass and carbon fibre

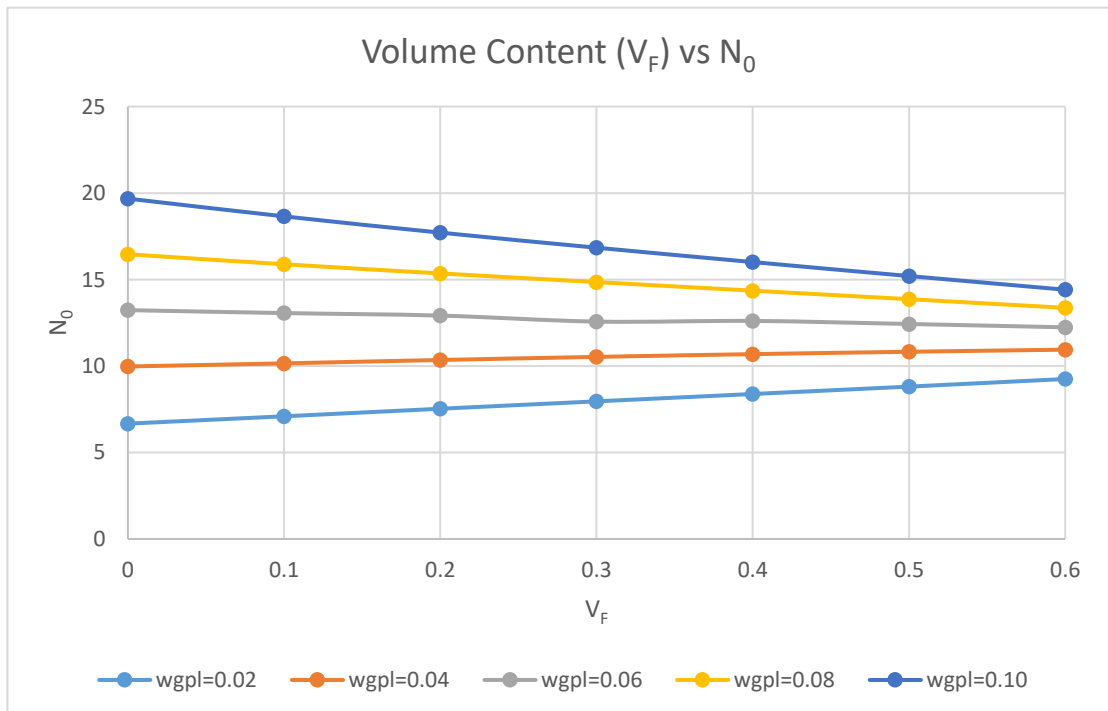


Figure 4-33 Non-Dimensional Buckling stress (N_0) vs Volume Content (VGPL) for a nanocomposite reinforced with Carbon fibre with 10 layers with equal thickness and equal fibre orientations of 45°

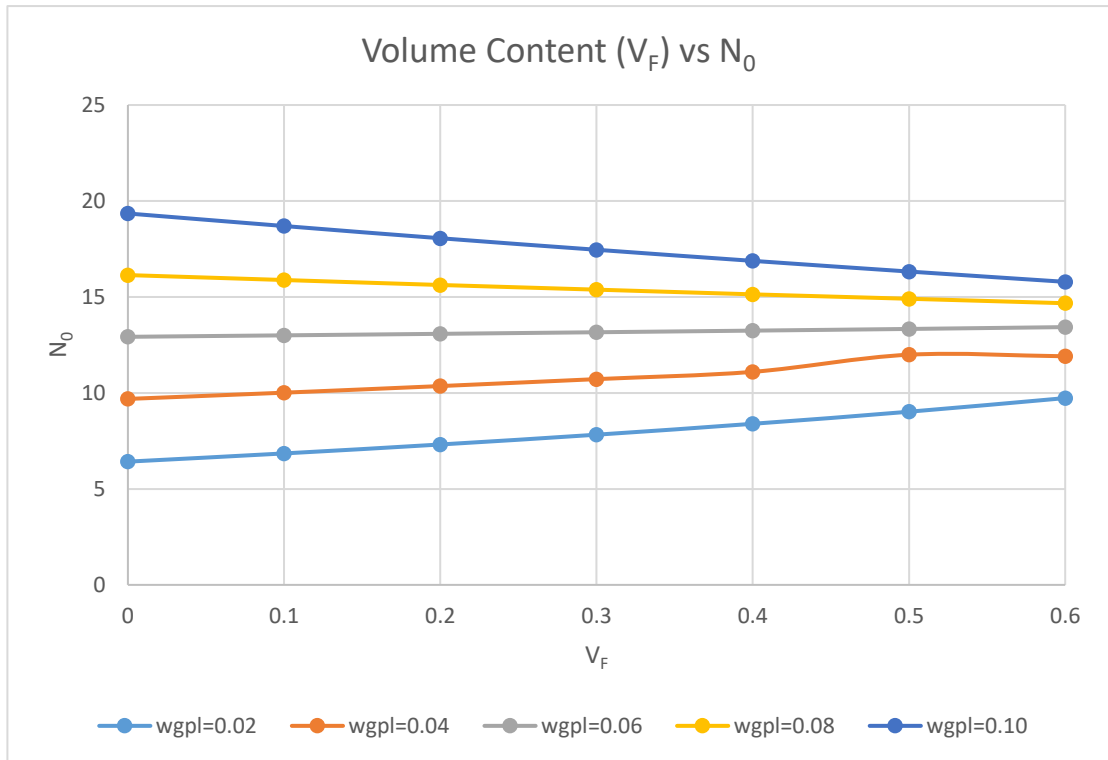


Figure 4-34 Non-Dimensional Buckling stress (N_0) vs Volume Content (V_{GPL}) for a nanocomposite reinforced with glass fibre with 10 layers with equal thickness and equal fibre orientations of 45°

4.7.1.3 Effect of Fibre Volume on 10 layer nanocomposite with 90° fibre orientation, reinforced with glass and carbon fibre

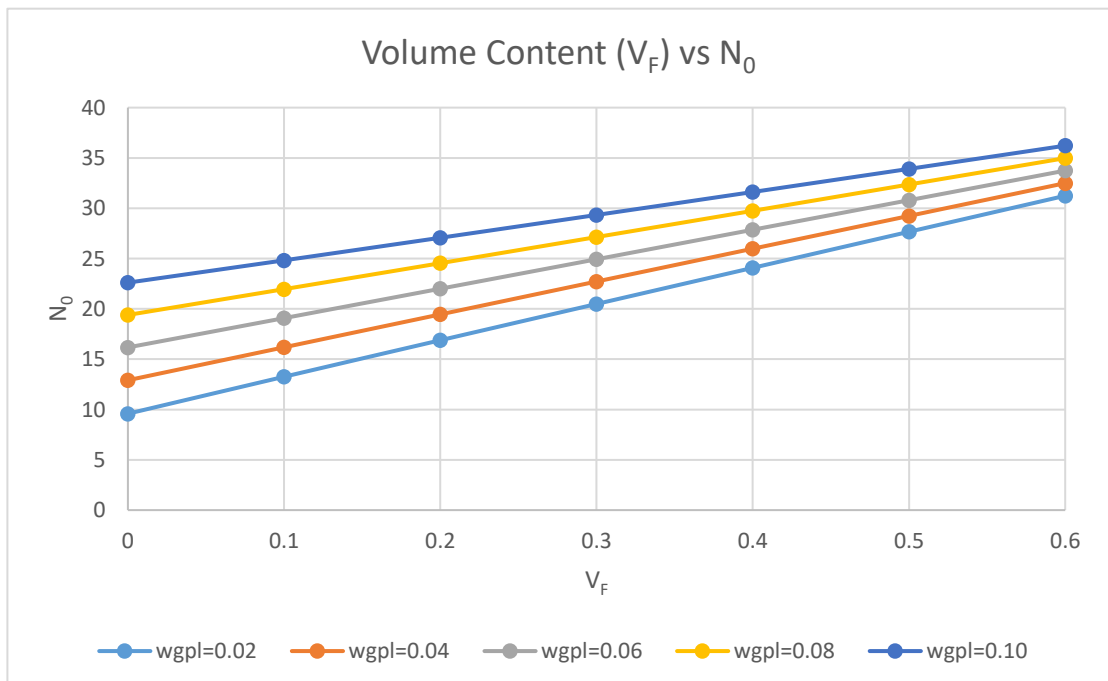


Figure 4-35 Non-Dimensional Buckling stress (N_0) vs Volume Content (V_{GPL}) for a nanocomposite reinforced with Carbon fibre with 10 layers with equal thickness and equal fibre orientation of 90°

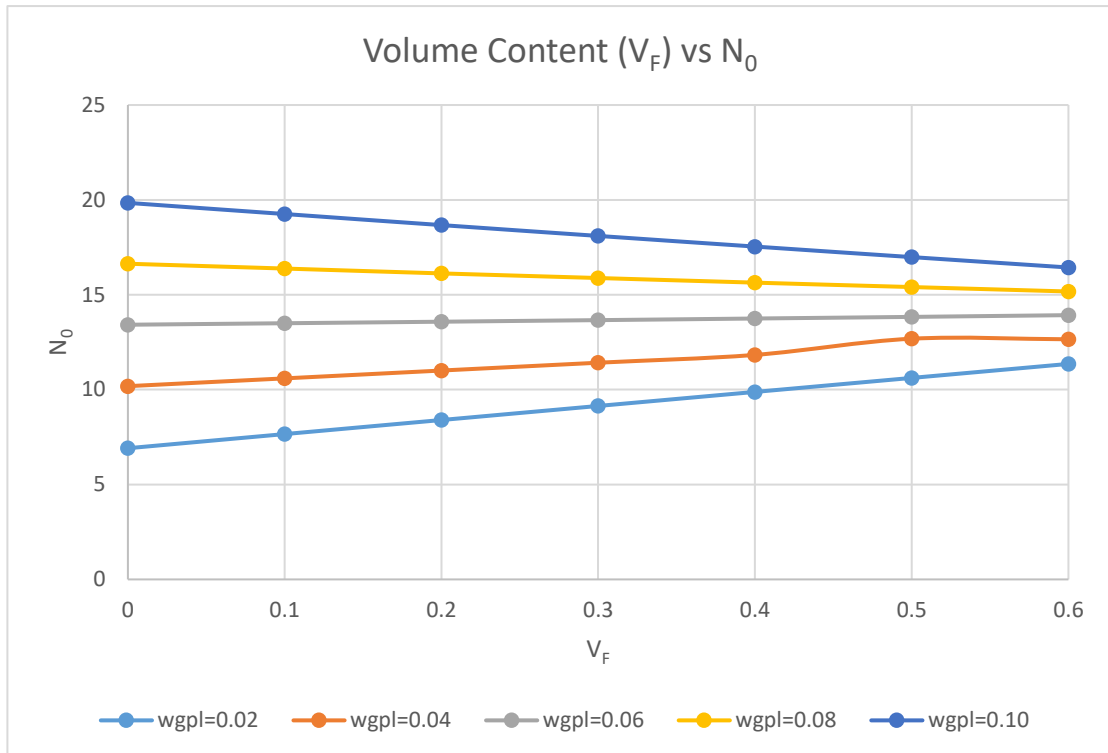


Figure 4-36 Non-Dimensional Buckling stress (N_0) vs Volume Content (V_{GPL}) for a nanocomposite reinforced with glass fibre with 10 layers with equal thickness and equal fibre orientation of 90°

4.7.2 Discussion of results

For the GFRL there is a difference in critical buckling stresses obtained when the fibre orientation is 45° and when it is 90° , however is it small. Jweeg (2015) determined that as the volume content increase buckling stress increases as well. Chiad (2018) found the same results as well. From the results on this section, it can be seen that whether the buckling stress increases or decreases when V_F is increased is dependent on factors such as graphene weight fraction, type of load on structure and fibre orientation. Thus as V_F increases, the buckling can increase or decrease depending on these properties. The results of this dissertation differ from those determined by Jweeg (2015) and Chiad (2018) because the matrix used by these scholars was not reinforced with GnPs nanofillers. In addition, as can be seen from result the amount of nanofiller in matrix is the main factor that determines if the buckling stress goes up or down. Therefore, the GFRNL with low W_{GPLs} increase critical buckling stress as the V_F increases and a GFRNL with a high W_{GPL} decrease critical buckling stress as the V_F increases.

In real life studies, these types of results are not realistic. Battawi (2018) discovered that the addition of more fibre on a composite material caused the material to be brittle and thus undermining the improvement in properties. In Battawi's research he discovered that the point at which the composite started acting brittle was at 5% fibre content (figure 1-4).

4.8. Discussion on the practicality of results

In this dissertation, the classical laminate plate theory is used. Thus, this research is conducted with the following assumptions. There are no flaws or gaps between the plies. There is no shear deformation on the laminate, thus the plies cannot slip on top of each other and the laminate acts as a single lamina. Moreover, the nanofill and reinforcement is assumed to be distributed uniformly and perfectly throughout of the laminate. These conditions may be difficult to achieve in real life since as stated by Kilic (2018) graphene to matrix interface and dispersion of graphene in matrix is still a big problem. Liang (2018) studies the solutions to this problem, however the solutions are not perfect yet, since they still have their own disadvantages and if these solutions are not conducted well they can possible make the laminate more weak.

The mass fabrications of graphene is another problem that makes some of these results unpractical. Figures 4-24 to 4-29 show the results for the effect of weight fraction on the critical buckling stress of the laminate. In these results any results corresponding to $W_{GPL} > 0.05$ are not practical since the cost of using this much graphene nanoplatelets would be too high. Thus, to overcome this problem a laminater with a high volume content should be used. An alternative is to use a material with W_{GPL} as close as possible to the cross-over point, because in this solution the laminate can have a low V_F while the W_{GPL} is not unreasonable large.

When different load conditions are applied to the laminate, the fibre orientation required to get the maximum buckling stress is changed. However due to manufacturing constrains there are only a few fibre orientations that are usually used. They are 0° , 90° , 45° and -45° (Allaire & Delgado, 2016). However with the passage of time many of the above mentioned problems will be overcome. Moreover there are ways of using the crurrent technology and means to obtain resonably performing nanocomposites.

CHAPTER 5

CONCLUSION AND RECOMMENDATIONS

Structural response of nanocomposite laminates

A laminated composite with layers made out of a polymer nanocomposite, reinforced with either carbon fibres or glass fibres, is analysed for buckling resistance using ANSYS. The laminate is composed of 3 layers, except when the laminate is tested for its response when number of layer and stacking orders are varied. The properties of the surface layers and the middle layers are different for different types of analysis. The effect of fibre orientation, number of layers, stacking sequence, thickness ratio, aspect ratio, graphene weight fraction, fibre content and the boundary conditions on the buckling stress experienced by the laminate is examined in this dissertation.

The effect of the fibre orientation on the critical buckling stress for a 3 ply laminated composite was studied in this dissertation. It is discovered that for a uniaxially loaded laminate, when the fibre orientation is parallel to the load, the laminate will have maximum buckling resistance and when the load is perpendicular to the fibre orientation, the buckling resistance is minimum. The effect of the middle layer fibre orientation on a 3 ply laminated composite's critical buckling stress is dependent on the thickness ratio. The lower the thickness ratio the greater the effect of the middle layer fibre orientation. However the lower the thickness ratio the lower the buckling stress, because as the thickness ratio decreases, the critical buckling stress decreases. When the thickness ratio is >0.6 the middle layer fibre orientation has very little effect on the critical buckling stress.

An increase in number of plies, graphene weight fraction and aspect ratio results in the increase of the critical buckling stress of the laminate. The rate at which the buckling stress increases when weight fraction is increased depends on the volume content of the laminate. There is a cross-over point where beyond this point the laminate that initially had the highest buckling stress will have the lowest buckling stress. Moreover, at the crossover point all the laminates with different V_F 's have an equal critical buckling stress. The volume content mostly affected by the weight fraction and fibre orientation. For a laminate with the conditions used in this dissertation, When $W_{GPL} < 0.06$ the buckling stress of the laminate increases as V_F is increased. When $W_{GPL} > 0.06$ the buckling stress of the laminate decreases as V_F increases. This is true for both CFRL and GFRL. The only exception is when CFRL has a fibre orientation of 90° , in this case all the laminates have an increasing critical buckling stress regardless of W_{GPL} .

Recommendations

In order to obtain the optimum nanocomposite laminate, the following is recommended. Since it would be very costly to use a very large amount of graphene nanoplatelets and carbon fibre, the weight fraction chosen for the laminate should correspond with the crossover point. At this point the fibre volume content of the laminate has little to no effect on the strength of the laminate, thus a low amount of fibres can be used. When the crossover point is greater than $W_{GPL}=0.05$ the largest reasonable value of W_{GPL} should be used while the V_F of the laminate is kept low.

The fibre orientation should be the same for all layers and should be parallel to the load. This is the best option for a uniaxially loaded laminate with only failure under buckling as a concern. However, when there are other forces and modes of failure to be considered, other stacking sequences should be considered. The most ideal thickness ratio is 0.6, since for thickness ratios greater than 0.6 there is very little effect on the critical buckling stress.

The greatest aspect ratio possible should be used and the greatest possible plate thickness should be used since the increases in thickness increases the moment of inertia of the plate. However, the plate cannot be too thick, because the assumptions of the classical laminate plate theory do not apply to a laminate that is too thick. The classical laminate plate theory is only valid when (width (a) and height (b) $> 10*H$) (Choudhury, et al., 2017).

Lastly, a cantilever boundary condition should be avoided if a plate is going to experience buckling. The most ideal boundary conditions is CCCC. However, if it is not possible to use the CCCC boundary conditions, whatever boundary condition used should make use of clamped supports instead of simply supported supports.

REFERENCES

- Ahmad, I., Yazdani, B. & Zhu, Y., 2015. Recent advances on carbon nanotubes and graphene reinforced ceramics nanocomposites. *Nanomaterials*, 5(1), pp. 90-114.
- Akpan, E. I., Shen, X., Wetzel, B. & Friedrich, K., 2019. *Design and Synthesis of Polymer Nanocomposites*. s.l.:Elsevier.
- Allaire, G. & Delgado, G., 2016. Stacking sequence and shape optimization of laminated composite plates via a level-set method. *Journal of the Mechanics and Physics of Solids*, Volume 97, pp. 168-196.
- Atashipour, S. R. & Girhammar, U. A., 2018. Influence of Grain Inclination Angle on Shear Buckling of Laminated Timber Sheathing Products. *Structures*, Volume 13, pp. 36-46.
- Balasubramanian, A., 2011. Plate analysis with different geometries and arbitrary boundary conditions. *Masters Dissertation*.
- Barber, A. H., Cohen, S. R. & Wagner, H. D., 2003. Measurement of carbon nanotube–polymer interfacial strength. *Applied Physics Letters*, 82(23), pp. 4140-4142.
- Battawi, A., 2018. factors affecting critical buckling load of reinforced beam. *International Journal of Current Engineering and Technology*, 7(4), pp. 1531-1535.
- Berthelot, J.-M. & Frederick, F. L., 1999. Composite materials: mechanical behavior and structural analysis. *New York: Springer*, pp. 3-14.
- Callister, W. D., 2007. *Material Science and Engineering*. 7th ed. Utah: John Wiley & Sons, Inc..
- Camargo, P. H. C., Satyanarayana, K. G. & Wypych, F., 2009. Nanocomposites: synthesis, structure, properties and new application opportunities. *Materials Research*, 12(1), pp. 1-39 .
- Carleton, J. E., 2016. *Introduction to structural analysis*. [Online] Available at: <http://www.learnaboutstructures.com/Structural-Analysis> [Accessed 28 November 2019].
- Chamis, C. C., 1983. Simplified Composite Micromechanics Equations for Hygral, Thermal and Mechanical Properties. *NASA*.
- Chamis, C. C., 1984. Simplified Composite Micromechanics Equations for Strength, Fracture Toughness, Impact Resistance and Environmental Effect. *NASA*.
- Changgu, L., Wei, X., Kysar, J. W. & Hone, J., 2008. Measurement of the elastic properties and intrinsic strength of monolayer graphene. *Science*, 321(5887), pp. 385-388.
- Chiad, J. S., Al-Waily, M. & Abdullah, M., 2018. Buckling Investigation of Isotropic Composite Plate Reinforced by Different Types of Powder. *Technology*, 9(8), pp. 305-317.

- Choudhury, A., Mondal, S. C. & Sarkar, S., 2017. Effect of Laminated Angle and Thickness on Analysis of Composite Plate Under Thermo Mechanical Loading. *Strojnický časopis-Journal of Mechanical Engineering* , 67((1)), pp. 5-22.
- Chung, D. D. & Chung, D., 2012. *Carbon Fiber Composites*. s.l.:Elsevier.
- Chung, D. D. L., 2017. Polymer-Matrix Composites: Structure and Processing.. *Carbon Composites*, pp. 161-217.
- Dai, G. & Mishnaevsky Jr, L., 2014. Graphene Reinforced Nanocomposites: 3D simulation of damage and fracture. *Computational Material Science*, pp. 684-692.
- de Oliveira, A. D. & Beatrice, C. A. G., 2018. Polymer Nanocomposites with Different Types of Nanofiller. *Nanocomposites-Recent Evolutions* .
- Derek, H., 1981. *introduction to composite materials*. s.l.:Cambridge University Press.
- Dhuban, S. B., Karuppanan, S., Mengal, A. N. & Patil, S. S., 2017. Effect of fiber orientation and ply stacking sequence on buckling behaviour of basalt-carbon hybrid composite laminates. *Indian Journal of Engineering and Materials Sciences* , Volume 23, pp. 187-193.
- Du, J. & Cheng, H.-m., 2012. The fabrication, Properties, and Uses of Graphene/polymer composites. *Macromolecular Chemistry and Physics*, 213(10-11), pp. 1060-1077.
- Feng, Z. et al., 2019. Fabrication of Graphene-Reinforced Nanocomposites with Improved Fracture Toughness in Net Shape for Complex 3D Structures via Digital Light Processing. *Journal of Carbon Research*, 5(2).
- Fiscsher , H., 2003. Polymer nanocomposites: from fundamental research to specific applications. *Materials Science and Engineering*, 23(6-8), pp. 763-772.
- Fu , S., Sun, Z., Huang, P. & Li, Y., 2019. Some Basic Aspects of Polymer Nanocomposites: A Critical Review. *Nano Materials Science* , 1(1), pp. 2-30.
- Halkyard, J., 2005. *Handbook of offshore Engineering*. Houston: Elsevier.
- Hallad, S. A. et al., 2018. Graphene Reinforced Natural Fiber Nanocomposites for Structural Applications. *IOP Conference Series: Materials Science and Engineering* , 376(1).
- Hamani, N. et al., 2013. Effect of Fiber Orientation on the Critical Buckling Load of Symmetric Composite Laminated Plates. *Advanced Materials Research*, Volume 629, pp. 95-99.
- Heidari-Rarani, M., Khalkhali-Sharifi, S. S. & Shokrieh, M. M., 2014. Effect of ply stacking sequence on buckling behavior of E-glass/epoxy. *Composite Material Science*, Volume 89, pp. 89-96.
- Herakovich, C. T., 1998. *Mechanics of Fibrous Composites*. New York: John Wiley & Sons.
- Hosseini, M. & Hadi, A., 2014. Buckling behavior of Composite Plates with Circular Embedded Delaminations under In-Plane Compressive loading. *Technical Journal of Engineering and Applied Sciences*, 3(13), pp. 1238-1245.

- Idowu, I. D. et al., 2015. The use of polypropylene in bamboo fibre composites and their mechanical properties—A review. *Journal of Reinforced Plastics and Composites*, 34(16), pp. 1347-1356.
- Jun, Y.-S., Um, J. G., Jiang, G. & Yu, A., 2018. A Study on the effects of graphene nanoplatelets (GnPs) sheet sizes from a few to hundred microns on the thermal, mechanical, and electrical properties of polypropylene (PP)/GnPs composites. *eXPRESS Polymer Letters*, 12(10), pp. 885-897.
- Jweeg, M. J., Al-waily, M. & Deli, A. A., 2015. Theoretical and Numerical Investigation of Buckling of Orthotropic Hyper Composite Plates. *International Journal of Mechanical & Mechatronics Engineering*, 15(4), pp. 1-12.
- Khandan, R. et al., 2012. Optimum design of fibre orientation in composite laminate plates for out-plane stresses. *Advances in Material Science and engineering*.
- Kilic, U., Daghash, S. & Ozbulut, O., 2018. Mechanical Characterization of Polymer Nanocomposites Reinforced with Graphene Nanoplatelets. *International Congress on polymers in Concrete*, pp. 689-695.
- Lau, K.-T. & Hui, D., 2002. Effectiveness of using carbon nanotubes as nano-reinforcements for advanced composite structures. *Carbon*, 9(40), pp. 1605-1606.
- Liang, A. et al., 2018. Recent Developments Concerning the Dispersion methods and mechanisms of Graphene. *Coatings*, 8(1), pp. 1-23.
- Liang, J.-Z., Du, Q., Tsui, C. P. & Tang, C. Y., 2016. Tensile Properties of Graphene nanoplatelets reinforced polypropylene composites. *Composites Part B: Engineering*, Volume 95, pp. 166-171.
- Mao, S. C. et al., 2008. In situ EBSD investigations of the asymmetric stress-induced martensitic transformation in TiNi shape memory alloys under bending. *Materials Science and Engineering*, 498((1-2)), pp. 278-282.
- Mehrabadi, S. J., Aragh, B. S., Khoshkharesh, V. & Taherpour, A., 2012. Mechanical buckling of nanocomposite rectangular plate reinforced by aligned and straight single-walled carbon nanotubes. *Composites Part B: Engineering*, 43(4), pp. 2031-2040.
- Mészáros, L. & Szakács, J., 2014. Elastic Recovery at Graphene Reinforced PA 6 Nanocomposites. *Nanocon*, pp. 51-55.
- Narayana, A. L., Rao, K. & Kumar, R. V., 2013. Effect of Plate Aspect Ratio on Buckling Strength of Rectangular Composite Plate with Square/rectangular Cutout Subjected to Various Linearly Varying In-Plane Loading Using Fem. *Recent Advances in Robotics, Aeronautical and Mechanical Engineering*, pp. 92-99.
- Nurhaniza, M. et al., 2010. Finite element analysis of composites materials for aerospace applications. *IOP Conference series*, 11(1).
- Okpala, C. C., 2013. Nanocomposites - An Overview. *International Journal of Engineering Research and Development*, 8(11), pp. 17-23.
- Pagano, N. J. & Pipes, R. B., 1971. The Influence of Stacking Sequence on laminate Strength. *Journal of Composite Materials*, 5(1), pp. 50-57.

- Pandya, S. et al., 2013. NANOCOMPOSITES AND IT'S APPLICATION-REVIEW. *International Journal of Pharmaceutical Sciences and Research*, 4(1), pp. 19-28.
- Parashar , A. & Mertiny, P., 2012. Representative volume element to estimate buckling behaviour of graphene/polymer nanocomposite. *Nanoscale research letters*, 7(1), p. 515.
- Radebe, I. S., Drosopoulos, G. A. & Adali, S., 2019. Buckling of non-uniformly distributed graphene and fibre reinforced multiscale angle-ply laminates. *Meccanica*, 54(14), pp. 2263-2279.
- Rafiee, M. A., Radiee, J. & Yu, Z., 2009. Buckling Resistance Graphene Nanocomposites. *Applied Physics Letters*, 95(22), pp. 223103-1 - 223103-3.
- Reddy, B. S., Kumar, J. S., Reddy, C. E. & Reddy , K., 2013. Buckling analysis of functionally graded material plates using higher order shear deformation theory. *Journal of Composites*.
- Rezaei, F., Yunus, R., Ibrahim, N. A. & Mahdi, E. S., 2008. Development of Short-Carbon-Fiber-Reinforced Polypropylene Composite for Car Bonnet. *Polymer-Plastics Technology and Engineering* , 47(4), pp. 351-357.
- Roylance, D., 2000. Laminated Composite Plates. *Massachusetts Institute of Technology Cambridge*.
- Song, M., Yang, J. & Kitipornchai, S., 2018. Bending and Buckling Analyses of Functionally Graded Polymer Composite Plates Reinforced with Graphene Nanoplatelets. *Composites Part B: Engineering*, pp. 106-113.
- STREM, n.d. *STREM Graphene Nanoplatelets*. [Online] Available at: https://www.strem.com/uploads/resources/documents/graphene_nanoplatelets_copy_1.pdf [Accessed 24 September 2019].
- Suleiman, O. M. E., Osman, M. Y. & Hassan, T., 2019. Effect of boundary conditions on buckling load for laminated composite plates. *Global Journal of Engineering Science and Researches*, 2(1), pp. 1-8.
- Suna, B., 2014. Design and Analysis of Laminated Composite Materials. *Doctoral Dissertation*.
- Tegaw, S. K., 2018. Determination of the effect of fiber volume fraction on the buckling Behavior of ant-symmetric angle ply laminate carbon fiber, boron fiber and glass fiber composite plates. *International Journal of Scientific & Engineering Research*, 9(7), pp. 890-901.
- University of New South Wales, 2018. *UNSW Sydney School of Material Science and Engineering*. [Online] Available at: <http://www.materials.unsw.edu.au/materials-changed-history> [Accessed 11 November 2019].

- Vodenitcharova, T. & Zhang, L. C., 2005. Bending and local buckling of a nanocomposite beam reinforced by a single-walled carbon nanotube. *International Journal of Solids and Structures*, 43(10), pp. 3006-3024.
- Wood, J., 2008. The top ten advances in materials science. *Materials Today*, 11(1-2), pp. 40-45.
- Zhang, Y., Franklin, N. W., Chen, R. J. & Dai, H., 2000. Metal coating on suspended carbon nanotubes and its implication to metal-tube interaction. *Chemical Physics Letters*, 331(1), pp. 35-41.

APPENDIX A

GFRNL LAYER PROPERTIES

A.1 Glass fibre reinforcement properties

A.1.1 Material properties where V_F is kept constant while varying W_{GPL}

$$V_F = 0.1$$

Table A-1 Glass fibre material properties when V_F is kept constant at 0.1, while W_{GPL} is varied.

W_{GPL}	E_{11} (Pa)	E_{22} (Pa)	G_{12} (Pa)	ν_{12}
0.00	10 390 000 000.00	4 198 884 219.68	1 558 226 945.76	0.335
0.01	19 533 286 038.04	15 660 457 225.15	5 843 115 552.51	0.333
0.02	28 674 729 364.18	26 349 445 877.87	9 867 883 173.84	0.332
0.03	37 814 334 098.45	36 518 036 795.10	13 713 227 672.03	0.330
0.04	46 952 104 354.64	46 319 237 759.73	17 430 400 423.15	0.328
0.05	56 088 044 240.37	55 851 269 580.94	21 053 514 729.84	0.327
0.06	65 222 157 857.07	65 180 073 575.73	24 606 156 746.28	0.325
0.07	74 354 449 299.97	74 351 565 722.47	28 105 155 425.66	0.323
0.08	83 484 922 658.17	83 398 702 346.63	31 562 840 652.35	0.322
0.09	92 613 582 014.63	92 345 751 358.15	34 988 452 555.19	0.320
0.10	101 740 431 446.13	101 210 978 695.90	38 389 052 299.90	0.319
0.11	110 865 475 023.40	110 008 396 048.63	41 770 128 640.75	0.317
0.12	119 988 716 811.00	118 749 931 479.39	45 136 013 544.95	0.315
0.13	129 110 160 867.43	127 441 233 673.30	48 490 167 192.70	0.314
0.14	138 229 811 245.12	136 092 236 954.39	51 835 394 969.51	0.312
0.15	147 347 671 990.41	144 707 566 171.83	55 173 987 908.30	0.310

$$V_F = 0.2$$

Table A-2 Glass fibre material properties when V_F is kept constant at 0.2, while W_{GPL} is varied.

W_{GPL}	E_{11} (Pa)	E_{22} (Pa)	G_{12} (Pa)	ν_{12}
0.00	17 280 000 000.00	5 052 801 030.26	1 879 031 569.05	0.320
0.01	25 407 365 367.15	17 978 094 189.90	6 749 447 423.29	0.319
0.02	33 533 092 768.16	29 167 073 173.82	11 016 139 009.76	0.317
0.03	41 657 185 865.29	39 262 918 341.55	14 888 818 715.72	0.316
0.04	49 779 648 315.24	48 625 858 414.98	18 490 968 049.30	0.314
0.05	57 900 483 769.22	57 473 351 036.34	21 900 027 501.06	0.313
0.06	66 019 695 872.95	65 944 438 130.43	25 167 025 320.44	0.311
0.07	74 137 288 266.64	74 132 169 458.88	28 326 953 211.21	0.310
0.08	82 253 264 585.04	82 101 167 070.13	31 404 607 175.05	0.308
0.09	90 367 628 457.44	89 897 711 484.21	34 418 048 860.01	0.307
0.10	98 480 383 507.67	97 555 818 103.64	37 380 746 450.53	0.305
0.11	106 591 533 354.13	105 101 048 053.81	40 302 947 660.15	0.304
0.12	114 701 081 609.78	112 552 981 291.75	43 192 588 036.46	0.302
0.13	122 809 031 882.16	119 926 869 555.10	46 055 908 266.10	0.301
0.14	130 915 387 773.44	127 234 769 855.59	48 897 883 734.35	0.300
0.15	139 020 152 880.36	134 486 339 482.93	51 722 529 742.57	0.298

$$V_F = 0.3$$

Table A-3 Glass fibre material properties when V_F is kept constant at 0.3, while W_{GPL} is varied.

W_{GPL}	E_{11} (Pa)	E_{22} (Pa)	G_{12} (Pa)	V_{12}
0.00	24 170 000 000.00	6 119 771 863.12	2 281 073 000.23	0.305
0.01	31 281 444 696.25	20 693 585 812.48	7 820 022 326.93	0.304
0.02	38 391 456 172.14	32 320 046 952.66	12 314 523 949.84	0.302
0.03	45 500 037 632.12	42 230 234 459.16	16 174 217 244.83	0.301
0.04	52 607 192 275.83	51 053 211 296.94	19 620 116 702.57	0.300
0.05	59 712 923 298.07	59 143 930 777.92	22 781 973 198.57	0.299
0.06	66 817 233 888.83	66 717 872 099.62	25 740 973 002.43	0.297
0.07	73 920 127 233.31	73 913 418 681.29	28 550 515 229.05	0.296
0.08	81 021 606 511.91	80 823 507 477.30	31 247 163 000.14	0.295
0.09	88 121 674 900.26	87 512 870 071.64	33 856 793 870.07	0.293
0.10	95 220 335 569.22	94 027 978 369.17	36 398 237 626.93	0.292
0.11	102 317 591 684.86	100 403 059 103.70	38 885 522 686.04	0.291
0.12	109 413 446 408.55	106 663 877 954.49	41 329 314 760.24	0.290
0.13	116 507 902 896.89	112 830 202 061.61	43 737 867 482.81	0.288
0.14	123 600 964 301.76	118 917 449 816.22	46 117 667 803.16	0.287
0.15	130 692 633 770.32	124 937 824 545.45	48 473 884 683.99	0.286

$$V_F = 0.4$$

Table A-4 Glass fibre material properties when V_F is kept constant at 0.4, while W_{GPL} is varied.

W_{GPL}	E_{11} (Pa)	E_{22} (Pa)	G_{12} (Pa)	ν_{12}
0.00	31 060 000 000.00	7 490 897 807.20	2 799 681 772.16	0.290
0.01	37 155 524 025.36	23 918 996 761.47	9 103 934 114.95	0.289
0.02	43 249 819 576.12	35 872 023 372.93	13 794 540 413.46	0.288
0.03	49 342 889 398.96	45 448 164 786.74	17 585 562 039.33	0.287
0.04	55 434 736 236.43	53 611 030 122.51	20 824 720 779.58	0.286
0.05	61 525 362 826.92	60 865 216 875.73	23 701 624 079.61	0.284
0.06	67 614 771 904.71	67 500 537 863.63	26 328 462 684.46	0.283
0.07	73 702 966 199.98	73 695 310 545.24	28 775 862 612.90	0.282
0.08	79 789 948 438.79	79 565 270 354.84	31 090 502 236.49	0.281
0.09	85 875 721 343.08	85 188 811 015.51	33 304 469 232.32	0.280
0.10	91 960 287 630.76	90 620 920 887.61	35 440 548 326.61	0.279
0.11	98 043 650 015.60	95 901 311 390.36	37 515 364 882.31	0.278
0.12	104 125 811 207.33	101 059 377 937.31	39 541 334 471.05	0.277
0.13	110 206 773 911.62	106 117 345 589.41	41 527 916 033.11	0.276
0.14	116 286 540 830.08	111 092 329 827.73	43 482 442 545.97	0.275
0.15	122 365 114 660.27	115 997 725 234.17	45 410 686 539.49	0.274

$$V_F = 0.5$$

Table A-5 Glass fibre material properties when V_F is kept constant at 0.5, while W_{GPL} is varied.

W_{GPL}	E_{11} (Pa)	E_{22} (Pa)	G_{12} (Pa)	V_{12}
0.00	37 950 000 000.00	9 317 852 834.74	3 494 149 396.81	0.275
0.01	43 029 603 354.47	27 812 840 149.32	10 672 008 061.47	0.274
0.02	48 108 182 980.10	39 903 857 992.01	15 497 167 432.19	0.273
0.03	53 185 741 165.80	48 949 858 840.36	19 142 317 430.31	0.272
0.04	58 262 280 197.02	56 310 123 844.96	22 112 605 200.24	0.271
0.05	63 337 802 355.76	62 639 553 506.50	24 661 450 933.57	0.270
0.06	68 412 309 920.59	68 292 601 702.42	26 929 979 362.94	0.269
0.07	73 485 805 166.65	73 477 842 222.98	29 003 016 835.41	0.269
0.08	78 558 290 365.65	78 326 016 164.65	30 934 619 051.46	0.268
0.09	83 629 767 785.90	82 923 239 819.50	32 760 863 487.46	0.267
0.10	88 700 239 692.30	87 328 547 241.73	34 506 749 817.18	0.266
0.11	93 769 708 346.33	91 583 760 582.05	36 190 148 682.05	0.265
0.12	98 838 176 006.11	95 719 336 916.51	37 824 173 782.32	0.264
0.13	103 905 644 926.35	99 757 983 319.61	39 418 665 921.74	0.263
0.14	108 972 117 358.40	103 716 974 585.96	40 981 154 112.50	0.262
0.15	114 037 595 550.23	107 609 686 125.78	42 517 496 773.45	0.261

A.1.2 Material properties where W_{GPL} is kept constant while varying V_F

$W_{GPL} = 0.02$

Table A-6 Glass fibre material properties when W_{GPL} is kept constant at 0.02, while V_F is varied.

V_F	E_{11} (Pa)	E_{22} (Pa)	G_{12} (Pa)	V_{12}
0	23 816 365 960.20	23 816 365 960.20	8 845 140 959.64	0.346
0.1	28 674 729 364.18	26 349 445 877.87	9 867 883 173.84	0.332
0.2	33 533 092 768.16	29 167 073 173.82	11 016 139 009.76	0.317
0.3	38 391 456 172.14	32 320 046 952.66	12 314 523 949.84	0.302
0.4	43 249 819 576.12	35 872 023 372.93	13 794 540 413.46	0.288
0.5	48 108 182 980.10	39 903 857 992.01	15 497 167 432.19	0.273
0.6	52 966 546 384.08	44 519 835 502.39	17 476 713 898.70	0.259

$W_{GPL} = 0.04$

Table A-7 Glass fibre material properties when W_{GPL} is kept constant at 0.04, while V_F is varied.

V_F	E_{11} (Pa)	E_{22} (Pa)	G_{12} (Pa)	V_{12}
0	44 124 560 394.05	44 124 560 394.05	16 432 349 874.99	0.343
0.1	46 952 104 354.64	46 319 237 759.73	17 430 400 423.15	0.328
0.2	49 779 648 315.24	48 625 858 414.98	18 490 968 049.30	0.314
0.3	52 607 192 275.83	51 053 211 296.94	19 620 116 702.57	0.300
0.4	55 434 736 236.43	53 611 030 122.51	20 824 720 779.58	0.286
0.5	58 262 280 197.02	56 310 123 844.96	22 112 605 200.24	0.271
0.6	61 089 824 157.62	59 162 529 340.64	23 492 715 576.21	0.257

W_{GPL} = 0.06*Table A-8 Glass fibre material properties when W_{GPL} is kept constant at 0.06, while V_F is varied*

V_F	E₁₁ (Pa)	E₂₂ (Pa)	G₁₂ (Pa)	V₁₂
0	64 424 619 841.19	64 424 619 841.19	24 057 925 246.80	0.339
0.1	65 222 157 857.07	65 180 073 575.73	24 606 156 746.28	0.325
0.2	66 019 695 872.95	65 944 438 130.43	25 167 025 320.44	0.311
0.3	66 817 233 888.83	66 717 872 099.62	25 740 973 002.43	0.297
0.4	67 614 771 904.71	67 500 537 863.63	26 328 462 684.46	0.283
0.5	68 412 309 920.59	68 292 601 702.42	26 929 979 362.94	0.269
0.6	69 209 847 936.47	69 094 233 913.41	27 546 031 473.78	0.256

W_{GPL} = 0.08*Table A-9 Glass fibre material properties when W_{GPL} is kept constant at 0.08, while V_F is varied*

V_F	E₁₁ (Pa)	E₂₂ (Pa)	G₁₂ (Pa)	V₁₂
0	84 716 580 731.31	84 716 580 731.31	31 721 869 382.38	0.335
0.1	83 484 922 658.17	83 398 702 346.63	31 562 840 652.35	0.322
0.2	82 253 264 585.04	82 101 167 070.13	31 404 607 175.05	0.308
0.3	81 021 606 511.91	80 823 507 477.30	31 247 163 000.14	0.295
0.4	79 789 948 438.78	79 565 270 354.84	31 090 502 236.49	0.281
0.5	78 558 290 365.65	78 326 016 164.65	30 934 619 051.46	0.268
0.6	77 326 632 292.52	77 105 318 531.89	30 779 507 670.18	0.254

$$W_{GPL} = 0.10$$

Table A-10 Glass fibre material properties when W_{GPL} is kept constant at 0.02, while V_F is varied

V_F	E_{11} (Pa)	E_{22} (Pa)	G_{12} (Pa)	V_{12}
0	105 000 479 384.59	105 000 479 384.59	39 424 184 691.53	0.332
0.1	101 740 431 446.13	101 210 978 695.90	38 389 052 299.90	0.319
0.2	98 480 383 507.67	97 555 818 103.64	37 380 746 450.53	0.305
0.3	95 220 335 569.22	94 027 978 369.17	36 398 237 626.93	0.292
0.4	91 960 287 630.76	90 620 920 887.61	35 440 548 326.61	0.279
0.5	88 700 239 692.30	87 328 547 241.73	34 506 749 817.18	0.266
0.6	85 440 191 753.84	84 145 162 772.53	33 595 959 132.28	0.253

A.2. Carbon fibre reinforcement

A.2.1 Material properties where V_F is kept constant while varying W_{GPL}

$$V_F = 0.1$$

Table A-11 Carbon fibre material properties when V_F is kept constant at 0.1, while W_{GPL} is varied.

W_{GPL}	E_{11} (Pa)	E_{22} (Pa)	G_{12} (Pa)	ν_{12}
0,00	29 450 000 000,00	4 017 899 761,34	1 555 928 443,18	0,34
0,01	38 593 286 038,04	14 113 374 555,12	5 816 639 840,82	0,333
0,02	47 734 729 364,18	23 286 510 874,36	9 804 880 775,51	0,332
0,03	56 874 334 098,45	32 103 972 749,55	13 610 167 032,02	0,330
0,04	66 012 104 354,64	40 746 557 423,40	17 287 567 086,75	0,328
0,05	75 148 044 240,37	49 289 860 249,75	20 872 817 884,04	0,327
0,06	84 282 157 857,07	57 771 076 711,24	24 390 123 275,85	0,325
0,07	93 414 449 299,97	66 210 638 207,37	27 856 459 186,48	0,323
0,08	102 544 922 658,18	74 620 700 921,71	31 284 084 272,13	0,322
0,09	111 673 582 014,63	83 008 950 812,10	34 682 072 051,26	0,320
0,10	120 800 431 446,13	91 380 485 942,66	38 057 282 311,11	0,319
0,11	129 925 475 023,40	99 738 821 554,85	41 414 997 440,33	0,317
0,12	139 048 716 811,00	108 086 460 486,82	44 759 351 199,73	0,315
0,13	148 170 160 867,43	116 425 233 494,50	48 093 624 845,78	0,314
0,14	157 289 811 245,12	124 756 510 940,60	51 420 456 135,52	0,312
0,15	166 407 671 990,41	133 081 339 212,61	54 741 989 716,76	0,310

$$V_F = 0.2$$

Table A-12 Carbon fibre material properties when V_F is kept constant at 0.2, while W_{GPL} is varied.

W_{GPL}	E_{11} (Pa)	E_{22} (Pa)	G_{12} (Pa)	ν_{12}
0,00	55 400 000 000,00	4 618 556 701,03	1 873 348 840,88	0,320
0,01	63 527 365 367,15	14 582 898 755,30	6 687 507 315,64	0,319
0,02	71 653 092 768,16	22 768 314 066,42	10 874 730 653,40	0,317
0,03	79 777 185 865,29	30 336 379 178,00	14 664 847 400,02	0,316
0,04	87 899 648 315,24	37 617 627 076,71	18 188 483 036,59	0,314
0,05	96 020 483 769,22	44 741 993 447,84	21 525 371 658,41	0,313
0,06	104 139 695 872,95	51 770 946 526,24	24 726 940 270,78	0,311
0,07	112 257 288 266,64	58 737 335 846,31	27 827 846 706,16	0,310
0,08	120 373 264 585,04	65 660 311 931,95	30 852 299 513,51	0,308
0,09	128 487 628 457,45	72 551 793 634,71	33 817 720 009,85	0,307
0,10	136 600 383 507,68	79 419 587 675,16	36 736 965 127,65	0,305
0,11	144 711 533 354,13	86 269 021 616,49	39 619 730 375,64	0,304
0,12	152 821 081 609,78	93 103 855 927,08	42 473 465 293,28	0,302
0,13	160 929 031 882,16	99 926 820 989,37	45 303 988 213,76	0,301
0,14	169 035 387 773,44	106 739 947 446,61	48 115 909 581,52	0,300
0,15	177 140 152 880,36	113 544 777 081,68	50 912 929 947,46	0,298

$$V_F = 0.3$$

Table A-13 Carbon fibre material properties when V_F is kept constant at 0.3, while W_{GPL} is varied.

W_{GPL}	E_{11} (Pa)	E_{22} (Pa)	G_{12} (Pa)	ν_{12}
0,00	81 350 000 000,00	5 323 529 411,76	2 270 267 057,97	0,305
0,01	88 461 444 696,25	15 068 571 548,23	7 709 879 628,26	0,304
0,02	95 571 456 172,14	22 261 394 951,79	12 074 792 996,83	0,302
0,03	102 680 037 632,12	28 660 891 934,10	15 807 846 590,28	0,301
0,04	109 787 192 275,83	34 711 201 269,93	19 138 861 159,17	0,300
0,05	116 892 923 298,07	40 576 745 368,54	22 198 974 372,64	0,299
0,06	123 997 233 888,83	46 332 481 461,74	25 068 473 240,95	0,297
0,07	131 100 127 233,31	52 017 465 621,04	27 799 263 584,68	0,296
0,08	138 201 606 511,91	57 654 048 694,99	30 426 392 583,52	0,295
0,09	145 301 674 900,26	63 255 945 498,04	32 974 379 234,14	0,293
0,10	152 400 335 569,22	68 832 038 814,23	35 460 891 548,14	0,292
0,11	159 497 591 684,86	74 388 335 487,22	37 898 983 171,12	0,291
0,12	166 593 446 408,55	79 929 043 450,25	40 298 507 488,57	0,290
0,13	173 687 902 896,89	85 457 198 468,86	42 667 041 729,53	0,288
0,14	180 780 964 301,76	90 975 045 922,47	45 010 508 341,80	0,287
0,15	187 872 633 770,32	96 484 282 493,29	47 333 603 348,62	0,286

$$V_F = 0.4$$

Table A-14 Carbon fibre material properties when V_F is kept constant at 0.4, while W_{GPL} is varied.

W_{GPL}	E_{11} (Pa)	E_{22} (Pa)	G_{12} (Pa)	V_{12}
0,00	107 300 000 000,00	6 162 576 687,12	2 780 823 635,86	0,290
0,01	113 395 524 025,36	15 571 240 621,95	8 927 059 409,62	0,289
0,02	119 489 819 576,12	21 765 389 333,13	13 430 380 659,91	0,288
0,03	125 582 889 398,96	27 070 494 566,90	17 050 743 107,38	0,287
0,04	131 674 736 236,43	32 004 360 799,36	20 142 889 794,14	0,286
0,05	137 765 362 826,92	36 747 779 766,31	22 894 661 161,43	0,284
0,06	143 854 771 904,71	41 380 342 500,39	25 414 821 931,40	0,283
0,07	149 942 966 199,98	45 942 557 725,73	27 770 709 776,89	0,282
0,08	156 029 948 438,78	50 457 218 136,08	30 006 244 272,42	0,281
0,09	162 115 721 343,08	54 938 131 121,83	32 151 292 789,67	0,280
0,10	168 200 287 630,76	59 394 149 574,06	34 226 874 326,26	0,279
0,11	174 283 650 015,60	63 831 211 478,37	36 248 210 292,44	0,278
0,12	180 365 811 207,33	68 253 448 597,71	38 226 594 484,95	0,277
0,13	186 446 773 911,62	72 663 824 902,44	40 170 583 144,27	0,276
0,14	192 526 540 830,08	77 064 522 086,53	42 086 777 034,14	0,275
0,15	198 605 114 660,27	81 457 181 820,68	43 980 349 898,21	0,274

$$V_F = 0.5$$

Table A-15 Carbon fibre material properties when V_F is kept constant at 0.5, while W_{GPL} is varied.

W_{GPL}	E_{11} (Pa)	E_{22} (Pa)	G_{12} (Pa)	ν_{12}
0,00	133 250 000 000,00	7 177 966 101,69	3 461 974 088,89	0,275
0,01	138 329 603 354,47	16 091 814 051,41	10 400 589 209,53	0,274
0,02	143 408 182 980,10	21 279 948 527,76	14 973 822 073,34	0,273
0,03	148 485 741 165,80	25 558 865 640,27	18 407 231 847,87	0,272
0,04	153 562 280 197,02	29 477 229 711,15	21 205 243 894,48	0,271
0,05	158 637 802 355,76	33 215 952 026,13	23 613 536 164,45	0,270
0,06	163 712 309 920,59	36 852 088 100,66	25 766 088 920,05	0,269
0,07	168 785 805 166,65	40 424 010 417,00	27 742 185 237,72	0,269
0,08	173 858 290 365,65	43 952 976 327,41	29 591 738 572,41	0,268
0,09	178 929 767 785,90	47 451 713 321,80	31 347 739 668,81	0,267
0,10	184 000 239 692,30	50 928 307 644,25	33 032 868 051,29	0,266
0,11	189 069 708 346,33	54 388 143 358,81	34 663 228 527,41	0,265
0,12	194 138 176 006,11	57 834 944 234,87	36 250 572 683,43	0,264
0,13	199 205 644 926,35	61 271 368 078,59	37 803 676 664,84	0,263
0,14	204 272 117 358,40	64 699 362 819,28	39 329 226 832,59	0,262
0,15	209 337 595 550,23	68 120 388 793,53	40 832 406 849,18	0,261

A.2.2 Material properties where W_{GPL} is kept constant while varying V_F

$W_{GPL} = 0.02$

Table A-16 Carbon fibre material properties when W_{GPL} is kept constant at 0.02, while V_F is varied.

V_F	E_{11} (Pa)	E_{22} (Pa)	G_{12} (Pa)	ν_{12}
0	23 816 365 960,20	23 816 365 960,20	8 845 140 959,64	0,346
0,1	28 674 729 364,18	26 349 445 877,87	9 867 883 173,84	0,332
0,2	33 533 092 768,16	29 167 073 173,82	11 016 139 009,76	0,317
0,3	38 391 456 172,14	32 320 046 952,66	12 314 523 949,84	0,302
0,4	43 249 819 576,12	35 872 023 372,93	13 794 540 413,46	0,288
0,5	48 108 182 980,10	39 903 857 992,01	15 497 167 432,19	0,273
0,6	52 966 546 384,08	44 519 835 502,39	17 476 713 898,70	0,259

$W_{GPL} = 0.04$

Table A - 17 Carbon fibre material properties when W_{GPL} is kept constant at 0.04, while V_F is varied.

V_F	E_{11} (Pa)	E_{22} (Pa)	G_{12} (Pa)	ν_{12}
0	44 124 560 394,05	44 124 560 394,05	16 432 349 874,99	0,343
0,1	46 952 104 354,64	46 319 237 759,73	17 430 400 423,15	0,328
0,2	49 779 648 315,24	48 625 858 414,98	18 490 968 049,30	0,314
0,3	52 607 192 275,83	51 053 211 296,94	19 620 116 702,57	0,300
0,4	55 434 736 236,43	53 611 030 122,51	20 824 720 779,58	0,286
0,5	58 262 280 197,02	56 310 123 844,96	22 112 605 200,24	0,271
0,6	61 089 824 157,62	59 162 529 340,64	23 492 715 576,21	0,257

$W_{GPL} = 0.06$

Table A-18 Carbon fibre material properties when W_{GPL} is kept constant at 0.06, while V_F is varied.

V_F	E_{11} (Pa)	E_{22} (Pa)	G_{12} (Pa)	V_{12}
0	64 424 619 841,19	64 424 619 841,19	24 057 925 246,80	0,339
0,1	65 222 157 857,07	65 180 073 575,73	24 606 156 746,28	0,325
0,2	66 019 695 872,95	65 944 438 130,43	25 167 025 320,44	0,311
0,3	66 817 233 888,83	66 717 872 099,62	25 740 973 002,43	0,297
0,4	67 614 771 904,71	67 500 537 863,63	26 328 462 684,46	0,283
0,5	68 412 309 920,59	68 292 601 702,42	26 929 979 362,94	0,269
0,6	69 209 847 936,47	69 094 233 913,41	27 546 031 473,78	0,256

$W_{GPL} = 0.08$

Table A-19 Carbon fibre material properties when W_{GPL} is kept constant at 0.08, while V_F is varied.

V_F	E_{11} (Pa)	E_{22} (Pa)	G_{12} (Pa)	V_{12}
0	84 716 580 731,31	84 716 580 731,31	31 721 869 382,38	0,335
0,1	83 484 922 658,17	83 398 702 346,63	31 562 840 652,35	0,322
0,2	82 253 264 585,04	82 101 167 070,13	31 404 607 175,05	0,308
0,3	81 021 606 511,91	80 823 507 477,30	31 247 163 000,14	0,295
0,4	79 789 948 438,78	79 565 270 354,84	31 090 502 236,49	0,281
0,5	78 558 290 365,65	78 326 016 164,65	30 934 619 051,46	0,268
0,6	77 326 632 292,52	77 105 318 531,89	30 779 507 670,18	0,254

$$W_{GPL} = 0.10$$

Table A-20 Carbon fibre material properties when W_{GPL} is kept constant at 0.10, while V_F is varied.

V_F	E_{11} (Pa)	E_{22} (Pa)	G_{12} (Pa)	V_{12}
0	105 000 479 384,59	105 000 479 384,59	39 424 184 691,53	0,332
0,1	101 740 431 446,13	101 210 978 695,90	38 389 052 299,90	0,319
0,2	98 480 383 507,67	97 555 818 103,64	37 380 746 450,53	0,305
0,3	95 220 335 569,22	94 027 978 369,17	36 398 237 626,93	0,292
0,4	91 960 287 630,76	90 620 920 887,61	35 440 548 326,61	0,279
0,5	88 700 239 692,30	87 328 547 241,73	34 506 749 817,18	0,266
0,6	85 440 191 753,84	84 145 162 772,53	33 595 959 132,28	0,253